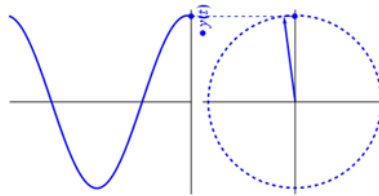


Complex-Valued Steady-State Models as Applied to Power Flow Analysis and Power System State Estimation

by

Prof. Robson Pires, D.Sc.
IEEE Senior Member, 2017
System Engineering Group - GESis
Institute of Electric Systems and Energy (ISEE)



Thesis submitted to the
Committee Members as a partial
requirement aiming the
candidate elevation from the
Associate IV degree to Full
Professor at Federal University
of Itajubá - UNIFEI, Itajubá,
Minas Gerais, MG
CEP: 37500-903, Brazil.

...

“The measure of greatness in a scientific idea is the extent to which it stimulates thought and opens up new lines of research.”

Paul A.M. Dirac

Acknowledgements

The Author is very grateful to the CNPQ - Conselho Nacional de Desenvolvimento Científico e Tecnológico, for the financial support during his sabbatical year from Dec. 2014 to Nov. 2015 - Process No. [200703/2014-5] at the “Bradley Department of Electrical and Computer Engineering”, Northern Virginia Center - VTech, Falls Church, VA - USA. Consequently, special thanks should be addressed to my longtime friend, Prof. Lamine Mili, who welcomed me and strongly contributed to this thesis. Also, I would like to express my gratitude to my advised students, Guilherme Chagas and Marcos Netto, who generalized the CV-PFA and CV-PSSE programs, respectively, aiming to simulate large power systems. Absolutely, I thankful to God for my good health and for putting brightness in my eyes; intuition in my heart and shiny scientific ideas in my mind to conduct these researches.

Contents

		Page
1	Introduction	1
2	Complex-Valued Functions and Variables	2
2.1	The Complex-Valued Wirtinger Calculus	2
2.1.1	Holomorphic Functions	2
2.1.2	Properties of Holomorphic Function	3
2.1.3	Non-holomorphic functions: $\mathbb{C}\mathbb{R}$ calculus	5
2.1.4	The Wirtinger Derivatives	6
2.1.5	Optimization with Complex Variables	9
2.1.6	The Co-gradient and Conjugate Co-gradient Operators	9
2.1.7	The Complex Jacobian Matrix	13
2.2	Framework for $\mathbb{C}\mathbb{R} - \text{Calculus}$	14
2.2.1	Hermitian conjugate matrix	14
2.2.2	SWAP operator	14
2.2.3	Mapping variables from \mathbb{R} towards \mathbb{C} domain	15
2.2.4	Mapping variables from \mathbb{C} towards \mathbb{C} domain	16
2.3	Partial Conclusions	17
3	Complex-Valued Power Flow Analysis (CV-PFA)	18
3.1	Nodal Equation	18
3.2	Complex-Valued Power Flow Equations	19
3.3	Wirtinger Derivatives Applied to the Power Flow Equations	19
3.4	Bus Models in the Complex Domain	21
3.4.1	Slack-Bus Type	21
3.4.2	PQ-Bus Type	21
3.4.3	PV-Bus Type	22
3.4.4	PQV-Bus Type	23
3.5	Complex-Valued Iterative Solution	23
3.5.1	The Newton-Raphson Algorithm	23
3.5.2	Structure of the Complex-Valued Power Flow Jacobian Matrix	24
3.5.3	The Fourth-Order Levenberg-Marquardt as Applied to CV-PFA	25
3.6	Numerical Results	27

3.6.1	Small Example: CV-Power Flow Analysis	27
3.6.2	IEEE Test Systems: well-conditioned systems	30
3.6.3	IEEE Test Systems: ill-conditioned systems	35
3.7	Partial Conclusions	37
4	Complex-Valued Power System State Estimation - (CV-PSSE)	39
4.1	Introduction	39
4.2	Complex-Valued WLS Power System State Estimation	40
4.2.1	Complex-Valued Nonlinear Measurement Model	40
4.2.2	Complex-Valued Gauss-Newton Algorithm	40
4.2.3	Complex-Valued High-Order Levenberg-Marquardt Algorithm	42
4.2.4	Complex-Valued PSSE Numerical Solutions	42
4.2.5	Direction of Maximum Rate of Change of the Cost Function	43
4.2.6	Numerical Decoupled Solutions	43
4.3	Complex-Valued Factorization Algorithms	44
4.3.1	Three-Angle Complex Rotation Algorithm	45
4.3.2	Complex-Valued Fast Givens Rotations	46
5	Complex-Valued Bad Data Processing	47
5.1	Nature of Complex Random Signals	47
5.2	CV-Multivariate Generalized Gaussian Distribution	48
5.3	Complex-Valued Measurements Models	52
5.3.1	Complex Linear Model	52
5.3.2	Complex Nonlinear Model	52
5.4	Complex-Valued Bad Data Detection and Identification Methods	52
5.4.1	Detection: Complex-Valued Chi-squared Test	53
5.4.2	Identification: Largest Normalized Residual Method	53
5.4.3	Bad Data Redemption as Pseudo Measurement	54
5.5	Numerical Results Without Bad Data Processing	54
5.5.1	Small Power System Example	54
5.5.2	IEEE-Test Systems and the Brazilian Equivalent Systems	58
5.6	Numerical Results Including Bad Data	63
5.6.1	Circular and Proper Complex Linear Model	63
5.6.2	Circular and Proper Complex NonLinear Model	65
5.6.3	Noncircular/Proper Complex NonLinear Model	67
5.6.4	Noncircular/Improper Complex NonLinear Model	67
5.7	Partial Conclusions	67
6	General Conclusions	68
6.1	Future Investigations	68
6.2	Papers Under Review	69
6.3	Advised Students	69

Bibliography 69

List of Figures

2.1	Contour Plot of the Scalar Real Function of Complex Scalar Variables.	12
3.1	IEEE-11 Bus: Condition Number.	26
3.2	Small 3-Bus System.	27
3.3	Sparsity structure of (a) real-valued Jacobian matrix; (b) complex-valued Jacobian matrix of the IEEE 14-bus system.	31
3.4	Sparsity structure of (a) real-valued Jacobian matrix; (b) complex-valued Jacobian matrix of the IEEE 30-bus system.	31
3.5	Sparsity structure of (a) real-valued Jacobian matrix; (b) complex-valued Jacobian matrix of the IEEE 57-bus system.	31
3.6	Sparsity structure of (a) real-valued Jacobian matrix; (b) complex-valued Jacobian matrix of the IEEE 118-bus system.	32
3.7	IEEE-14 Bus: voltage and angle profiles.	33
3.8	IEEE-30 Bus: voltage and angle profiles.	34
3.9	IEEE-57 Bus: voltage and angle profiles.	34
3.10	IEEE-118 Bus: voltage and angle profiles.	35
3.11	IEEE-11 Bus: one line diagram.	35
3.12	IEEE-11 Bus: Voltage profile.	38
3.13	CV-Power Flows and State Variables Plotting.	38
5.1	Scatter plots for (a) circular, (b) proper but noncircular, and (c) improper (and thus noncircular) data.	51
5.2	Covariance and complementary covariance function plots for the corresponding processes in Fig. 5.1: (a) circular (b) proper but noncircular; and (c) improper.	51
5.3	2-Bus power system.	55
5.4	Sparsity structure of (a) real-valued Jacobian matrix; (b) real-valued gain matrix; (c) complex-valued Jacobian matrix; (d) complex-valued Hessian matrix of the IEEE 14-bus system.	59
5.5	Sparsity structure of (a) real-valued Jacobian matrix; (b) real-valued gain matrix; (c) complex-valued Jacobian matrix; (d) complex-valued Hessian matrix of the IEEE 30-bus system.	60
5.6	Sparsity structure of (a) real-valued Jacobian matrix; (b) real-valued gain matrix; (c) complex-valued Jacobian matrix; (d) complex-valued Hessian matrix of the Brazilian equivalent 340-bus system.	61

5.7	Sparsity structure of (a) real-valued Jacobian matrix; (b) real-valued gain matrix; (c) complex-valued Jacobian matrix; (d) complex-valued Hessian matrix of the Brazilian equivalent 730-bus system.	62
5.8	Small 3-Bus Example System.	63
5.9	Small 2-Bus Example System.	65

List of Tables

3.1	Branches Data.	28
3.2	Bus Data.	28
3.3	Correction Vector.	29
3.4	State Variables.	29
3.5	Complex-Valued <i>Mismatches</i> Vector.	29
3.6	CV-Power Flow Report.	30
3.7	Features of the IEEE Test systems	30
3.8	Sparsity and Numerical Analysis	32
3.9	Maximum bias between states and location	33
3.10	ill-conditioned IEEE-11 Bus Data.	36
3.11	ill-conditioned IEEE-11 Bus Branches Data.	36
3.12	State Variables and Complex Power Injections.	37
5.1	Branches Data	55
5.2	Estimated State Variables	57
5.3	CV-Estimated Quantities	58
5.4	CV-Residual Vector	58
5.5	Features of the IEEE-Standards and Brazilian Grids	63
5.6	Parameters and Performance Indices	64

Abstract

Nonlinear systems of equations in complex domain are frequently encountered in applied mathematics, e.g., power systems, signal processing, control theory, neural networks and biomedicine, to name a few. The solution of these problems often requires a first- or second-order approximation of these nonlinear functions to generate a new step or descent direction to meet the solution iteratively. However, such methods cannot be applied to real functions of complex variables because they are necessarily non-analytic in their argument, i.e., the Taylor series expansion in their argument alone does not exist. To overcome this problem, the nonlinear function is usually redefined as a function of the real and imaginary parts of its complex argument so that standard methods can be applied. Although not widely known, it is possible to build an expansion of these nonlinear functions in its original complex variables by noting that functions of complex variables can be analytic in their argument and its complex conjugate as a whole. This property lies in the fact that if a function is analytic in the space spanned by $\Re\{x\}$ and $\Im\{x\}$ in \mathbb{R} , it is also analytic in the space spanned by x and x^* in \mathbb{C} . The main contribution of this work is the application of this methodology to a complex Taylor series expansions aiming algorithms commonly used for solving complex-valued nonlinear systems of equations emerged from power systems problems. In our proposal, a complex-valued power flow analysis (CV_PFA) model solved by Newton-Raphson method is revisited and enhanced. Nonetheless, especially emphasis is addressed to Gauss-Newton method when derived in complex domain for solving power system state estimation (CV_PSSE) problems, whichever they are applied in transmission or distribution systems. The factorization method of the complex Jacobian matrices emerged from CV_PFA and CV_PSSE approaches is the *Three Angle Complex Rotation (TACR)* algorithm that comes from the Givens Rotations algorithm in real domain. In this research one demonstrates that Wirtinger derivatives can lead to greater insights in the structure of both problems, i.e., CV_PFA & CV_PSSE. Moreover, it can often be exploited to mitigate computational overhead, storage cost and enhance the network's component modeling as FACTS devices, e.g., STATCOM, VSC-HVDC, besides easily handle PMU measurements and embedding new technologies towards smart grids. Finally, in order to add numerical robustness, a fourth-order Levenberg-Marquardt algorithm is employed to the CV_PFA & CV_PSSE approaches because of its nice bi-quadratic convergence property, instead of the well-known quadratic convergence property of the classical Newton-Raphson and Gauss-Newton algorithms. Recall that these latter algorithms are prone to collapse when the power system network is ill-conditioned, i.e., it is heavily loaded or presents branches with high R/X ratio. These results are partially presented in this thesis because they are still under study and development. But most of them will appear in forthcoming papers submitted to IEEE-PES Transactions on Power Systems and coming up Top Conferences.

Keywords: Complex-valued power flow, complex-valued power system state estimation, Newton-Raphson, Gauss-Newton and Robust Levenberg-Marquardt algorithms in complex domain.

List of Symbols

\mathcal{J}	Real-valued cost function of complex variables
\underline{x}_c	State variables vector in the conjugate coordinates system
$x; x^*$	Complex and complex conjugate state variable
$a; a^*$	Complex and complex conjugate tap position
\mathbf{I}	Identity matrix
\mathbf{J}	Complex-valued Jacobian matrix
\mathbf{H}	CV-Jacobian matrix in the complex conjugate coordinates
\mathbf{G}	Complex-valued Hessian matrix
$(\cdot)_c$	Quantity in the complex conjugate coordinates
$\Re\{\cdot\}$	Real part of a complex variable
$\Im\{\cdot\}$	Imaginary part of a complex variable
$\ \cdot\ $	Euclidean norm
$\ \cdot\ _\infty$	Infinity norm
$(\cdot)^\dagger$	denotes the Moore-Penrose pseudoinverse
$(\cdot)^*$	denotes the complex conjugate
$(\cdot)^T$	denotes complex transpose
$(\cdot)^H$	denotes complex conjugate transpose, i.e., Hermitian operator

Complex-Valued Steady-State Models as Applied to Power Flow Analysis and Power System State Estimation

1 Introduction

This thesis is a tribute to the Steinmetz's work [1]. The reasons and motivations are stated throughout the whole document as follows. Numerical solutions for solving power system applications are typically carried out in the real domain. For instance, the power flow analysis and power system state estimation are well known tools, among others. It turns out that these solutions are not well suited for modeling voltage and current phasor. To overcome this difficulty, the proposal described in this thesis aims to model the aforementioned applications in a unified system of coordinates, e.g., complex-domain. Nonetheless, the solution methods of these problems often require a first- or second-order approximation of the set of power-flow equations, i.e., nonlinear functions. However, such methods cannot be applied to nonlinear functions of complex variables because they are non-analytic in their arguments and therefore, for these functions Taylor series expansions do not exist. Hence, for many decades this problem has been solved redefining the nonlinear functions as separate functions of the real and imaginary parts of their complex arguments so that standard methods can be applied. Although not widely known, it is also possible to construct an extended nonlinear functions that includes not only the original complex state variables, but also their complex conjugates and then apply the Wirtinger calculus [2], [3]. This property lies on the fact that if a function is analytic in the space spanned by $\Re\{x\}$ and $\Im\{x\}$ in \mathbb{R} , it is also analytic in the space spanned by x and x^* in \mathbb{C} . In complex analysis of one and several complex variables, *Wirtinger operators* are partial differential operators of the first order which behave in a very similar manner to the ordinary derivatives with respect to one real variable, when applied to *holomorphic* functions, *nonholomorphic* functions or simply differentiable functions on complex domain. These operators allow the construction of a differential calculus for such functions that is entirely analogous to the ordinary differential calculus for functions of real variables [4]. Then, taken into account the Wirtinger calculus, in this thesis is derived the steady-state models as applied to power flow analysis and power system state estimation [5], [6].

Therefore, the classical Newton-Raphson and Gauss-Newton methods in complex domain aiming the numerical solution of the power flow analysis and power system state estimation, including the factorization of the complex Jacobian matrices emerged from this approaches, are derived. Additionally, in order to add numerical robustness, a fourth-order Levenberg-Marquardt algorithm is employed to the CV_PFA & CV_PSSE approaches because of its nice bi-quadratic convergence property, instead of the well-known quadratic convergence property of the Newton-Raphson and Gauss-Newton algorithms. Recall that these algorithms are prone to collapse when the electrical network is ill-conditioned, i.e., it is heavily loaded or presents branches with high R/X ratio. Moreover, the factorization of the Jacobian matrices emerged from the the referred applications are performed through the Three Angle Complex Rotation (TACR) [7] or the Complex-Valued Fast Givens Rotations (CVFGR) [8] algorithms.

This thesis is organized as follows. The theoretical foundation is based on *Wirtinger Calculus* which is summed up in Section 2. Section 3 describes the complex-valued model solution aiming the power flow analysis (CV-PFA) problem. In Section 4 is derived the complex-valued static model solution addressed for the power system state estimation (CV-PSSE) problem. Section 5 presents the complex-valued bad data processing. Finally, in Section 6 are gathered some conclusions. Furthermore, the next steps to be investigated in near future are highlighted.

2 Complex-Valued Functions and Variables

A complex-valued function is a mapping from a given *domain* Ω into the complex scalar ($f \in \mathbb{C}$), vector ($\mathbf{F} \in \mathbb{C}^n$), or matrix ($\mathbf{F} \in \mathbb{C}^{n \times m}$) domain. For them, one can define the same basic concepts applied to complex variables as *real and imaginary parts, absolute value, and conjugate*. Hereinafter, the scalar case will be focused.

The gradient-based optimization procedures, that is the partial derivatives or gradient used in adaptation of complex parameters, is *not* based on the standard complex derivative taught in regular mathematics and engineering complex variables courses [5]. Shall be noticed that *complex derivatives* exists *if and only if* a function of complex variable z is *complex analytic* in z .

Nonetheless, the same real-valued function viewed as a function of the real-valued real and imaginary components of the complex variable can have a (real) gradient when partial derivatives are taken with respect to those two (real) components. In this way we can shift from viewing the real-valued function as a non-differentiable mapping between \mathbb{C} and \mathbb{R} to treating it as a differentiable mapping between \mathbb{R}^2 and \mathbb{R} . Indeed, the modern graduate-level textbook in complex variables theory by Remmert [4] continually and easily shifts back and forth between the real function $\mathbb{R}^2 \rightarrow \mathbb{R}$ or \mathbb{R}^2 perspective and the complex function $\mathbb{C} \rightarrow \mathbb{C}$ perspective of a complex or real scalar-valued function,

$$f(z) = f(r) = f(x, y),$$

of complex variable $z = (x + jy)$,

$$z \in \mathbb{C} \iff r = \begin{pmatrix} x \\ y \end{pmatrix} \in \mathbb{R}^2.$$

In order to avoid the constant back-and-forth shift between a real function (“ \mathbb{R} -calculus”) perspective and a complex function (“ \mathbb{C} -calculus”) perspective which a careful analysis of non-analytic complex functions is required, one refer to the mathematics framework underlying the derivatives given hereafter as a “ $\mathbb{C}\mathbb{R}$ -calculus” or simply “*Wirtinger Calculus*” [5]. However, because the real gradient perspective arises within a complex variables framework, a direct reformulation of the problem to the real domain is awkward. Instead, it greatly simplifies derivations if one can represent the real gradient as a redefined, new complex gradient operator. As one shall see in the sequence, the complex gradient is an extension of the standard complex derivative to non-complex analytic functions.

2.1 The Complex-Valued Wirtinger Calculus

Most of the contents of this section is based on the work of Professors Kreutz-Delgado (2009) - [5], Danilo Mandic (2009) [9], Are HjØrungnes (2011) - [10] and Pablo’s PhD Thesis (2013) - [11].

When dealing with complex variables, the notion of derivative is not as direct and intuitive as in the real variable case. Usually, traditional courses on complex variable calculus start with the concept of *holomorphic function*.

2.1.1 Holomorphic Functions

Definition 2.1.1. Let $\Omega \subseteq \mathbb{C}$ be the domain of the scalar function $f : \Omega \rightarrow \mathbb{C}$. Thus, $f(z)$ is an holomorphic function in the domain Ω if the limit



$$f'(z) = \lim_{\Delta z \rightarrow 0} \frac{f(z + \Delta z) - f(z)}{\Delta z} \quad (1)$$

exist for all $z \in \Omega$.

For a function to be holomorphic, the previous limit (1) must be independent of the direction which f approaches to zero in the complex plane. This, although can be seen as a minor issue, is indeed a very strong condition imposed on the function $f(z)$. Then, the complex derivative of a function of $z = x + j y$, i.e.,

$$f(z) = u(x, y) + j v(x, y), \quad (2)$$

to exist in the standard *holomorphic* sense, the real partial derivatives of u and v must not only exist, but they also must satisfy the **Cauchy-Riemann** equations:

$$\frac{\partial u}{\partial x} = \frac{\partial v}{\partial y}, \quad \frac{\partial v}{\partial x} = -\frac{\partial u}{\partial y}. \quad (3)$$

Proof. For a function to be holomorphic, it must satisfy (1) independently of the path of approximation to the point z when $\Delta z = \Delta x + j \Delta y \rightarrow 0$. If we expand (1) in real and imaginary parts of z , and of f yields

$$f'(z) = \lim_{\Delta x \rightarrow 0, \Delta y \rightarrow 0} \frac{u(x + \Delta x, y + \Delta y) + j v(x + \Delta x, y + \Delta y) - u(x, y) + j v(x, y)}{\Delta x + j \Delta y} \quad (4)$$

Let us consider now the two simplest cases for the approach of $\Delta x \rightarrow 0$ and $\Delta y \rightarrow 0$, that correspond to the coordinate axes:

Case 1: $\Delta y = 0$, while $\Delta x \rightarrow 0$.

$$\begin{aligned} f'(z) &= \lim_{\Delta x \rightarrow 0} \left(\frac{u(x+\Delta x, y) + j v(x+\Delta x, y) - u(x, y) - j v(x, y)}{\Delta x} \right) \\ &= \lim_{\Delta x \rightarrow 0} \left(\frac{u(x+\Delta x, y) - u(x, y)}{\Delta x} + j \frac{v(x+\Delta x, y) - v(x, y)}{\Delta x} \right) \\ &= \frac{\partial u(x, y)}{\partial x} + j \frac{\partial v(x, y)}{\partial x}. \end{aligned} \quad (5)$$

Case 2: $\Delta x = 0$, while $\Delta y \rightarrow 0$.

$$\begin{aligned} f'(z) &= \lim_{\Delta y \rightarrow 0} \left(\frac{u(x, y+\Delta y) + j v(x, y+\Delta y) - u(x, y) - j v(x, y)}{j \Delta y} \right) \\ &= \lim_{\Delta y \rightarrow 0} \left(\frac{u(x, y+\Delta y) - u(x, y)}{j \Delta y} + j \frac{v(x, y+\Delta y) - v(x, y)}{j \Delta y} \right) \\ &= \frac{\partial v(x, y)}{\partial y} - j \frac{\partial u(x, y)}{\partial y}. \end{aligned} \quad (6)$$

To ensure uniqueness of the limit (4), equation (5) must be equal to equation (6). Identifying *real* and *imaginary* parts, we get the **Cauchy-Riemann equations**. ■

2.1.2 Properties of Holomorphic Function

Let us take a look on the properties of holomorphic functions. Although the notation that is used in complex calculus is very similar to the one used in real calculus, an holomorphic function $f(z)$ has a certain structure that makes itself somewhat special. Specifically, the following results are equivalent:

- The derivative $f'(z)$ exists and is continuous.
- The function $f(z)$ is holomorphic (that is, *analytic*¹ in z).
- All the derivatives of the function $f(z)$ exist, and $f(z)$ admits convergent power series expansion.
- The real $u(x, y)$ and imaginary $v(x, y)$ parts of the function $f(z)$ are *harmonic functions*, that is, they satisfy Laplace equations:

$$\frac{\partial^2 u(x, y)}{\partial x^2} + \frac{\partial^2 u(x, y)}{\partial y^2} = 0, \quad \text{and} \quad \frac{\partial^2 v(x, y)}{\partial x^2} + \frac{\partial^2 v(x, y)}{\partial y^2} = 0. \quad (7)$$

It is clear that, when a function is holomorphic, we are imposing a big structure and strong properties on it. A *holomorphic function* can also be known as *complex differentiable*, *complex analytic* or *regular*. Thus if either $u(x, y)$ or $v(x, y)$ fail to be harmonic, the function $f(z)$ is not differentiable.

Although many important complex functions are holomorphic and thus complex differentiable, unavoidably we are going to find lots of functions that are not. It seems that there are not many functions in the *engineering fields* that satisfies the conditions to be holomorphic and complex differentiable. The following theorem explains the main reason.

Theorem 1. (*The Real-Valued Holomorphic Functions*) *Let $\Omega \subseteq \mathbb{C}$ be a domain in the complex plane, and let $f(z) : \Omega \subseteq \mathbb{C}$ be a real holomorphic function. Then, $f(z)$ must be the constant function, for all z .*

Proof. If $f(z)$ takes only real values, necessarily $v(x, y) = \text{Im}(z) = 0$. Then, if $f(z)$ is holomorphic, it must satisfy the Cauchy-Riemann equations (3). So the real part $u(x, y)$ must be constant throughout the z plane, that is,

$$f(z) = \text{const.}, \forall z. \quad (8)$$

■

This is a classical result that reduces the set of real holomorphic functions to only the constant function. In practice, cost functions (as was stated at the beginning of Section 1) are *real* but *necessarily non-constant*, so they are not holomorphic functions, and their study cannot be done by using classical tools for complex variables.

Notice that if we are looking for an optimization procedure to find the optimal point of a real, non-constant cost function, we find that the function is not holomorphic. Thus, its derivative with respect to the independent complex variable z does not exist in the conventional sense.

For all these reasons, it is necessary an alternate formulation for the calculus of derivatives of real functions with complex variables and, in general, nonholomorphic functions.

¹A function is analytic in a domain if it admits convergent power series expansion in such domain. That implies the function has derivatives of all orders. For a complex function of complex variable, the term *analytic* has been recently substituted by the term *holomorphic*, although both are synonyms and we could interchange them. Specifically, we can say that a function of real variable that admits real power series expansions is analytic (*real analytic*), while a function of complex variable that admits complex power series expansion is holomorphic (*complex analytic*).

2.1.3 Non-holomorphic functions: $\mathbb{C}\mathbb{R}$ calculus

Now, it is convenient to define a generalization or extension of the standard partial derivative to *nonholomorphic* functions of $z = x + j y$ that are nonetheless differentiable with respect to x and y and which incorporates the *real gradient* information directly within the complex variables framework. This procedure is called *real-derivative*, or \mathbb{R} – *derivative*, of a possibly nonholomorphic function in order to avoid confusion with the standard *complex-derivative*, or \mathbb{C} – *derivative*, of a holomorphic function which was presented in the previous subsection. The goal is that the *real-derivative* to reduce to the standard *complex-derivative* when applied to holomorphic functions. In essence, the so-called *conjugate coordinates* can be defined as:

$$\begin{aligned} \text{Conjugate Coordinates : } c \triangleq (z, z^*) = (z, z^*) \in \mathbb{C} \times \mathbb{C}, \quad z = x + j y \\ \text{and} \\ z^* = x - j y \end{aligned} \tag{9}$$

which serves as a formal substitute for the real $r = (x, y)^T \in \mathbb{R}$ representation of the point $z = x + j y \in \mathbb{C}$.

Definition 2.1.2. For a general complex- or real-valued function $f(c) = f(z, z^*)$ consider the *pair* of partial derivatives of $f(c)$ *formally*² referred as *Wirtinger derivatives*.

$$\begin{aligned} \mathbb{R} - \text{Derivative of } f(c) \triangleq \left. \frac{\partial f(z, z^*)}{\partial z} \right|_{z^* = \text{const.}} \\ \text{and} \end{aligned} \tag{10}$$

$$\text{Conjugate } \mathbb{R} - \text{Derivative of } f(c) \triangleq \left. \frac{\partial f(z, z^*)}{\partial z^*} \right|_{z = \text{const.}}$$

where the formal partial derivatives are taken to be standard complex partial derivatives (\mathbb{C} – *derivatives*) which is taken with respect to z in the first case and in the sequel with respect to z^* . As noted in (10) the first expression is called *real-derivative* (\mathbb{R} – *derivative*) and the second expression is the *conjugate* \mathbb{R} – *derivative* (or \mathbb{R}^* – *derivative*). This introduces the so-called *Wirtinger calculus* or $\mathbb{C}\mathbb{R}$ – *calculus* (Kreutz–Delgado, 2006) [5]. Other definitions is presented in the sequence.

Complex Derivative Identities - The most common useful Wirtinger derivatives are showed below:

$$\frac{\partial f^*}{\partial z^*} = \left(\frac{\partial f}{\partial z} \right)^* \tag{11}$$

$$\frac{\partial f^*}{\partial z} = \left(\frac{\partial f}{\partial z^*} \right)^* \tag{12}$$

²These statements are formal because one cannot truly vary $z = x + j x$ while keeping $z^* = x - j x$ constant, and vice versa. Actually, z and z^* are independent in the sense that $\frac{\partial z}{\partial z^*} = \frac{\partial z^*}{\partial z} = 0$.

$$df = \frac{\partial f}{\partial z} dz + \frac{\partial f}{\partial z^*} dz^* \quad \text{Differential Rule,} \quad (13)$$

$$\frac{\partial h(f(c))}{\partial z} = \frac{\partial h(f(z, z^*))}{\partial z} = \frac{\partial h}{\partial f} \frac{\partial f}{\partial z} + \frac{\partial h}{\partial f^*} \frac{\partial f^*}{\partial z} \quad \text{Chain Rule,} \quad (14)$$

$$\frac{\partial h(f(c))}{\partial z^*} = \frac{\partial h(f(z, z^*))}{\partial z^*} = \frac{\partial h}{\partial f} \frac{\partial f}{\partial z^*} + \frac{\partial h}{\partial f^*} \frac{\partial f^*}{\partial z^*} \quad \text{Chain Rule,} \quad (15)$$

$$f(z) \in \mathbb{R} \Leftrightarrow \frac{\partial f}{\partial z^*} = \left(\frac{\partial f}{\partial z} \right)^*. \quad (16)$$

All of these properties extend naturally to the multivariate case, *substituting the scalars by vectors and derivatives by gradients.*

2.1.4 The Wirtinger Derivatives

The aforementioned derivatives presented above are related with the *real* and *imaginary* parts derivatives in the following way.

Theorem 2. (*Relation between Wirtinger calculus and real derivatives*): Let $z \in \mathbb{C}$ and let $x = \text{Re}\{z\}$ and $y = \text{Im}\{z\}$. The partial derivative of f with respect to the complex variable, $\frac{\partial}{\partial z}$, and its counterpart, i.e., the complex conjugate variable, $\frac{\partial}{\partial z^*}$, are defined as

$$\begin{aligned} \frac{\partial f(c)}{\partial z} &\triangleq \left. \frac{\partial f(z, z^*)}{\partial z} \right|_{z^*=\text{const.}} \\ \frac{\partial f(z, z^*)}{\partial z} \Big|_{z^*=\text{const.}} &= \frac{1}{2} \left[\frac{\partial}{\partial x} - j \frac{\partial}{\partial y} \right], \end{aligned} \quad (17)$$

and

$$\begin{aligned} \frac{\partial f(c)}{\partial z^*} &\triangleq \left. \frac{\partial f(z, z^*)}{\partial z^*} \right|_{z=\text{const.}} \\ \frac{\partial f(z, z^*)}{\partial z^*} \Big|_{z=\text{const.}} &= \frac{1}{2} \left[\frac{\partial}{\partial x} + j \frac{\partial}{\partial y} \right]. \end{aligned} \quad (18)$$

respectively. Thus, the (conjugate) gradient operator acts as a partial derivatives with respect to z (z^*), treating z^* (z) as a constant. However, in order to better express any change in a function with respect to a change in z , the following additional definition of *complex gradient operator* or $\frac{\partial}{\partial c}$ allows to represent the aforementioned definition in an unified manner,

$$\frac{\partial}{\partial c} = \left(\frac{\partial}{\partial z}, \frac{\partial}{\partial z^*} \right). \quad (19)$$

Proof. Firstly, let us express the differential of the function of two real variables $f(x, y)$:

$$df(x, y) = \frac{\partial f}{\partial x} dx + \frac{\partial f}{\partial y} dy. \quad (20)$$

As $f(x, y) = u(x, y) + j v(x, y)$, the chain rule of derivation defined in (14) can be applied yielding

$$df(x, y) = \frac{\partial u}{\partial x} dx + j \frac{\partial v}{\partial x} dx + \frac{\partial u}{\partial y} dy + j \frac{\partial v}{\partial y} dy. \quad (21)$$

Now, taken into account that $x = \frac{1}{2}(z + z^*)$ and $y = \frac{1}{2}j(z^* - z)$ the following changes of variable over the differentials of the real $dx = \frac{(dz + dz^*)}{2}$ and imaginary parts $dy = j \frac{(dz^* - dz)}{2}$ can takes place, yielding to

$$df = \frac{1}{2} \left(\frac{\partial u}{\partial x} + \frac{\partial v}{\partial y} + j \left(\frac{\partial v}{\partial x} - \frac{\partial u}{\partial y} \right) \right) dz + \frac{1}{2} \left(\frac{\partial u}{\partial x} - \frac{\partial v}{\partial y} + j \left(\frac{\partial v}{\partial x} + \frac{\partial u}{\partial y} \right) \right) dz^*. \quad (22)$$

Thus, the differential of f becomes:

$$df = \frac{1}{2} \left(\frac{\partial f}{\partial x} - j \frac{\partial f}{\partial y} \right) dz + \frac{1}{2} \left(\frac{\partial f}{\partial x} + j \frac{\partial f}{\partial y} \right) dz^*. \quad (23)$$

Finally, we only have to expand the differential of f but depending on the complex conjugate variables z and z^* ,

$$df(c) = df(z, z^*) = \frac{\partial f}{\partial z} dz + \frac{\partial f}{\partial z^*} dz^*. \quad (24)$$

Comparing terms in (23) and (24) allows to verify the equalities stated in (17) and (18). ■

These two expressions relate the \mathbb{R} and \mathbb{R}^* derivatives with the derivatives with respect to the *real* and *imaginary* parts of the complex variables. This duality gives name to the $\mathbb{C}\mathbb{R}$ calculus [5].

Example 2.1. As a result from the relationship outlined above, let us assume that z and z^* are independent, then the following relations are straightforward:

$$\frac{\partial z}{\partial z} = \frac{1}{2} \left(\frac{\partial(x + jy)}{\partial x} - j \frac{\partial(x + jy)}{\partial y} \right) = \frac{1}{2} \left(\frac{\partial x}{\partial x} + j \underbrace{\frac{\partial y}{\partial x}}_{=0} - j \underbrace{\frac{\partial x}{\partial y}}_{=0} + \frac{\partial y}{\partial y} \right) = 1, \quad (25)$$

$$\frac{\partial z^*}{\partial z^*} = \frac{1}{2} \left(\frac{\partial(x - jy)}{\partial x} + j \frac{\partial(x - jy)}{\partial y} \right) = \frac{1}{2} \left(\frac{\partial x}{\partial x} - j \underbrace{\frac{\partial y}{\partial x}}_{=0} + j \underbrace{\frac{\partial x}{\partial y}}_{=0} + \frac{\partial y}{\partial y} \right) = 1, \quad (26)$$

$$\frac{\partial z}{\partial z^*} = \frac{1}{2} \left(\frac{\partial(x + jy)}{\partial x} + j \frac{\partial(x + jy)}{\partial y} \right) = \frac{1}{2} \left(\frac{\partial x}{\partial x} + j \underbrace{\frac{\partial y}{\partial x}}_{=0} + j \underbrace{\frac{\partial x}{\partial y}}_{=0} - \frac{\partial y}{\partial y} \right) = 0, \quad (27)$$

$$\frac{\partial z^*}{\partial z} = \frac{1}{2} \left(\frac{\partial(x - jy)}{\partial x} - j \frac{\partial(x - jy)}{\partial y} \right) = \frac{1}{2} \left(\frac{\partial x}{\partial x} - j \underbrace{\frac{\partial y}{\partial x}}_{=0} - j \underbrace{\frac{\partial x}{\partial y}}_{=0} - \frac{\partial y}{\partial y} \right) = 0. \quad (28)$$

Based on the above relations, *Cauchy-Riemann equations in real domain* (3) can be reduced into a single condition in *complex domain*. That illustrates the elegance of $\mathbb{C}\mathbb{R}$ Calculus as follows.

Theorem 3. (*Cauchy-Riemann equations under Wirtinger calculus*): Let $f(z)$ be a scalar function of complex variable z . Then, f is holomorphic (complex analytic in z) if, and only if, it does not depend on the conjugate variable z^* . That is:

$$\frac{\partial f}{\partial z^*} = 0. \quad (29)$$

Consequently, the \mathbb{R} derivative of a function, $\frac{\partial f}{\partial z}$, is identical to the complex classical derivative $f'(z)$ as defined in (1), when $f(z, z^*)$ does not depend on z^* .

$$f(z) \text{ is holomorphic} \Leftrightarrow \frac{\partial f}{\partial z^*} = 0. \Leftrightarrow \frac{\partial f}{\partial z} = f'(z). \quad (30)$$

Proof. Simply applying *Cauchy-Riemann equations* (3) on condition (29), we can see that

$$\begin{aligned} \frac{\partial f}{\partial z^*} &= \frac{1}{2} \left(\frac{\partial f}{\partial x} + j \frac{\partial f}{\partial y} \right) = \frac{1}{2} \left(\frac{\partial(u+jv)}{\partial x} + j \frac{\partial(u+jv)}{\partial y} \right) \\ &= \frac{1}{2} \left(\left(\frac{\partial u}{\partial x} - \frac{\partial v}{\partial y} \right) + j \left(\frac{\partial v}{\partial x} + \frac{\partial u}{\partial y} \right) \right) = 0. \end{aligned} \quad (31)$$

In order to proof (30) just substitutes (29) in (24). ■

Example 2.2. Now, consider the special case when the scalar-valued function is

$$f(c) = f(z, z^*) = z^* z = |z|^2 = x^2 + y^2$$

then,

$$\begin{aligned} \frac{\partial f(c)}{\partial z} &= \frac{1}{2} \left(\frac{\partial(x^2+y^2)}{\partial x} - j \frac{\partial(x^2+y^2)}{\partial y} \right) = (x - j y) = z^*, \\ \frac{\partial f(c)}{\partial z^*} &= \frac{1}{2} \left(\frac{\partial(x^2+y^2)}{\partial x} + j \frac{\partial(x^2+y^2)}{\partial y} \right) = (x + j y) = z. \end{aligned}$$

which shows us that z^* is formally considered as a constant when derived with respect to z and vice versa. But, this is a classical example that lies on the set of only *real holomorphic functions* (*Theorem 2*).

Although many important functions are holomorphic, including the functions z^n , e^z , $\ln(z)$, $\sin(z)$, and $\cos(z)$, and hence differentiable in the standard complex variables sense, there are commonly encountered useful functions which are not. For instance, the functions: $f(z) = z^*$; $f(z) = \text{Re}(z) = \frac{z+z^*}{2} = x$ and $g(z) = \text{Im}(z) = \frac{z-z^*}{2j} = y$; $f(z) = |z|^2 = z^* z = x^2 + y^2$, among others, fail to satisfy the Cauchy-Riemann condition, therefore, all of them are not harmonic.

Fortunately, all of the real-valued *non-holomorphic* functions shown above can be viewed as functions of both z and its complex conjugate z^* , as this simple fact is of significance to overcome this apparent difficulty.

2.1.5 Optimization with Complex Variables

In this section one starts to apply the concepts defined above and specially focused now on the multivariate case with real-valued scalar functions of complex multivariate variables. Indeed, the model for the cost function is:

$$f(\underline{\mathbf{Z}}) : \mathbb{C}^n \rightarrow \mathbb{R}, \quad (32)$$

where

$$\underline{\mathbf{Z}} = \begin{bmatrix} z_1 \\ \vdots \\ z_n \end{bmatrix} \in \mathbb{C}^n. \quad (33)$$

2.1.6 The Co-gradient and Conjugate Co-gradient Operators

Definition 2.1.3. Let f be a real-valued function whose independent variable is a complex vector $\underline{\mathbf{Z}}$, as defined in (32). Then, the co-gradient (\mathbb{R} gradient) and conjugate cogradient (\mathbb{R}^* gradient) are defined as in (Kreutz–Delgado, 2006) [5]:

$$\nabla_{\underline{\mathbf{Z}}} f(\underline{\mathbf{Z}}) = \left[\frac{\partial f}{\partial z_i} \right]_i \in \mathbb{C}^n, \quad (34)$$

$$\nabla_{\underline{\mathbf{Z}}^*} f(\underline{\mathbf{Z}}) = \left[\frac{\partial f}{\partial z_i^*} \right]_i \in \mathbb{C}^n. \quad (35)$$

which in expanded form becomes:

$$\nabla_{\underline{\mathbf{Z}}} f(\underline{\mathbf{Z}}) = \frac{1}{2} \begin{bmatrix} \frac{\partial}{\partial x_1} - j \frac{\partial}{\partial y_1} \\ \vdots \\ \frac{\partial}{\partial x_n} - j \frac{\partial}{\partial y_n} \end{bmatrix}, \quad (36)$$

and

$$\nabla_{\underline{\mathbf{Z}}^*} f(\underline{\mathbf{Z}}) = \frac{1}{2} \begin{bmatrix} \frac{\partial}{\partial x_1} + j \frac{\partial}{\partial y_1} \\ \vdots \\ \frac{\partial}{\partial x_n} + j \frac{\partial}{\partial y_n} \end{bmatrix}. \quad (37)$$

The relations of these operators with respect to the gradients of the *real* and *imaginary* parts are extensions of the Wirtinger derivatives (17) and (18):

$$\nabla_{\underline{\mathbf{Z}}} f(\underline{\mathbf{Z}}) = \frac{1}{2} (\nabla_{\mathbf{X}} - j \nabla_{\mathbf{Y}}), \quad (38)$$

$$\nabla_{\underline{\mathbf{Z}}^*} f(\underline{\mathbf{Z}}) = \frac{1}{2} (\nabla_{\mathbf{X}} + j \nabla_{\mathbf{Y}}). \quad (39)$$

Example 2.3. : Consider the real-valued function of a complex vector $\underline{\mathbf{Z}}$ as

$$f(\mathbf{c}) = f(\underline{\mathbf{Z}}, \underline{\mathbf{Z}}^*) = \underline{\mathbf{Z}}^H \underline{\mathbf{Z}} = z_1 z_1^* + z_2 z_2^*.$$

For this function one can readily determine the *co-gradient* and *conjugate co-gradient* operators which are:

$$\nabla_{\underline{\mathbf{Z}}} f(\underline{\mathbf{Z}}) = \begin{bmatrix} z_1^* \\ z_2^* \end{bmatrix} = \underline{\mathbf{Z}}^*, \quad (40)$$

$$\nabla_{\underline{\mathbf{Z}}^*} f(\underline{\mathbf{Z}}) = \begin{bmatrix} z_1 \\ z_2 \end{bmatrix} = \underline{\mathbf{Z}}. \quad (41)$$

It is straightforward to see that *Cauchy-Riemann equations*, *holomorphic conditions*, *rules of complex derivation*, and the rest of the concepts presented in the previous sections, are naturally extended to the multivariate case. For instance, the Cauchy-Riemann condition for f to be *holomorphic* in the multivariate case is:

$$\nabla_{\underline{\mathbf{Z}}^*} f(\underline{\mathbf{Z}}) = \mathbf{0} \in \mathbb{C}^n. \quad (42)$$

Stationary Points - The function f can have an arbitrary shape, but as a function of a complex vector, it can be seen as a group of mountains in a multidimensional space. This landscape has *valleys* and *peaks*, corresponding to *local maxima* and *minima* of the real-valued function. These points are called *extreme points* or *stationary points*, and they share a nice property: the \mathbb{R} and \mathbb{R}^* gradients of the cost function vanish at them [11].

Let f be a real-valued function as defined in (32). Then, the following two conditions are, each one, necessary and sufficient in order to optimize f with respect to a complex vector $\underline{\mathbf{Z}}$. At the extreme point $\underline{\mathbf{Z}}_e = \underline{\mathbf{Z}}$, it holds:

$$\nabla_{\underline{\mathbf{Z}}} f(\underline{\mathbf{Z}})|_{\underline{\mathbf{Z}}=\underline{\mathbf{Z}}_e} = \mathbf{0}, \quad (43)$$

$$\nabla_{\underline{\mathbf{Z}}^*} f(\underline{\mathbf{Z}})|_{\underline{\mathbf{Z}}=\underline{\mathbf{Z}}_e} = \mathbf{0}. \quad (44)$$

Proof. This result is just a multidimensional extension to the well-known result for scalar complex variables, where the extreme points of a function f defined as $f(z) : \mathbb{C} \rightarrow \mathbb{R}$, are found when:

$$\left. \frac{\partial f(z)}{\partial z} \right|_{z=z_e} = 0, \quad (45)$$

$$\left. \frac{\partial f(z)}{\partial z^*} \right|_{z=z_e} = 0. \quad (46)$$

■

Any algorithm that optimizes the cost function f should reach one of these extreme points, where the criterion represented by the function is *maximized*, *minimized*, or reaches an *inflexion point*.

While one changes the vector $\underline{\mathbf{Z}}$, in fact it is changing the real value of the cost function f . For each $\underline{\mathbf{Z}}$, the value of f is determined, but in general, the reverse does not always hold, so f is not an *injective function*.

This means that one can move freely the vector in any direction, as one were walking on the mountains, and watch for the effects on the objective function (that would be the height over the multidimensional surface).

An interesting question is: *which direction is the one that achieves the maximum rate of change?* If it is on the slopes of a valley, that direction leads us directly to the local minimum.

The Direction of Maximum Rate of Change - To answer that question, one looks at how a small change on the vector variable is translated to the value of the cost function. The main result of this section is stated in the following theorem:

Let $f(\underline{\mathbf{Z}}) : \mathbb{C}^n \rightarrow \mathbb{R}$ be a real-valued function of complex multivariate variable. Then, the direction of maximum rate of change is given by

$$\nabla_{\underline{\mathbf{Z}}^*} f(\underline{\mathbf{Z}}) = \mathbf{0}. \quad (47)$$

And thus, moving $\underline{\mathbf{Z}}$ in the same direction of (47), the cost function f is *maximized*. On the other hand, moving in the opposite direction, e.g., $-\nabla_{\underline{\mathbf{Z}}^*} f(\underline{\mathbf{Z}})$, the cost function f is *minimized*.

Proof. Using the differential rule (13) for vectors, yields to

$$df = (\nabla_{\underline{\mathbf{Z}}} f(\underline{\mathbf{Z}}))^T d\underline{\mathbf{Z}} + (\nabla_{\underline{\mathbf{Z}}^*} f(\underline{\mathbf{Z}}))^T d\underline{\mathbf{Z}}^* \in \mathbb{R}. \quad (48)$$

Identifying the expression $\nabla_{\mathbf{X}} = \frac{1}{2}(\nabla_{\underline{\mathbf{Z}}} + \nabla_{\underline{\mathbf{Z}}^*})$ of the real part of a complex vector:

$$df = 2 \times \text{Re} \left\{ (\nabla_{\underline{\mathbf{Z}}} f(\underline{\mathbf{Z}}))^T d\underline{\mathbf{Z}} \right\}. \quad (49)$$

Using the multivariate equivalent of property (12) for real-valued functions, (49) becomes:

$$df = 2 \times \text{Re} \left\{ (\nabla_{\underline{\mathbf{Z}}^*} f(\underline{\mathbf{Z}}))^H d\underline{\mathbf{Z}} \right\} = 2 \times \langle \nabla_{\underline{\mathbf{Z}}^*} f(\underline{\mathbf{Z}}), d\underline{\mathbf{Z}} \rangle. \quad (50)$$

This expression is proportional to the scalar product of two complex-valued vectors, $\nabla_{\underline{\mathbf{Z}}^*} f(\underline{\mathbf{Z}})$ and $d\underline{\mathbf{Z}}$. *From basic geometry, one knows that the scalar product $(\langle \cdot, \cdot \rangle)$ is maximized when the two vectors has the same direction, and minimized when they have opposite directions.* In general, one is interested on minimizing the cost functions, because they usually represent an *undesirable quality* or an *error* of the system. ■

Another interesting situation occurs when vectors $\nabla_{\underline{\mathbf{Z}}^*} f(\underline{\mathbf{Z}})$ and $d\underline{\mathbf{Z}}$ are orthogonal. The scalar product of two orthogonal vector is null. One can interpret this fact as if the rate of change df vanishes, so the cost function does not change. It is interesting to see that, obviously, the *isobars* of

the cost functions are defined by this situation. In fact, the locus of points orthogonal to the vector $\nabla_{\mathbf{z}^*} f(\mathbf{z})$ locally define the points where the cost function f takes the same value. The following example is a practical aid to better understand this issue.

Example 2.4. Consider the scalar-valued function given by

$$f(c) = f(z, z^*) = z^*z = |z|^2 = x^2 + y^2, \quad (51)$$

which is the squared Euclidean distance to the origin. Assuming that z and z^* are independent, the formal derivatives \mathbb{R} and \mathbb{R}^* of this function are expressed as

$$\frac{\partial f(c)}{\partial z} = \frac{1}{2} \left(\frac{\partial (x^2 + y^2)}{\partial x} - \frac{\partial (x^2 + y^2)}{\partial y} \right) = (x - jy) = z^*, \quad (52)$$

$$\frac{\partial f(c)}{\partial z^*} = \frac{1}{2} \left(\frac{\partial (x^2 + y^2)}{\partial x} + \frac{\partial (x^2 + y^2)}{\partial y} \right) = (x + jy) = z. \quad (53)$$

Fig. (2.1) displays on the complex plane the *level curves* of the scalar real function of complex scalar variables given by (51) [11]. The two derivatives are represented by an arrow marking the directions of change for derivatives. In this case, they are mutually orthogonal, but this is not a general property.

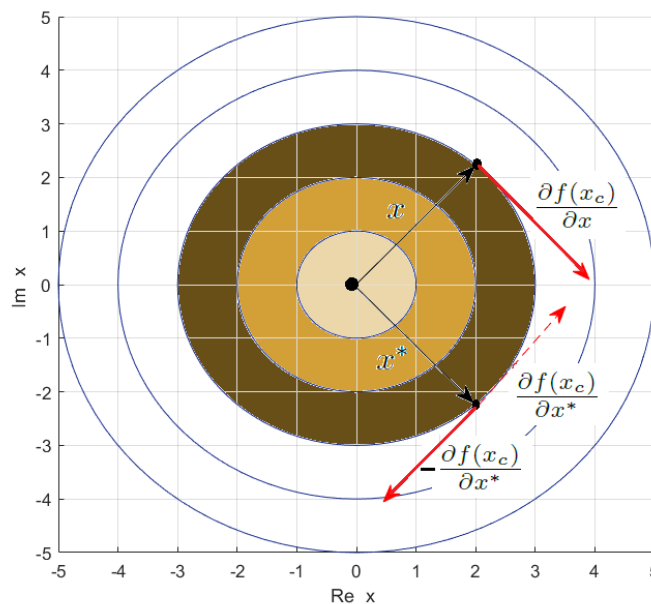


Figure 2.1: Contour Plot of the Scalar Real Function of Complex Scalar Variables.

Moreover, its analysis allow us to infer that the direction of maximum rate of change of the objective function is given by the conjugate gradient defined as $-\frac{\partial f}{\partial z^*}$. Observe that its positive direction is referred to a maximization problem whereas the opposite direction concerns to the cost function minimization.

Therefore, the vector

$$-\frac{\partial f}{\partial z^*}, \quad (54)$$

represents the direction of *maximum descent*, and the orthogonal direction represents the direction of no local change.

Note that the same reasoning cannot be applied the gradient, i.e., $\frac{\partial f}{\partial z}$. Looking at (49), it is easy to see that it does not represent an scalar product, so it does not gives any insight about the geometry of the gradient of the cost function.

2.1.7 The Complex Jacobian Matrix

Let $f(c) = f(z, z^*) \in \mathbb{C}^m$ be a mapping

$$f := \mathbb{C}^n \rightarrow \mathbb{C}^m$$

The generalization of (13) yields the *vector form of differential rule*³,

$$df(c) = \frac{\partial f(c)}{\partial c} dc = \frac{\partial f(c)}{\partial z} dz + \frac{\partial f(c)}{\partial z^*} dz^* \quad (55)$$

where the $m \times n$ matrix $\frac{\partial f}{\partial z}$ is called the *Jacobian*, or *Jacobian Matrix*, of the mapping f , and the $m \times n$ matrix $\frac{\partial f}{\partial z^*}$ the *conjugate Jacobian* of f . The Jacobian of f is often denoted by \mathbf{J}_f and is computed by applying the *co-gradient operator* component-wise to f ,

$$\mathbf{J}_f(c) = \frac{\partial f(c)}{\partial z} = \begin{pmatrix} \frac{\partial f_1(c)}{\partial z} \\ \vdots \\ \frac{\partial f_m(c)}{\partial z} \end{pmatrix} = \begin{pmatrix} \frac{\partial f_1(c)}{\partial z_1} & \cdots & \frac{\partial f_1(c)}{\partial z_n} \\ \vdots & \ddots & \vdots \\ \frac{\partial f_m(c)}{\partial z_1} & \cdots & \frac{\partial f_m(c)}{\partial z_n} \end{pmatrix} \in \mathbb{C}^{m \times n}, \quad (56)$$

and similarly the conjugate Jacobian, denoted by \mathbf{J}_f^* is computed by applying the *conjugate co-gradient operator* component-wise to f ,

$$\mathbf{J}_f^c(c) = \frac{\partial f(c)}{\partial z^*} = \begin{pmatrix} \frac{\partial f_1(c)}{\partial z^*} \\ \vdots \\ \frac{\partial f_m(c)}{\partial z^*} \end{pmatrix} = \begin{pmatrix} \frac{\partial f_1(c)}{\partial z_1^*} & \cdots & \frac{\partial f_1(c)}{\partial z_n^*} \\ \vdots & \ddots & \vdots \\ \frac{\partial f_m(c)}{\partial z_1^*} & \cdots & \frac{\partial f_m(c)}{\partial z_n^*} \end{pmatrix} \in \mathbb{C}^{m \times n}. \quad (57)$$

With the above notation one can write the *differential rule* in (55) as

$$df(c) = \mathbf{J}_f(c) dz + \mathbf{J}_f^c(c) dz^*. \quad (58)$$

that when under the properties (11) and (12) component-wise to f , yields to the following identities:

$$\frac{\partial f^*(c)}{\partial z^*} = \left(\frac{\partial f(c)}{\partial z} \right)^* = (\mathbf{J}_f(c))^* \quad \text{and} \quad \frac{\partial f^*(c)}{\partial z} = \left(\frac{\partial f(c)}{\partial z^*} \right)^* = (\mathbf{J}_f^c(c))^* \quad (59)$$

Note from (59) that,

$$(\mathbf{J}_f(c))^* = \left(\frac{\partial f(c)}{\partial z} \right)^* = \frac{\partial f^*(c)}{\partial z^*} \neq \mathbf{J}_f^c(c) = \frac{\partial f(c)}{\partial z^*}. \quad (60)$$

³At this point, the expression $\frac{\partial f(c)}{\partial c} dc$ only has meaning as a shorthand expression for $\frac{\partial f}{\partial z} dz + \frac{\partial f}{\partial z^*} dz^*$, each term of which must be interpreted formally as z and z^* cannot be varied independently of each other.

Nonetheless, *in the important special case that $f(c)$ is real-valued* (in which case $f^*(c) = f(c)$) one have

$$f(c) \in \mathbb{R}^m \Rightarrow (\underline{\mathbf{J}}_f(c))^* = \frac{(\partial f(c))^*}{\partial z} = \frac{\partial f(c)}{\partial z^*} = \underline{\mathbf{J}}_f^c(c). \quad (61)$$

With (58), equation (61) yields to the following important fact which holds for real-valued functions of complex variables $f(c)$ ⁴,

$$\begin{aligned} f(c) \in \mathbb{R}^m \Rightarrow df(c) &= \underline{\mathbf{J}}_f(c) dz + (\underline{\mathbf{J}}_f(c) dz)^* \\ &= 2 \times Re \{ \underline{\mathbf{J}}_f(c) dz \} = 2 \times Re \{ \underline{\mathbf{J}}_f^c(c) dz^* \}. \end{aligned} \quad (62)$$

In other words, for *holomorphic functions* $\underline{\mathbf{J}}^* \neq \underline{\mathbf{J}}^c$, whereas for real functions of complex variable, i.e., *non-holomorphic functions*, the following equality holds: $\underline{\mathbf{J}}^* = \underline{\mathbf{J}}^c$.

Finally, the *complex* derivatives showed above allow us to claim that they are often described by more elegant expressions than their *real* counterparts.

2.2 Framework for $\mathbb{C}\mathbb{R}$ – Calculus

2.2.1 Hermitian conjugate matrix

Also, the following definition will be required hereafter: Let $z \in \mathbb{C}^m$; then $\overset{\mathbb{R}}{z} \triangleq (Re\{z\}, Im\{z\}) \in \mathbb{R}$, $\overset{\mathbb{C}}{z} \triangleq (z, z^*) \in \mathbb{C}$ and $\overset{\mathbb{C}^*}{z} \triangleq (z^*, z) = \overset{\mathbb{C}}{z} \in \mathbb{C}$. Furthermore the linear map

$$J \triangleq \begin{bmatrix} I_n & j I_n \\ I_n & -j I_n \end{bmatrix} \quad (63)$$

which is a *isomorphism* from \mathbb{R} to \mathbb{C} and its inverse is given by $J^{-1} = \frac{1}{2}J^H$, this latter defined as *Hermitian conjugate* matrix. While I_n is the identity matrix of n order.

Example 2.5. : Taking into account the above definition, i.e.,

$$\begin{aligned} J &= \begin{bmatrix} 1 & +j \\ 1 & -j \end{bmatrix} \rightarrow J^{-1} = \frac{1}{2}J^H = \frac{1}{2}(J^*)^T = \frac{1}{2} \left(\begin{bmatrix} 1 & +j \\ 1 & -j \end{bmatrix}^* \right)^T = \\ &= \frac{1}{2} \begin{bmatrix} 1 & -j \\ 1 & +j \end{bmatrix}^T = \frac{1}{2} \begin{bmatrix} 1 & 1 \\ -j & +j \end{bmatrix} \therefore J^H = \begin{bmatrix} 1 & 1 \\ -j & +j \end{bmatrix} \triangleq \begin{matrix} \textit{Hermitian} \\ \textit{conjugate} \\ \textit{matrix} \end{matrix} \end{aligned}$$

2.2.2 SWAP operator

Additionally, it is advised to define a *swap* operator as

$$S \triangleq \begin{bmatrix} 0 & I_n \\ I_n & 0 \end{bmatrix} \quad (64)$$

which is a *isomorphism* from \mathbb{C} to the *dual space* \mathbb{C}^* which obeys the properties

$$S^{-1} = S^T = S, \quad (65)$$

⁴The real part of a vector (or matrix) is the vector (or matrix) of the real parts. Note that the mapping $dz \rightarrow df(c)$ is not linear.

showing that S is symmetric and its own inverse, $S^2 = I$.

In fact the *swap* operator is a block permutation matrix which permutes blocks of rows or blocks of columns depending on whether S pre-multiplies or post-multiplies a matrix, respectively.

Example 2.6. : Now considering the operator defined above, i.e.,

$S = \begin{bmatrix} 0 & 1 \\ 1 & 0 \end{bmatrix} \rightarrow S^{-1} = S^T = S = \begin{bmatrix} 0 & 1 \\ 1 & 0 \end{bmatrix}$, for $n = 1$, and let a $2n \times 2n$ matrix A be block partitioned as

$$A = \begin{pmatrix} A_{11} & A_{12} \\ A_{21} & A_{22} \end{pmatrix}.$$

then pre-multiplication by S results in a block swap of the top n rows *en masse* with the bottom n rows,

$$SA = \begin{pmatrix} A_{21} & A_{22} \\ A_{11} & A_{12} \end{pmatrix}.$$

Alternatively, post-multiplication by S results in a block swap of the first n columns with the last n columns,

$$AS = \begin{pmatrix} A_{12} & A_{11} \\ A_{22} & A_{21} \end{pmatrix}.$$

It is also useful to note the result of a "sandwiching" by S ,

$$SAS = \begin{pmatrix} A_{22} & A_{21} \\ A_{12} & A_{11} \end{pmatrix}.$$

Additionally, it is straightforward to show that

$$I = \frac{1}{2} J^T S J \tag{66}$$

for J given by (63).

2.2.3 Mapping variables from \mathbb{R} towards \mathbb{C} domain

Now the linear map in (63) also defines one-to-one correspondence between the *real* gradient $\frac{\partial}{\partial \mathbb{R}}$ and *complex* gradient $\frac{\partial}{\partial \mathbb{C}}$, namely,

$$\frac{\partial}{\partial \mathbb{R}} = J^T \frac{\partial}{\partial \mathbb{C}}. \tag{67}$$

Similarly, the *real* Hessian $\frac{\partial^2}{\partial \mathbb{R} \partial \mathbb{R}^T}$ can be transformed into several *complex* Hessian matrices, two of which are

$$\frac{\partial^2}{\partial \mathbb{R} \partial \mathbb{R}^T} = \frac{\partial}{\partial \mathbb{R}} \left(\frac{\partial}{\partial \mathbb{R}} \right)^T = J^T \frac{\partial}{\partial \mathbb{C}} \left(\frac{\partial}{\partial \mathbb{C}^T} J \right) = J^T \frac{\partial^2}{\partial \mathbb{C} \partial \mathbb{C}^T} J, \tag{68}$$

$$\frac{\partial^2}{\partial z^{\mathbb{R}} \partial z^{\mathbb{R}T}} = \frac{\partial}{\partial z^{\mathbb{R}}} \left(\frac{\partial}{\partial z^{\mathbb{R}}} \right)^T = J^H \frac{\partial}{\partial z^{\mathbb{C}}} \left(\frac{\partial}{\partial z^{\mathbb{C}T}} J \right) = J^H \frac{\partial^2}{\partial z^{\mathbb{C}} \partial z^{\mathbb{C}T}} J. \quad (69)$$

Notice that the complex Hessian matrix derived above is function of J^T in (68) while of J^H , *i.e.*, *Hermitian* conjugate matrix, in (69).

2.2.4 Mapping variables from \mathbb{C} towards \mathbb{C} domain

Consider a matrix $M \in \mathbb{C}^{2n \times 2n}$ has the property that it is a linear mapping from C to C , such that one can state

$$M \in (C, C) = \{M \mid Mc \in C, \forall c \in C \text{ and } M \text{ is linear}\} \subset (\mathbb{C}^{2n}, \mathbb{C}^{2n}) = \mathbb{C}^{2n \times 2n} \quad (70)$$

where (C, C) is a *real* vector space of linear operators, while $(\mathbb{C}^{2n}, \mathbb{C}^{2n})$ is a *complex* vector space of linear operators. Both are vector spaces over *different fields*, they cannot have a vector-subspace/vector-parent-space relationship to each other. Note that $(C, C) \subset (\mathbb{C}^{2n}, \mathbb{C}^{2n})$ is just the statement that any matrix which maps from $C \subset \mathbb{C}^{2n}$ to $C \subset \mathbb{C}^{2n}$ is also a linear mapping from \mathbb{C}^{2n} to \mathbb{C}^{2n} .

In order to determine the *necessary* and *sufficient* conditions for a matrix $M \in \mathbb{C}^{2n \times 2n}$ to be an element of (C, C) suppose that the vector $c = \text{col}(z, z^*) \in C$ always maps to a vector $s = \text{col}(\xi, \bar{\xi}) \in C$ under the action of M , *e.g.*, $s = Mc$. This relationship when expressed in block matrix is

$$\begin{pmatrix} \xi \\ \bar{\xi} \end{pmatrix} = \begin{bmatrix} M_{11} & M_{12} \\ M_{21} & M_{22} \end{bmatrix} \begin{pmatrix} z \\ z^* \end{pmatrix}. \quad (71)$$

The first block row of this matrix equation yields the conditions

$$\xi = M_{11}z + M_{12}z^*,$$

while the complex conjugate of the second block row yields

$$\xi = M_{21}^*z^* + M_{22}^*z,$$

and subtracting these two sets of equations results in the following condition on the block elements of M ,

$$(M_{11} - M_{22}^*)z - (M_{12} - M_{21}^*)z^* = 0.$$

With $z = (x + jy)$, the equality stated above can be spitted into two sets of conditions as

$$[(M_{11} - M_{22}^*) + (M_{12} - M_{21}^*)]x = 0$$

and

$$[(M_{11} - M_{22}^*) - (M_{12} - M_{21}^*)]y = 0.$$

Since these equations must hold for any x and y , they are equivalent to

$$(M_{11} - M_{22}^*) + (M_{12} - M_{21}^*) = 0$$

and

$$(M_{11} - M_{22}^*) - (M_{12} - M_{21}^*) = 0.$$

Therefore, adding and subtracting these two equations yields the *necessary* and *sufficient* condition for M to be admissible (i.e., to act as a linear mapping from C to C),

$$M = \begin{bmatrix} M_{11} & M_{12} \\ M_{21} & M_{22} \end{bmatrix} \in \mathbb{C}^{2n \times 2n} \text{ is an element of } (C, C) \text{ iff } M_{11} = M_{22}^* \text{ and } M_{12} = M_{21}^*. \quad (72)$$

The *necessary* and *sufficient* admissibility condition (72) is better expressed in the following equivalent form

$$M \in (C, C) \iff M = SM^*S \iff M = SMS \quad (73)$$

which is straightforward to verify.

Given an arbitrary matrix $M \in \mathbb{C}^{2n \times 2n}$, we can define a natural mapping of M into $(C, C) \subset \mathbb{C}^{2n \times 2n}$ by

$$P(M) \triangleq \frac{M + SM^*S}{2} \in (C, C), \quad (74)$$

in which case the admissibility condition (73) has an equivalent restatement as

$$M \in (C, C) \iff P(M) = M. \quad (75)$$

Finally, it is also straightforward to demonstrate that

$$\forall M \in \mathbb{C}^{2n \times 2n}, P(P(M)) = P(M). \quad (76)$$

I.e., P is an idempotent mapping of $\mathbb{C}^{2n \times 2n}$ onto (C, C) , $P^2 = P$.

2.3 Partial Conclusions

In this section the Wirtinger derivatives is derived and it is showed how easy becomes up to now to operate any application in conjugate coordinates. It is shown that holomorphic functions are in fact a subset of functions of complex variables that does not depend upon their corresponding complex conjugate variables. Consequently, the Wirtinger derivatives is a general operator that allows us to expand any nonlinear function in Taylor's serie, i.e., whichever they are holomorphic or non-holomorphic, aiming the derivation of classical algorithms usually applied to power systems problems, as Newton-Raphson and Gauss-Newton, to cite a few.

3 Complex-Valued Power Flow Analysis (CV-PFA)

Numerical solutions for solving power system application are typically carried out in the real domain. Examples are power flow analysis and power system state estimation, among others. It turns out that these solutions are not well suited for modeling voltage and current phasor, which were introduced by Steinmetz [1,12]. To circumvent this difficulty, iterative and non-iterative algorithms carried out in the complex domain were proposed recently in the literature; applications in power transmission and distributions systems are described in [13], [14], [15] for iterative methods and [16], [17] [18] for non-iterative methods. Iterative complex-valued power flow calculation is addressed by Wang [16] by using the Wirtinger calculus [3], [2]. On the other hand, [15] makes use of the method proposed by Brandwood [19]. However, both approach does not use any Wirtinger derivatives. Instead, they use nodal network equations to derive a first- or second-order Newton-Raphson algorithm. Furthermore, in order to add numerical robustness, a fourth-order Levenberg-Marquardt algorithm is employed to the CV_PFA approach because of its nice bi-quadratic convergence property, instead of the well-known quadratic convergence property of the classical Newton-Raphson. Recall that this algorithm is prone to collapse when the power system network is ill-conditioned, i.e., it is heavily loaded or presents branches with high R/X ratio.

In this section is presented the derivation of a complex-valued power flow (CV-PFA) derived straightforwardly from Wirtinger's Work [3], in contrast to the approach brought by [13], [14]. Firstly, the whole power flow modeling starts based on the classical nodal equation as presented in [20]. In the second approach the analytical model is derived through the general power flow equations. The main reason for this latter option is the transformer model with tap position off-nominal, including phase-shifters [21], [22]. Further discussions on this issue are addressed throughout the derivation of the approaches.

3.1 Nodal Equation

This approach requires the Nodal Admittance matrix building, e.g.,

$$\underline{I} = \mathbf{Y}_{\text{bus}} \underline{V}, \quad (77)$$

thus the complex nodal power can be expressed as

$$\underline{S} = \text{diag}(\underline{V}) \underline{I}^*, \quad (78)$$

or

$$\underline{S} = \text{diag}(\underline{V}) \mathbf{Y}_{\text{bus}}^* \underline{V}^*. \quad (79)$$

Then, the nodal complex power at $bus - k$, i.e., S_k , is

$$S_k = V_k Y_{kk}^* V_k^* + V_k \sum_{\substack{m=0 \\ m \neq k}}^N Y_{km}^* V_m^*, \quad (80)$$

where $N + 1$ is the number of network nodes, and the node 0 is assigned as the *slack node*.

3.2 Complex-Valued Power Flow Equations

The complex-valued power flow equations that model any type of branch in an electrical network, i.e., transmission lines and phase- and phase-shifting-transformers are as follows:

$$S_{km} = V_k \left(\frac{y_{km}^*}{a_{km} a_{km}^*} - j b_{km}^{sh} \right) V_k^* - V_k \frac{y_{km}^*}{a_{km}} V_m^*, \quad (81)$$

$$S_{mk} = V_m \left(y_{km}^* - j b_{km}^{sh} \right) V_m^* - V_m \frac{y_{km}^*}{a_{km}^*} V_k^*. \quad (82)$$

and

$$S_{km}^* = V_k^* \left(\frac{y_{km}}{a_{km}^* a_{km}} + j b_{km}^{sh} \right) V_k - V_k^* \frac{y_{km}}{a_{km}^*} V_m, \quad (83)$$

$$S_{mk}^* = V_m^* \left(y_{km} + j b_{km}^{sh} \right) V_m - V_m^* \frac{y_{km}}{a_{km}} V_k. \quad (84)$$

In the set of equations (81-84), the general off-nominal tap transformer model is composed by an ideal transformer with complex turns ratio $a e^{j\phi} : 1$ in series with its admittance or impedance [21].

3.3 Wirtinger Derivatives Applied to the Power Flow Equations

Firstly, let us assume that the complex power injections, S_k and S_m , are equal to the power flows S_{km} and S_{mk} , respectively. Then, applying the Wirtinger calculus to the complex power flow equation given by (81) yields

$$\left. \frac{\partial S_k}{\partial V_k} \right|_{V_k^* = Const} = \left(\frac{y_{km}^*}{a_{km} a_{km}^*} - j b_{km}^{sh} \right) V_k^* - \frac{y_{km}^*}{a_{km}} V_m^*, \quad (85)$$

$$\left. \frac{\partial S_k}{\partial V_k^*} \right|_{V_k = Const} = V_k \left(\frac{y_{km}^*}{a_{km} a_{km}^*} - j b_{km}^{sh} \right), \quad (86)$$

$$\left. \frac{\partial S_k}{\partial V_m} \right|_{V_m^* = Const} = 0.0, \quad (87)$$

$$\left. \frac{\partial S_k}{\partial V_m^*} \right|_{V_m = Const} = -V_k \frac{y_{km}^*}{a_{km}}, \quad (88)$$

$$\left. \frac{\partial S_k}{\partial a_{km}} \right|_{a_{km}^* = Const} = -V_k \left(\frac{y_{km}^*}{a_{km}^2 a_{km}^*} \right) V_k^* + V_k \frac{y_{km}^*}{a_{km}^2} V_m^*, \quad (89)$$

$$\left. \frac{\partial S_k}{\partial a_{km}^*} \right|_{a_{km} = Const} = -V_k \left(\frac{y_{km}^*}{a_{km} (a_{km}^*)^2} \right) V_k^*. \quad (90)$$

and given by (82) yields

$$\left. \frac{\partial S_m}{\partial V_m} \right|_{V_m^* = \text{Const}} = \left(y_{km}^* - j b_{km}^{sh} \right) V_m^* - \frac{y_{km}^*}{a_{km}^*} V_k^*, \quad (91)$$

$$\left. \frac{\partial S_m}{\partial V_m^*} \right|_{V_m = \text{Const}} = V_m \left(y_{km}^* - j b_{km}^{sh} \right), \quad (92)$$

$$\left. \frac{\partial S_m}{\partial V_k} \right|_{V_k^* = \text{Const}} = 0.0, \quad (93)$$

$$\left. \frac{\partial S_m}{\partial V_k^*} \right|_{V_k = \text{Const}} = - V_m \frac{y_{km}^*}{a_{km}^*}, \quad (94)$$

$$\left. \frac{\partial S_m}{\partial a_{km}} \right|_{a_{km}^* = \text{Const}} = 0.0, \quad (95)$$

$$\left. \frac{\partial S_m}{\partial a_{km}^*} \right|_{a_{km} = \text{Const}} = V_m \frac{y_{km}^*}{(a_{km}^*)^2} V_k^*. \quad (96)$$

and given by (83) yields

$$\left. \frac{\partial S_k^*}{\partial V_k} \right|_{V_k^* = \text{Const}} = V_k^* \left(\frac{y_{km}}{a_{km}^* a_{km}} + j b_{km}^{sh} \right), \quad (97)$$

$$\left. \frac{\partial S_k^*}{\partial V_k^*} \right|_{V_k = \text{Const}} = \left(\frac{y_{km}}{a_{km}^* a_{km}} + j b_{km}^{sh} \right) V_k - \frac{y_{km}}{a_{km}^*} V_m, \quad (98)$$

$$\left. \frac{\partial S_k^*}{\partial V_m} \right|_{V_m^* = \text{Const}} = - V_k^* \frac{y_{km}}{a_{km}^*}, \quad (99)$$

$$\left. \frac{\partial S_k^*}{\partial V_m^*} \right|_{V_m = \text{Const}} = 0.0, \quad (100)$$

$$\left. \frac{\partial S_k^*}{\partial a_{km}} \right|_{a_{km}^* = \text{Const}} = - V_k^* \left(\frac{y_{km}}{a_{km}^* a_{km}^2} \right) V_k, \quad (101)$$

$$\left. \frac{\partial S_k^*}{\partial a_{km}^*} \right|_{a_{km} = \text{Const}} = - V_k^* \left(\frac{y_{km}}{(a_{km}^*)^2 a_{km}} \right) V_k + V_k^* \frac{y_{km}}{(a_{km}^*)^2} V_m. \quad (102)$$

Finally, applying Wirtinger calculus to (84) yields

$$\left. \frac{\partial S_m^*}{\partial V_k} \right|_{V_k^* = \text{Const}} = - V_m^* \frac{y_{km}}{a_{km}}, \quad (103)$$

$$\left. \frac{\partial S_m^*}{\partial V_k^*} \right|_{V_k = \text{Const}} = 0.0, \quad (104)$$

$$\left. \frac{\partial S_m^*}{\partial V_m} \right|_{V_m^* = \text{Const}} = V_m^* \left(y_{km} + j b_{km}^{sh} \right), \quad (105)$$

$$\left. \frac{\partial S_m^*}{\partial V_m^*} \right|_{V_m = \text{Const}} = \left(y_{km} + j b_{km}^{sh} \right) V_m - \frac{y_{km}}{a_{km}} V_k, \quad (106)$$

$$\left. \frac{\partial S_m^*}{\partial a_{km}} \right|_{a_{km}^* = \text{Const}} = V_m^* \frac{y_{km}}{a_{km}^2} V_k, \quad (107)$$

$$\left. \frac{\partial S_m^*}{\partial a_{km}^*} \right|_{a_{km} = \text{Const}} = 0.0. \quad (108)$$

3.4 Bus Models in the Complex Domain

3.4.1 Slack-Bus Type

The complex voltage at a *slack*-bus type is known, once the magnitude and phase-angle values are specified for the reference bus.

3.4.2 PQ-Bus Type

With the active- and reactive-power demand specified for a *PQ* node, the following complex mismatches functions are expressed as

$$M_k = S_k - (P_{ks} + j Q_{ks}), \quad (109)$$

$$M_k^* = S_k^* - (P_{ks} - j Q_{ks}), \quad (110)$$

where P_{ks} and Q_{ks} , are the specified active- and reactive-power injection at node k , respectively.

In order to derive the Newton-Raphson algorithm in the complex domain, the Jacobian matrix elements in complex form corresponding to each *PQ* – *Bus* are formed based on the Wirtinger derivatives of M_k and M_k^* with respect to the complex and the complex conjugate nodal voltage magnitudes, yielding

$$\left. \frac{\partial M_k}{\partial V_k} \right|_{V_k^* = \text{Const}} = \sum_{m \in \Omega_i}^N \left. \frac{\partial S_k}{\partial V_k} \right|_{V_k^* = \text{Const}}, \quad (111)$$

$$\left. \frac{\partial M_k}{\partial V_k^*} \right|_{V_k = \text{Const}} = \sum_{m \in \Omega_i}^N \left. \frac{\partial S_k}{\partial V_k^*} \right|_{V_k = \text{Const}}, \quad (112)$$

$$\left. \frac{\partial M_k}{\partial V_m} \right|_{V_m^* = \text{Const}} = 0.0, \quad (113)$$

$$\left. \frac{\partial M_k}{\partial V_m^*} \right|_{V_m = \text{Const}} = \sum_{m \in \Omega_i}^N \left. \frac{\partial S_k}{\partial V_m^*} \right|_{V_m = \text{Const}}, \quad (114)$$

and

$$\left. \frac{\partial M_k^*}{\partial V_k} \right|_{V_k^* = \text{Const}} = \sum_{m \in \Omega_i}^N \left. \frac{\partial S_k^*}{\partial V_k} \right|_{V_k^* = \text{Const}}, \quad (115)$$

$$\left. \frac{\partial M_k^*}{\partial V_k^*} \right|_{V_k = \text{Const}} = \sum_{m \in \Omega_i}^N \left. \frac{\partial S_k^*}{\partial V_k^*} \right|_{V_k = \text{Const}}, \quad (116)$$

$$\left. \frac{\partial M_k^*}{\partial V_m} \right|_{V_m^* = \text{Const}} = \sum_{m \in \Omega_i}^N \left. \frac{\partial S_k^*}{\partial V_m} \right|_{V_m^* = \text{Const}}, \quad (117)$$

$$\left. \frac{\partial M_k^*}{\partial V_m^*} \right|_{V_m = \text{Const}} = 0.0. \quad (118)$$

Here Ω_i in (111-118) is the set of neighboring buses connected to the k^{th} – *bus* and N is the total number of buses. Moreover, in (113-114) and (117-118), $m \neq 0$ and $m \neq k$. We highlight that the *right hand side (rhs)* of (116) is the nodal complex current at node k while the *rhs* of (111) is the complex conjugate of the nodal current at node k .

3.4.3 PV-Bus Type

As the active-power generation and the terminal voltage magnitude at a *PV – bus* are both specified, i.e., P_{ks} and V_{ks} , respectively, the sum of M_k in (109) and M_k^* in (110) gives the complex residual function, M_{kg} , which is related to the active-power constraint as follows:

$$\begin{aligned} M_{kg} &= M_k + M_k^*, \\ &= S_k + S_k^* - 2 \times P_{ks}. \end{aligned} \quad (119)$$

The second complex residual function E_{kg} for a generator node k is formed, using the voltage magnitude constraint given by

$$|E_{kg}| = |V_k|^2 - |V_{ks}|^2, \quad (120)$$

where the $|V_{ks}|$ is the specified voltage magnitude at Node k .

As $|V_k|^2 = V_k V_k^*$, (120) can be expressed in the complex domain as

$$E_{kg} = V_k V_k^* - |V_{ks}|^2, \quad (121)$$

and the Jacobian matrix elements associated with a Generator node k are obtained by taking the partial derivatives of the complex residual functions in (119) and (121) with respect to V_k and V_k^* , yielding

$$\frac{\partial M_{kg}}{\partial V_k} \Big|_{V_k^*=Const} = \frac{\partial M_k}{\partial V_k} \Big|_{V_k^*=Const} + \frac{\partial M_k^*}{\partial V_k} \Big|_{V_k^*=Const}, \quad (122)$$

$$\frac{\partial M_{kg}}{\partial V_k^*} \Big|_{V_k=Const} = \frac{\partial M_k}{\partial V_k^*} \Big|_{V_k=Const} + \frac{\partial M_k^*}{\partial V_k^*} \Big|_{V_k=Const}, \quad (123)$$

$$\frac{\partial M_{kg}}{\partial V_m} \Big|_{V_m^*=Const} = \frac{\partial M_k}{\partial V_m} \Big|_{V_m^*=Const} + \frac{\partial M_k^*}{\partial V_m} \Big|_{V_m^*=Const}, \quad (124)$$

$$\frac{\partial M_{kg}}{\partial V_m^*} \Big|_{V_m=Const} = \frac{\partial M_k}{\partial V_m^*} \Big|_{V_m=Const} + \frac{\partial M_k^*}{\partial V_m^*} \Big|_{V_m=Const}, \quad (125)$$

where in (124-125), $m \neq 0$ and $m \neq k$. Moreover, note that the *rhs* of (122-125) are defined in (111-118). On the other hand, the partial derivatives of E_{kg} in (121) with respect to V_k and V_k^* are expressed as

$$\frac{\partial E_{kg}}{\partial V_k} \Big|_{V_k^*=Const} = V_k^*, \quad (126)$$

$$\frac{\partial E_{kg}}{\partial V_k^*} \Big|_{V_k=Const} = V_k, \quad (127)$$

and the partial derivaives with respect to V_m and V_m^* are given by

$$\frac{\partial E_{kg}}{\partial V_m} \Big|_{V_m^*=Const} = 0.0, \text{ for } m \neq 0 \text{ and } m \neq k, \quad (128)$$

$$\frac{\partial E_{kg}}{\partial V_m^*} \Big|_{V_m=Const} = 0.0, \text{ for } m \neq 0 \text{ and } m \neq k, \quad (129)$$

3.4.4 PQV-Bus Type

This type of bus is referred to model On-Load-Tap-Changer (*OLTC*), which can be a phase-transformer for local and nearby bus voltage regulation or a phase-shifting-transformer for controlling the active power flow transmitted over a line [23]. It is also suited to model a DC link of a voltage-sourced converter [24], [25]. As the active- and reactive-power demand are specified, the complex mismatches functions as stated in (109) and (110) are employed. Nonetheless, it is worth to recall that the *OLTC* tap position allows us to regulate the voltage magnitude at either k - or m -bus. Let us assume that the m -bus voltage is regulated, leading to the following mismatches functions:

$$M_m = a_{km} - a_{km}^* - 2 \times \Im\{a_{km}\}, \quad (130)$$

$$E_m = V_m V_m^* - |V_{m_s}|^2, \quad (131)$$

Here $\Im\{a_{km}\}$ is the specified imaginary part of the complex tap value, e.g, for a phase-transformer, we have $\Im\{a_{km}\} = 0.0$; otherwise, it is a phase-shifter-transformer and instead of (130), (119) is used. In (131), V_{m_s} is the specified voltage at node m , i.e., the regulated nodal voltage, yielding the partial derivatives of (130) and (131) given by

$$\left. \frac{\partial M_m}{\partial a_{km}} \right|_{a_{km}^* = Const} = 1.0, \quad (132)$$

$$\left. \frac{\partial M_m}{\partial a_{km}^*} \right|_{a_{km} = Const} = -1.0, \quad (133)$$

and

$$\left. \frac{\partial E_m}{\partial V_m} \right|_{V_m^* = Const} = V_m^*, \quad (134)$$

$$\left. \frac{\partial E_m}{\partial V_m^*} \right|_{V_m = Const} = V_m. \quad (135)$$

When (119) is used, the corresponding partial derivatives are those defined in (89-90) and (101-102).

3.5 Complex-Valued Iterative Solution

3.5.1 The Newton-Raphson Algorithm

When the slack bus is excluded, the state variables vector in the complex conjugate coordinate becomes

$$\underline{\mathbf{x}}_c = [V_1, V_2, \dots, V_{N-1}, V_1^*, V_2^*, \dots, V_{N-1}^*]^T, \quad (136)$$

and the mismatches vector reduces to

$$\underline{M}(\underline{\mathbf{x}}_c) = [M_1, M_2, \dots, M_{N-1}, M_1^*, M_2^*, \dots, M_{N-1}^*]^T. \quad (137)$$

If Node k (for $k = 1, 2, \dots, N-1$) is a *PV-bus* or a *PQV-bus*, the pair of elements M_k and M_k^* in (137) are replaced by M_{kg} and E_{kg} as in (119) and (121) or replaced by M_m and E_m as in (130) and (131), respectively. Here, the objective is to calculate $\underline{\mathbf{x}}_c$ that satisfies

$$\underline{M}(\underline{\mathbf{x}}_c) = 0. \quad (138)$$

It follows that the linearization of (138) from one step to the sequel is given by

$$\underline{M} \left(\underline{\mathbf{x}}_c^{(\nu-1)} \right) + \mathbf{J}(\underline{\mathbf{x}}_c^{(\nu-1)}) \Delta \underline{\mathbf{x}}_c^{(\nu)} = 0, \quad (139)$$

and

$$\underline{\mathbf{x}}_c^{(\nu)} = \underline{\mathbf{x}}_c^{(\nu-1)} - \left[\mathbf{J}^{(\nu-1)} \right]^{-1} \underline{M} \left(\underline{\mathbf{x}}_c^{(\nu-1)} \right), \quad (140)$$

or

$$\Delta \underline{\mathbf{x}}_c^{(\nu)} = - \left[\mathbf{J}^{(\nu-1)} \right]^{-1} \underline{M} \left(\underline{\mathbf{x}}_c^{(\nu-1)} \right), \quad (141)$$

where \mathbf{J} is the complex-valued Jacobian matrix in the complex conjugate coordinate. So, the update equation is given by

$$\underline{\mathbf{x}}_c^{(\nu)} = \underline{\mathbf{x}}_c^{(\nu-1)} + \Delta \underline{\mathbf{x}}_c^{(\nu)}. \quad (142)$$

The convergence criterion can be the same that is often assumed in the \mathbb{R} – domain, *i.e.*,

$$\left\| \Delta \underline{\mathbf{x}}_c^{(\nu)} \right\|_{\infty} \leq tol \ (\approx 10^{-3}). \quad (143)$$

where $\|\cdot\|_{\infty}$ is defined as the infinity norm and ν is the iteration counter. In the complex domain, the convergence criterion is chosen to be the infinity norm of the $\Delta \underline{\mathbf{x}}_c^{(\nu)}$ of the complex conjugate partition as explained next.

3.5.2 Structure of the Complex-Valued Power Flow Jacobian Matrix

The complex-valued power flow Jacobian matrix exhibits the following structure:

$$\mathbf{J} = \begin{bmatrix} \frac{\partial M_{kg}}{\partial V_k} & \frac{\partial M_{kg}}{\partial V_m} & \frac{\partial M_{kg}}{\partial a_{km}} & \frac{\partial M_{kg}}{\partial V_k^*} & \frac{\partial M_{kg}}{\partial V_m^*} & \frac{\partial M_{kg}}{\partial a_{km}^*} \\ \frac{\partial M_k}{\partial V_k} & \frac{\partial M_k}{\partial V_m} & \frac{\partial M_k}{\partial a_{km}} & \frac{\partial M_k}{\partial V_k^*} & \frac{\partial M_k}{\partial V_m^*} & \frac{\partial M_k}{\partial a_{km}^*} \\ 0.0 & 0.0 & \frac{\partial M_m}{\partial a_{km}} & 0.0 & 0.0 & \frac{\partial M_m}{\partial a_{km}^*} \\ \frac{\partial E_{kg}}{\partial V_k} & 0.0 & 0.0 & \frac{\partial E_{kg}}{\partial V_k^*} & 0.0 & 0.0 \\ \frac{\partial M_k^*}{\partial V_k} & \frac{\partial M_k^*}{\partial V_m} & \frac{\partial M_k^*}{\partial a_{km}} & \frac{\partial M_k^*}{\partial V_k^*} & \frac{\partial M_k^*}{\partial V_m^*} & \frac{\partial M_k^*}{\partial a_{km}^*} \\ 0.0 & \frac{\partial E_m}{\partial V_m} & 0.0 & 0.0 & \frac{\partial E_m}{\partial V_m^*} & 0.0 \end{bmatrix}. \quad (144)$$

In (144), the partial derivatives in the 1st and 4th rows correspond to PV-buses, those in the 2nd and 5th rows correspond to PQ-buses and those in the 3th and 6th rows correspond to PQV-buses. In order to factorize the CV-Jacobian matrix in (144), two *QR*-algorithms are considered and investigated [8] and [7]; the latter is written in polar coordinates. Both are the extension of the well-known real-valued algorithm described in [26], which was successfully applied to PSSE by [27], [28], and [29]. Recall that the *QR*-algorithm should be applied to an augmented matrix in order to avoid explicitly storing the *Q*-matrix. To this end, the *QR*-transformation is applied to \mathbf{J}_a given by

$$\mathbf{J}_a^{(\nu-1)} = \left[\mathbf{J}^{(\nu-1)} \underline{M} \left(\underline{\mathbf{x}}_c^{(\nu-1)} \right) \right]. \quad (145)$$

On the other hand, it turns out that if we store the sequence of rotations in compact form, the complex-valued Jacobian matrix can be kept constant, implying that only the right-hand-side vector is updated throughout the final iterations. Here, the solution of (141) is reached by performing a simple back-substitution over the factorization of (145), yielding

$$\tilde{\mathbf{J}}_{\mathbf{a}}^{(\nu-1)} = \left[\mathbf{T}_{\mathbf{c}} \widetilde{\mathbf{M}}_{\mathbf{c}} \right]. \quad (146)$$

where $\mathbf{T}_{\mathbf{c}}$ is an upper triangular matrix of dimension- $2n \times 2n$, and $\widetilde{\mathbf{M}}_{\mathbf{c}}$ comprises the corresponding rows in the updated *rhs* vector, *dimension*- $2n \times 1$, for $n = N - 1$. Then, (141) can be expressed through

$$\Delta \underline{\mathbf{x}}_{\mathbf{c}}^{(\nu)} = \mathbf{T}_{\mathbf{c}} \widetilde{\mathbf{M}}_{\mathbf{c}}. \quad (147)$$

Note that when executing the algorithm given by (147), only the complex conjugate state vector, $\underline{\mathbf{x}}^*$, has to be updated. Therefore, the steps defined in (141) and (143) can be numerically decoupled, suggesting that only the Jacobian matrix associated with $\underline{\mathbf{x}}^*$ has to be stored and factorized.

3.5.3 The Fourth-Order Levenberg-Marquardt as Applied to CV-PFA

In the state-of-the-art of numerical analysis, many proposals can be found aiming to solve ill-conditioned nonlinear system of equations as [30], [31], [32], [33], [34] to cite a few. In power systems analysis, Brown's and Brent's methods have been applied to solve ill-conditioned systems [35], [36], [37], [38], [39] and [40]. Nonetheless, in [41] the researchers have employed Yang's proposal [42] which is based on the Levenberg-Marquardt algorithm that is usually derived for optimization problem [6].

After tireless checking of the numerical robustness stated in [42], [43], [44] and [45] by using the nonlinear systems of equations in real domain, as Rosenbrok's; Brown's 1 and 2; Brown-Conte and Powell's test functions extracted from [34], the algorithm proposed by Yang [42] and Fan [43] have presented best performance and easy encoding task. In this work the Yang's proposal is presented as applied to CV-PFA. Nonetheless, as the goal is to enhance the numerical robustness, the Barel's format equation [6] is assumed once it is based on the Jacobian instead of the Gain matrix as stated in [42]. The motivation can be seen in the Fig. 3.1 presented in the sequel which is referred to the application showed on page 35.

Recall that the key idea of the Yang's proposal is to enhance the condition number of the coefficient matrix when updating the states throughout the iterative process, i.e.

$$\Delta \underline{\mathbf{x}}_{\mathbf{c}}^{(\nu)} = - \left(\begin{array}{c} \mathbf{J}^{(\nu-1)} \\ \sqrt{\eta_{\nu}} I \end{array} \right)^{-1} \left(\begin{array}{c} \underline{\mathbf{M}}(\underline{\mathbf{x}}_{\mathbf{c}}^{(\nu-1)}) \\ 0 \end{array} \right), \quad (148)$$

where $\eta_{\nu} > 0$ is the Levenberg-Marquardt (LM) regularization parameter which influences both the length and direction of the updates to be applied to the state variables at each iteration aiming to satisfy (138). It is calculated as $\eta_{\nu} = \mu_{\nu} \|\underline{\mathbf{M}}(\underline{\mathbf{x}}_{\mathbf{c}}^{(\nu-1)})\|$ where μ_{ν} is typically set to 10^{-5} .

Now, instead of using only one LM step as stated in (148), two additional approximation steps are computed by using the previous Jacobian matrix. The second correction step is

$$\Delta \underline{\mathbf{y}}_{\mathbf{c}}^{(\nu)} = - \left(\begin{array}{c} \mathbf{J}^{(\nu-1)} \\ \sqrt{\eta_{\nu}} I \end{array} \right)^{-1} \left(\begin{array}{c} \underline{\mathbf{M}}(\underline{\mathbf{y}}_{\mathbf{c}}^{(\nu-1)}) \\ 0 \end{array} \right), \quad (149)$$

where $\underline{\mathbf{y}}_{\mathbf{c}}^{(\nu-1)} = \underline{\mathbf{x}}_{\mathbf{c}}^{(\nu)}$ as stated in (142). And the third step is

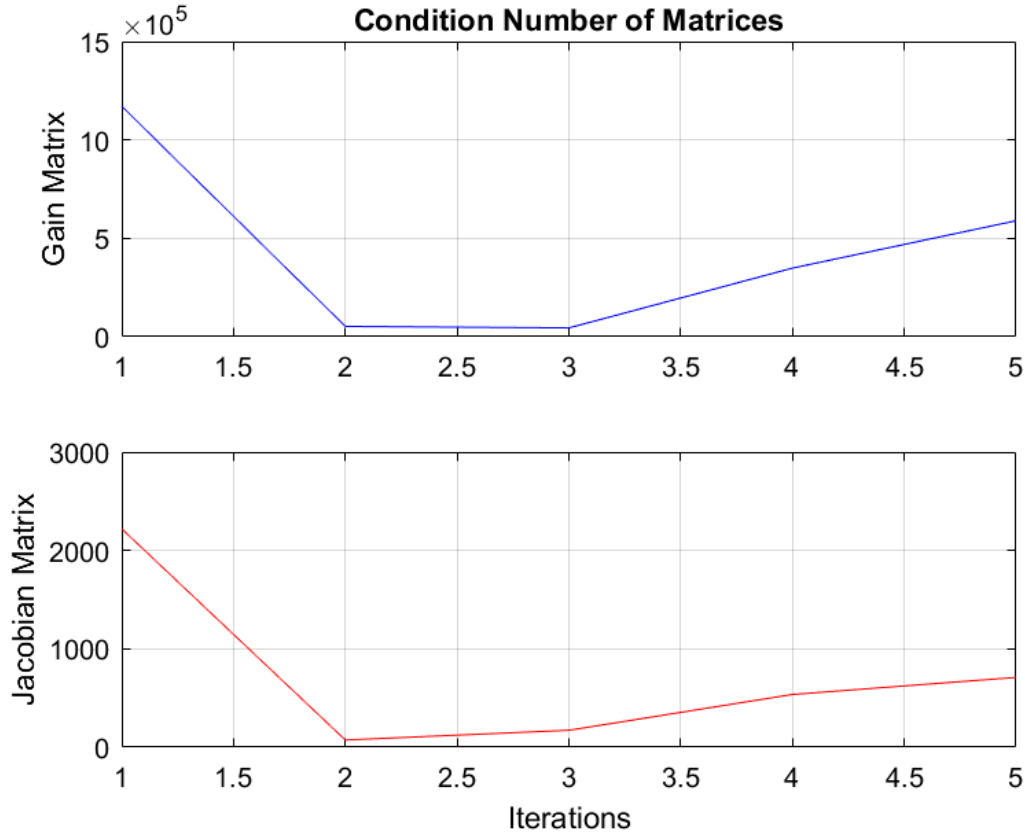


Figure 3.1: IEEE-11 Bus: Condition Number.

$$\Delta \mathbf{z}_c^{(\nu)} = - \left(\begin{array}{c} \mathbf{J}^{(\nu-1)} \\ \sqrt{\eta_\nu} I \end{array} \right)^{-1} \left(\begin{array}{c} \underline{M}(\mathbf{z}_c^{(\nu-1)}) \\ 0 \end{array} \right), \quad (150)$$

where $\mathbf{z}_c^{(\nu-1)} = \mathbf{y}_c^{(\nu)} = \mathbf{y}_c^{(\nu-1)} + \Delta \mathbf{z}_c^{(\nu)}$. Thus, the convergence checking should be carried out over this last approximation step, yielding

$$\left\| \Delta \mathbf{z}_c^{(\nu)} \right\|_\infty \leq tol \ (\approx 10^{-3}). \quad (151)$$

If (151) is satisfied, *stop and print out the results*. Otherwise, calculate the ratio of error deduction $err_\nu = Ared_\nu / Pred_\nu$, where

$$Ared_\nu = \left\| \underline{M}(\mathbf{x}_c^{(\nu-1)}) \right\|^2 - \left\| \underline{M}(\mathbf{x}_c^{(\nu-1)} + \Delta \mathbf{x}_c^{(\nu)} + \Delta \mathbf{y}_c^{(\nu)} + \Delta \mathbf{z}_c^{(\nu)}) \right\|^2, \quad (152)$$

$$\begin{aligned} Pred_\nu = & \left\| \underline{M}(\mathbf{x}_c^{(\nu-1)}) \right\|^2 - \left\| \underline{M}(\mathbf{x}_c^{(\nu-1)} + \mathbf{J}^{(\nu-1)} \Delta \mathbf{x}_c^{(\nu)}) \right\|^2 + \\ & \left\| \underline{M}(\mathbf{y}_c^{(\nu-1)}) \right\|^2 - \left\| \underline{M}(\mathbf{y}_c^{(\nu-1)} + \mathbf{J}^{(\nu-1)} \Delta \mathbf{y}_c^{(\nu)}) \right\|^2 + \\ & \left\| \underline{M}(\mathbf{z}_c^{(\nu-1)}) \right\|^2 - \left\| \underline{M}(\mathbf{z}_c^{(\nu-1)} + \mathbf{J}^{(\nu-1)} \Delta \mathbf{z}_c^{(\nu)}) \right\|^2. \end{aligned} \quad (153)$$

The state vector is updated through

$$\mathbf{x}_c^{(\nu)} = \begin{cases} \mathbf{x}_c^{(\nu-1)} + \Delta \mathbf{x}_c^{(\nu)} + \Delta \mathbf{y}_c^{(\nu)} + \Delta \mathbf{z}_c^{(\nu)}, & \text{if } err_\nu \geq p_0 \\ \mathbf{x}_c^{(\nu-1)}, & \text{otherwise.} \end{cases} \quad (154)$$

where p_0 is a parameter that is chosen between 0 and 1. Finally the LM regularization parameter η_ν is updated as

$$\eta_\nu = \begin{cases} 4 \eta_\nu & \text{if } \text{err}_\nu < p_1 \\ \eta_\nu & \text{if } \text{err}_\nu \in [p_1, p_2] \\ \max \left\{ \frac{\eta_\nu}{4}, \lambda \right\} & \text{if } \text{err}_\nu > p_2 \end{cases} \quad (155)$$

where $0 < p_0 \leq p_1 \leq p_2 < 1$ and $\eta_\nu > \lambda > 0$. Now the iteration counter is update, i.e., $\nu = \nu + 1$ and it is checked if the maximum iteration number is reached; if that is the case, terminate the algorithm and print out the results, otherwise starts the whole process going back to equation (148).

Remark that Jacobian matrix \mathbf{J} is evaluated only once at the ν -th iteration, which is an appealing property for the biquadratic convergence rate of the proposed approach. The latter can be proved easily using the same theorems shown in [42]. Note that the calculation of the Jacobian matrix is time consuming for large-scale systems. Thanks to the biquadratic convergence rate of the proposed approach, the number of iterations is reduced significantly. On the other hand, the linearization error of the nonlinear equation is compensated through the two additional approximate LM steps. This improves the numerical robustness of the proposed approach remarkably under highly stressed operating conditions.

Finally, note that there are several parameters that should be set before the iterative LM-based CV-PFA has started. Among them, the initial value of μ , the p_0 , p_1 , p_2 and λ . The initial value of μ , which is usually set to 10^{-5} , has little impact on the iterative process once it is either updated, whereas for p_0 , p_1 , p_2 and λ , we set them as $p_0 = 10^{-4}$, $p_1 = 0.25$, $p_2 = 0.75$ and $\lambda = 0.65$ following the recommendation stated in [42]. We find that this set of values works well for different test systems.

3.6 Numerical Results

3.6.1 Small Example: CV-Power Flow Analysis

In the sequel the CV-Power Flow modeling is applied to a small example system which diagram is showed in Fig. 3.2, while the corresponding branch parameters and bus data, both in pu ($V_{base} = 230 \text{ kV}$; $S_{base} = 100 \text{ MVA}$), are presented in Table 3.1 and 3.2, respectively.

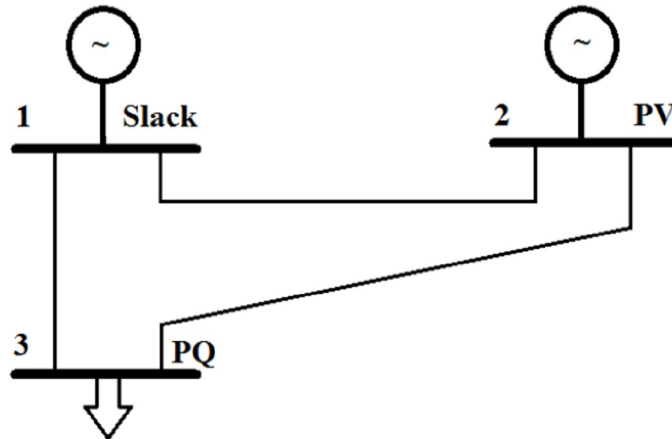


Figure 3.2: Small 3-Bus System.

Table 3.1: Branches Data.

Branch $i \rightarrow j$	Serie		Shunt	
	R pu	X pu	Charging MVar	Y/2 pu
1-2	0.0012	0.0021	39.2	0.196
1-3	0.0150	0.0400		
2-3	0.3000	1.6000		

Table 3.2: Bus Data.

Bus	Specified Quantities in pu			
Type	P_g	V	P_{load}	Q_{load}
PV-2	1.0000	1.0000	0.2160	0.0918
PQ-3			2.700	1.620

The nodal admittance matrix, i.e., Y_{bus} , yields to

$$Y_{bus} = \begin{bmatrix} 213.3474 & -j 380.8922 & -205.1282 & +j 358.9744 & -8.2192 & +j 21.9178 \\ -205.1282 & +j 358.9744 & 205.2414 & -j 359.3821 & -0.1132 & +j 0.6037 \\ -8.2192 & +j 21.9178 & -0.1132 & +j 0.6037 & 8.3324 & -j 22.3256 \end{bmatrix}$$

The whole set of intermediary results throughout the iterative process is presented in the sequence.

As in the real-domain, the elements of the complex-valued Jacobian matrix remain practically unchanged after the second iteration, which suggest that we may keep them constant thereafter. Moreover, the computation of some entries can be avoided because they are complex conjugates of other variables; it turns out that these elements are PV-nodes.

$$J^{(\nu=0)} = \begin{bmatrix} 413.6193 \times e^{-j 60.268} & 0.4232 \times e^{-j 74.484} & 413.6193 \times e^{+j 60.268} & 0.4232 \times e^{+j 74.484} \\ & 0.1960 \times e^{+j 90.000} & 0.6143 \times e^{-j 100.619} & 23.8298 \times e^{+j 69.533} \\ 1.0000 \times e^{j 0.000} & & 1.0000 \times e^{j 0.000} & \\ 0.6143 \times e^{+j 100.619} & 23.8298 \times e^{-j 69.533} & & 0.1960 \times e^{+j 90.000} \end{bmatrix}$$

$$J^{(\nu=1)} = \begin{bmatrix} 414.4312 \times e^{-j 60.323} & 0.4232 \times e^{-j 74.616} & 414.4312 \times e^{+j 60.323} & 0.3842 \times e^{+j 69.158} \\ & 3.1443 \times e^{-j 148.587} & 0.5577 \times e^{-j 105.946} & 21.6334 \times e^{+j 64.207} \\ 1.0000 \times e^{-j 0.132} & & 1.0000 \times e^{+j 0.132} & \\ 0.5577 \times e^{+j 105.946} & 23.8298 \times e^{-j 69.665} & & 3.1443 \times e^{+j 148.587} \end{bmatrix}$$

$$J^{(\nu=2)} = \begin{bmatrix} 414.3163 \times e^{-j 60.313} & 0.4232 \times e^{-j 74.599} & 414.3180 \times e^{+j 60.313} & 0.3765 \times e^{+j 68.935} \\ & 3.5321 \times e^{-j 143.603} & 0.5465 \times e^{-j 106.168} & 21.2006 \times e^{+j 63.984} \\ 1.0000 \times e^{-j 0.115} & & 1.0000 \times e^{+j 0.115} & \\ 0.5452 \times e^{+j 106.041} & 23.8298 \times e^{-j 69.648} & & 3.5232 \times e^{+j 144.712} \end{bmatrix}$$

$$J^{(\nu=3)} = \begin{bmatrix} 414.3115 \times e^{-j 60.313} & 0.4232 \times e^{-j 74.599} & 414.3133 \times e^{+j 60.313} & 0.3763 \times e^{+j 68.932} \\ & 3.5408 \times e^{-j 143.485} & 0.5463 \times e^{-j 106.171} & 21.1905 \times e^{+j 63.982} \\ 1.0000 \times e^{-j 0.115} & & 1.0000 \times e^{+j 0.115} & \\ 0.5449 \times e^{+j 106.040} & 23.8298 \times e^{-j 69.648} & & 3.5316 \times e^{+j 144.620} \end{bmatrix}$$

Interestingly, the numerical values of the state variables corrections; state variables and mismatches vectors calculated in the complex domain are displayed in the Tables 3.3-3.5. Remark that they are the same as those calculated in the real domain. Consequently, the values of the power injections and of the power flows calculated in the real and in the complex domain are also the same; they are displayed in Tables 3.6.

Table 3.3: Correction Vector.

<i>Convergence Criteria : $\ \underline{\Delta X}\ _{\infty} < tol. \approx 10^{-4}$</i>				
$\underline{\Delta X}$	$\underline{\Delta X}^{(\nu=0)}$	$\underline{\Delta X}^{(\nu=1)}$	$\underline{\Delta X}^{(\nu=2)} \times 10^{-3}$	$\underline{\Delta X}^{(\nu=3)} \times 10^{-6}$
ΔV_2	$0.0023 \times e^{+j 90.00}$	$0.0003 \times e^{-j 90.39}$	$0.0127 \times e^{-j 90.08}$	$0.1708 \times e^{+j 89.92}$
ΔV_3	$0.1278 \times e^{-j 138.75}$	$0.0185 \times e^{-j 174.56}$	$0.4267 \times e^{-j 179.44}$	$0.2326 \times e^{-j 179.18}$
ΔV_2^*	$0.0023 \times e^{-j 90.00}$	$0.0003 \times e^{+j 90.37}$	$0.0127 \times e^{+j 90.07}$	$0.1708 \times e^{-j 89.91}$
ΔV_3^*	$0.1278 \times e^{+j 138.75}$	$0.0203 \times e^{+j 178.81}$	$0.4795 \times e^{+j 173.22}$	$0.2615 \times e^{+j 173.47}$
$\ \underline{\Delta X}\ _{\infty}$	0.127809	0.020316	4.795255×10^{-4}	2.614490×10^{-7}

Table 3.4: State Variables.

\underline{X}	$ \underline{X} ^{(\nu=0)}$	$ \underline{X} ^{(\nu=1)}$	$ \underline{X} ^{(\nu=2)}$	$ \underline{X} ^{(\nu=3)}$
V_2	$1.000 \times e^{j 0.0}$	$1.000 \times e^{+j 0.132}$	$1.000 \times e^{+j 0.115}$	$1.000 \times e^{+j 0.115}$
V_3	$1.000 \times e^{j 0.0}$	$0.907 \times e^{-j 5.326}$	$0.889 \times e^{-j 5.548}$	$0.889 \times e^{-j 5.552}$
V_2^*	$1.000 \times e^{-j 180}$	$1.000 \times e^{-j 0.132}$	$1.000 \times e^{-j 0.115}$	$1.000 \times e^{-j 0.115}$
V_3^*	$1.000 \times e^{-j 180}$	$0.907 \times e^{+j 5.326}$	$0.887 \times e^{+j 5.421}$	$0.887 \times e^{+j 5.420}$

Table 3.5: Complex-Valued *Mismatches* Vector.

\underline{M}	$\underline{M}(\underline{X})^{(\nu=0)}$	$\underline{M}(\underline{X})^{(\nu=1)}$	$\underline{M}(\underline{X})^{(\nu=2)}$	$\underline{M}(\underline{X})^{(\nu=3)} \times 10^{-3}$
M_{2g}	$-1.5680 + j 0.0000$	$0.2178 + j 0.0000$	$0.0093 + j 0.0000$	$0.1229 + j 0.0000$
M_3	$+2.7000 + j 1.4240$	$0.1363 + j 0.3648$	$0.0021 + j 0.0087$	$0.0011 + j 0.0047$
M_{2g}^*	$+0.0000 + j 0.0000$	$0.0000 - j 0.0000$	$0.0000 - j 0.0000$	$0.0000 - j 0.0000$
M_3^*	$+2.7000 - j 1.4240$	$0.1363 - j 0.3648$	$0.0021 - j 0.0087$	$0.0011 - j 0.0047$

Table 3.6: CV-Power Flow Report.

S_k	<i>Coordinates</i>	
	<i>Retangular</i>	<i>Polar</i>
	$(P_k \pm j Q_k)$	$ S_k \times e^{\pm j \varphi}$
S_1	$+2.0788 + j 2.2844$	$3.0887 \times e^{+j 47.697}$
S_2	$+0.7841 - j 0.5449$	$0.9548 \times e^{-j 34.802}$
S_3	$-2.6999 - j 1.6199$	$3.1487 \times e^{-j 149.036}$
S_{km}		
	$(P_{km} \pm j Q_{km})$	$ S_{km} \times e^{\pm j \theta_{km}}$
S_{12}	$-0.7183 + j 0.4114$	$0.8277 \times e^{+j 150.199}$
S_{21}	$+0.7192 - j 0.4099$	$0.8277 \times e^{-j 29.686}$
S_{13}	$+2.7972 + j 1.8730$	$3.3663 \times e^{+j 33.806}$
S_{31}	$-2.6368 - j 1.4171$	$2.9935 \times e^{-j 151.745}$
S_{23}	$+0.0649 - j 0.1350$	$0.1498 \times e^{-j 64.323}$
S_{32}	$-0.0631 - j 0.2028$	$0.2124 \times e^{-j 107.289}$

3.6.2 IEEE Test Systems: well-conditioned systems

Table 3.7 provides the parameters of the IEEE test power systems while Figs. 3.3-3.6 display the sparsity structures of the Jacobian matrices in the the \mathbb{C} -domain given by (144) as compared to those derived in the \mathbb{R} -domain.

Table 3.7: Features of the IEEE Test systems

IEEE-Test Bus Systems	-14	-30	-57	-118
No. of PV-bus (N_{PV})	4	5	6	53
No. of PQ-bus (N_{PQ})	9	24	50	64
No. of transformers	3	4	15	9
No. of transmission lines + shunt	21	43	83	200
\mathbb{R} -Valued: $n = (N_{PV} + 2 \times N_{PQ})$	22	53	106	181
\mathbb{C} -Valued: $2n = 2 \times (N_{PV} + N_{PQ})$	26	58	112	234

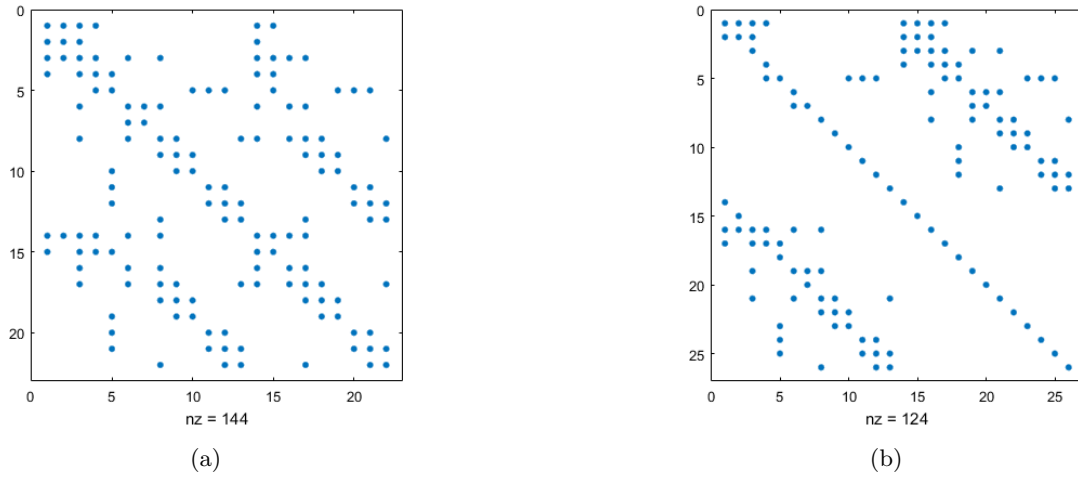


Figure 3.3: Sparsity structure of (a) real-valued Jacobian matrix; (b) complex-valued Jacobian matrix of the IEEE 14-bus system.

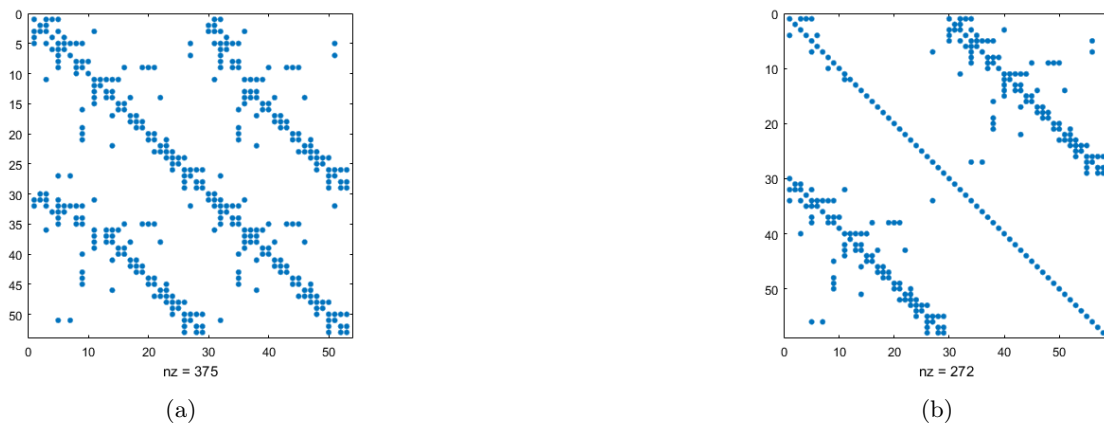


Figure 3.4: Sparsity structure of (a) real-valued Jacobian matrix; (b) complex-valued Jacobian matrix of the IEEE 30-bus system.

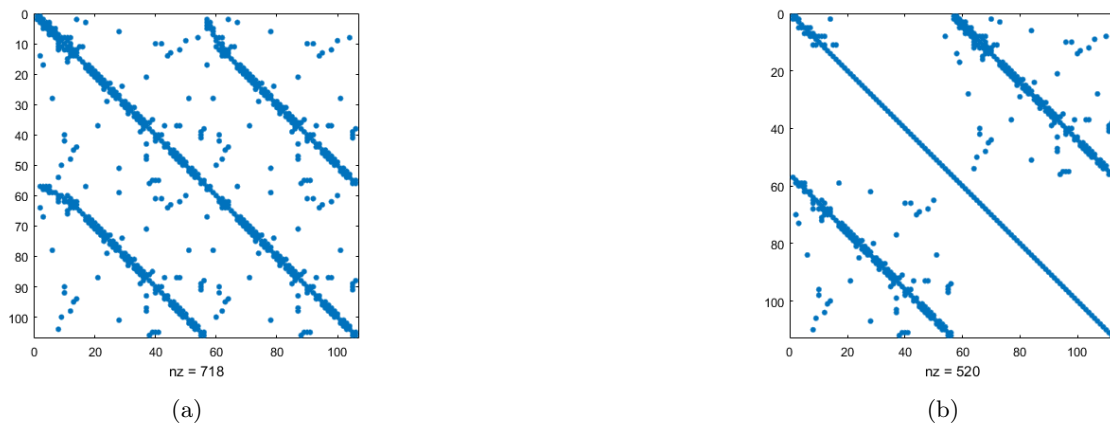


Figure 3.5: Sparsity structure of (a) real-valued Jacobian matrix; (b) complex-valued Jacobian matrix of the IEEE 57-bus system.

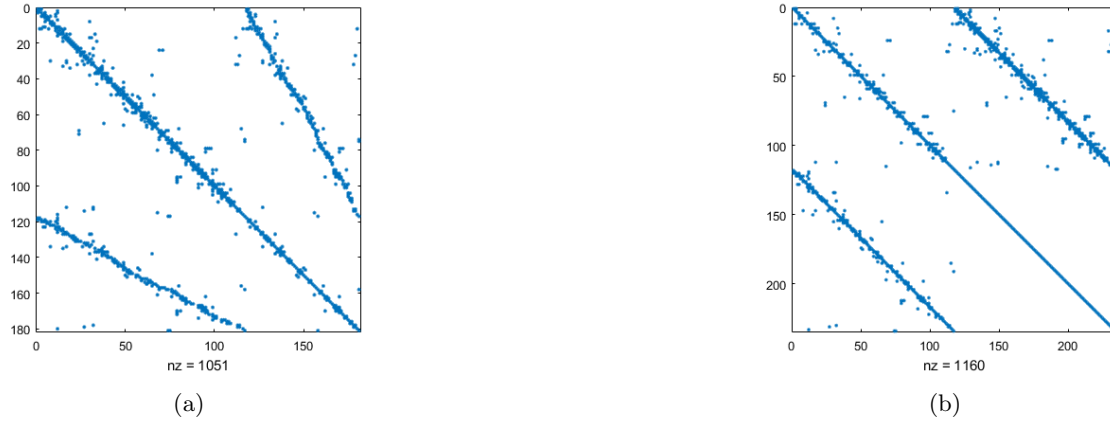


Figure 3.6: Sparsity structure of (a) real-valued Jacobian matrix; (b) complex-valued Jacobian matrix of the IEEE 118-bus system.

Clearly, the diagonal blocks in the complex Jacobian matrix are practically diagonal matrices, which prompt its factorization. On the other hand, Table 3.8 provides the number of iterations, the condition number and the non-zero counts associated with the real-valued and complex-valued Jacobian matrices.

Table 3.8: Sparsity and Numerical Analysis

IEEE-Test Systems	-14	-30	-57	-118
No. of iterations:				
✓ RV-NR power flow	4	4	4	4
✓ CV-NR/LM power flow	4/2	4/2	5/2	4/2
Condition Number:				
✓ RV-Jacobian matrix	117.8	473.3	826.1	3166.9
✓ CV-Jacobian matrix	118.0	487.5	815.8	3276.8
✓ RV/CV Ratio	0.99	0.97	1.01	0.97
Nonzero counts:				
✓ RV-Jacobian matrix	144	375	718	1051
✓ CV-Jacobian matrix	124	272	520	1160
✓ RV/CV Ratio	1.16	1.38	1.38	0.90

Table 3.8 allows us to infer that the complex-valued power flow algorithm has numerical performance and sparsity structure very similar to the real-valued counterpart; specifically, it requires the same number of iterations to reach the solution ($tol. \sim 10^{-4}$) and it exhibits the same numerical robustness and sparsity structure. Furthermore, as the fourth-order Levenberg-Marquadt algorithm based on power flow analysis, **CV-LMPFA** for short, is now available in complex domain; notice that it requires just 2 (two) iterations to reach the convergence in all of the well-conditioned IEEE test systems.

Figs. 3.7 to 3.10 display the profiles of the voltage and phase angle at each bus of the IEEE 14-, 30-, 57-, and 118-bus systems. Remark that the results produced by the real- and complex-valued Newton-Raphson power flow analysis are completely overlaid. Furthermore, in Table 3.9 is presented the relative maximum bias between the corresponding state variables calculated in the complex and

in the real domain are the same; the small difference indicated in the table is due to numerical approximations, i.e., arithmetic of real and complex numbers.

Table 3.9: Maximum bias between states and location

IEEE Test Systems	14-bus	30-bus	57-bus	118-bus
$\ \Delta \underline{\mathbf{V}}\ _{\infty} \times 10^{-7} _{(bus)}$	41.2 ₍₉₎	3.77 ₍₂₁₎	77.9 ₍₂₅₎	1.48 ₍₄₎
$\ \Delta \underline{\delta}\ _{\infty} \times 10^{-7} _{(bus)}$	26.1 ₍₆₎	1.82 ₍₁₃₎	50.6 ₍₂₆₎	1.40 ₍₄₎

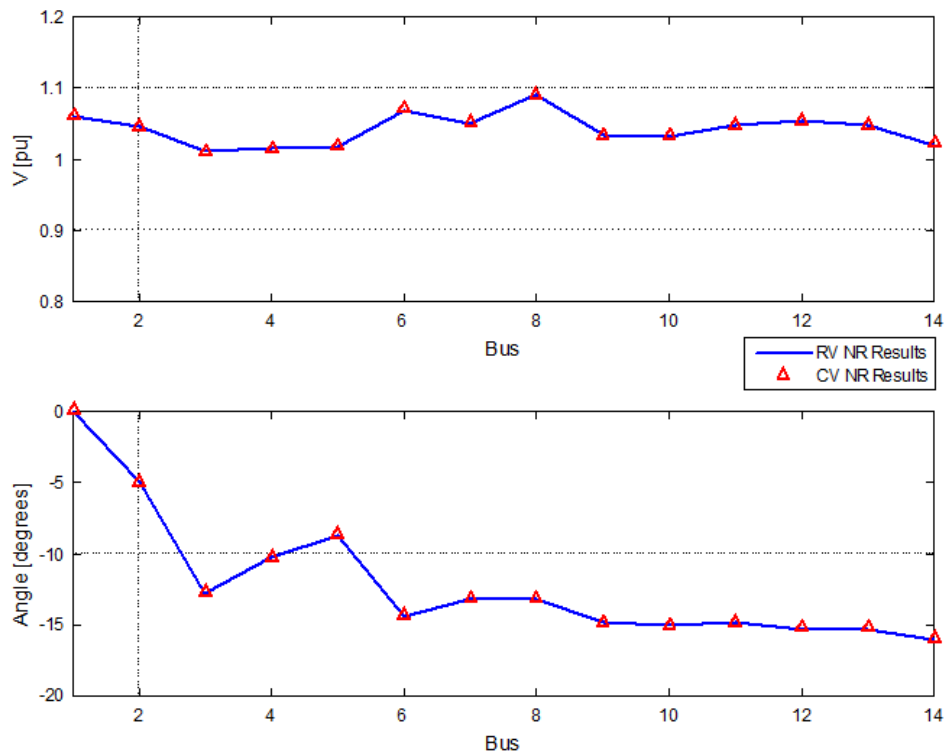


Figure 3.7: IEEE-14 Bus: voltage and angle profiles.

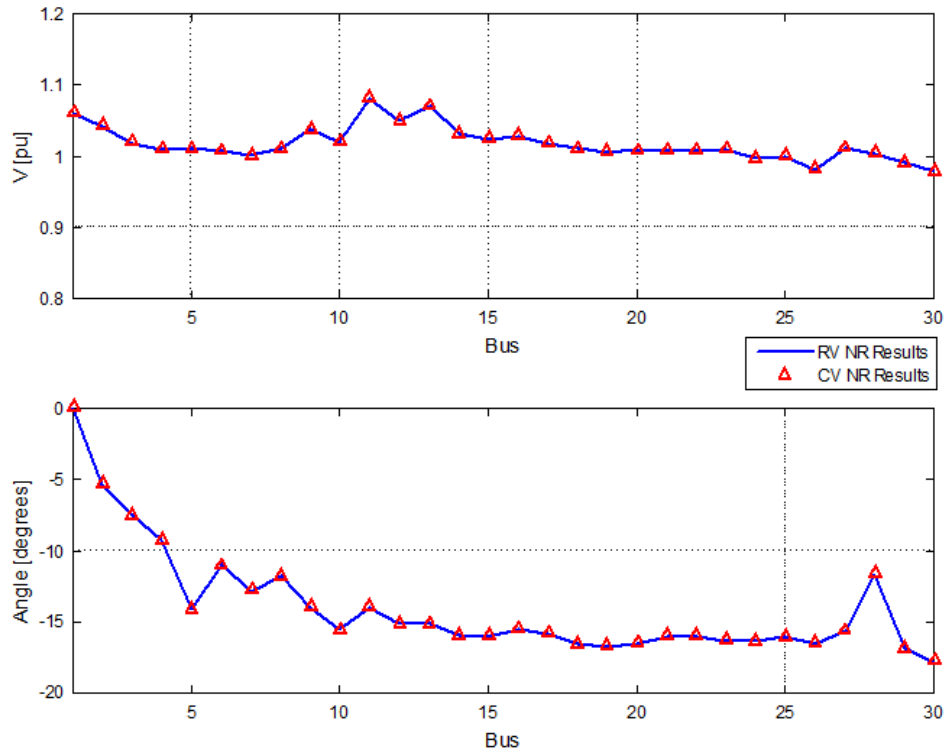


Figure 3.8: IEEE-30 Bus: voltage and angle profiles.

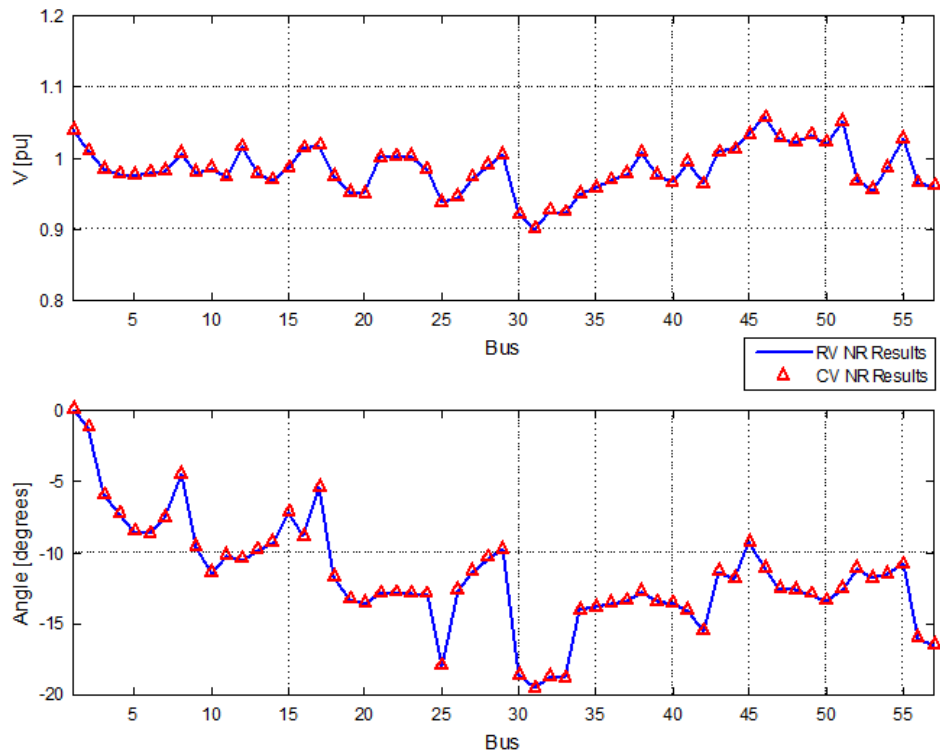


Figure 3.9: IEEE-57 Bus: voltage and angle profiles.

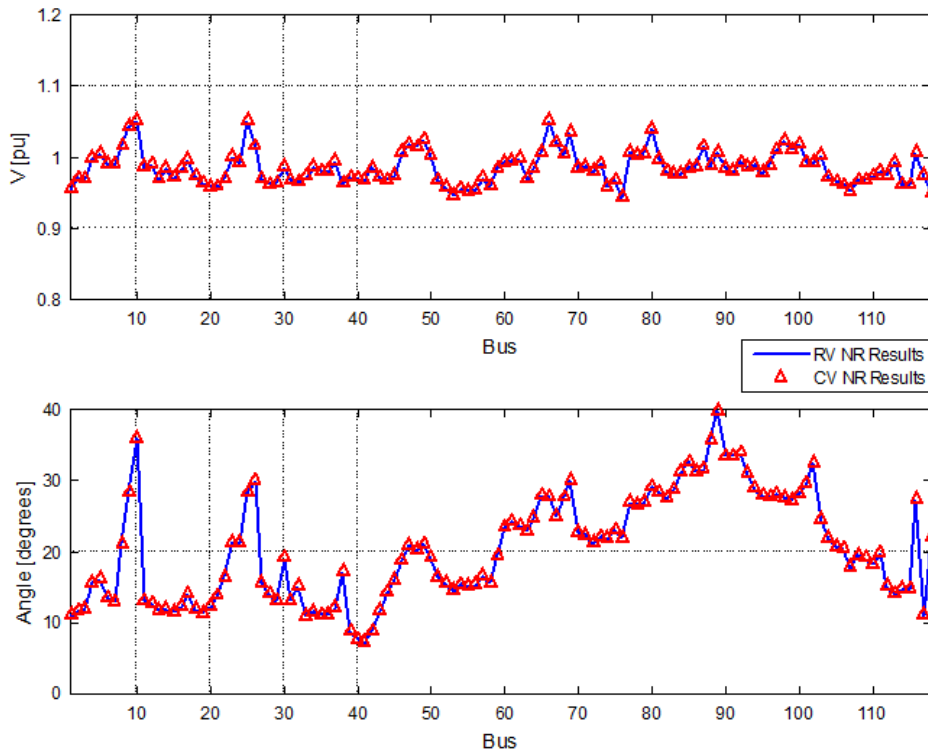


Figure 3.10: IEEE-118 Bus: voltage and angle profiles.

3.6.3 IEEE Test Systems: ill-conditioned systems

The simulations carried out on the well-known ill-conditioned IEEE 11-Bus system are presented in the sequence. The main features of this systems are its heavily loaded condition and radial topology. The complex-valued Levenberg-Marquardt approach (**CV-LMPFA**) got successful performance in all cases while the complex-valued Newton-Raphson algorithm (**CV-NRPFA**) has collapsed. The one line diagram for the 11-Bus system is depicted in Fig. 3.11.

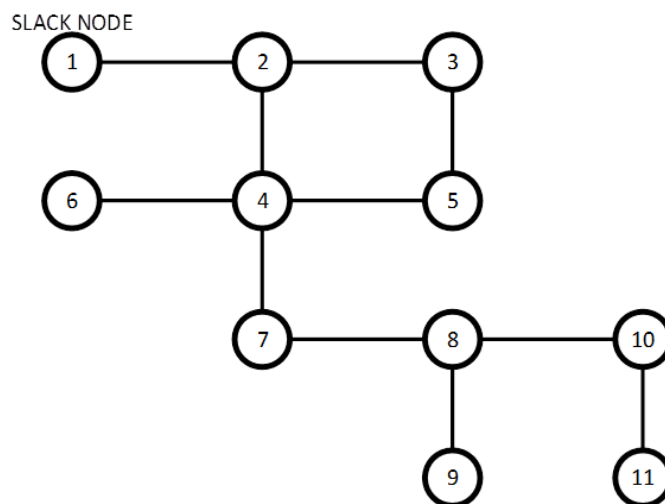


Figure 3.11: IEEE-11 Bus: one line diagram.

The power flow network data for the ill-conditioned 11-Bus system are presented in Tables 3.10 and 3.11.

Table 3.10: ill-conditioned IEEE-11 Bus Data.

Bus		V	δ	Load		Generator			
No.	code	pu	degree	MW	MVAr	Mw	MVAr	Qmin	Qmax
1	1	1.024	0.0	0.0	0.0	0.0	0.0	0	0
2	2	1.000	0.0	0.0	0.0	0.0	0.0	-1	+1
3	0	1.000	0.0	12.8	6.2	0.0	0.0	0	0
4	2	1.000	0.0	0.0	0.0	0.0	0.0	-1	+1
5	0	1.000	0.0	16.5	8.0	0.0	0.0	0	0
6	0	1.000	0.0	9.0	6.8	0.0	0.0	0	0
7	2	1.000	0.0	0.0	0.0	0.0	0.0	-1	+1
8	2	1.000	0.0	0.0	0.0	0.0	0.0	-1	+1
9	0	1.000	0.0	2.6	0.9	0.0	0.0	0	0
10	2	1.000	0.0	0.0	0.0	0.0	0.0	-1	+1
11	0	1.000	0.0	15.8	5.7	0.0	0.0	0	0

Table 3.11: ill-conditioned IEEE-11 Bus Branches Data.

Branches		Impedance		Half Susceptance	Transformer
From	To	R (pu)	X (pu)	(pu)	Tap
1	2	0.0	0.0706	0	1
2	3	0.0	0.1540	0	1
2	4	0.0377	0.0413	0	1
3	5	0.1228	0.1803	0	1
4	5	0.0	0.4593	0	1
4	6	0.0	0.0176	0	1
4	7	0.6114	0.8117	0	1
7	8	0.6209	0.2167	0	1
8	9	0.0718	0.7179	0	1
8	10	0.4097	0.5600	0	1
10	11	0.0264	0.2646	0	1

The state variables and corresponding power injections for the ill-conditioned IEEE-11 bus system are showed in Table 3.12. The iterative process has reached the solution in 5 iterations ($tol. \sim 10^{-3}$).

Table 3.12: State Variables and Complex Power Injections.

Bus No.	Voltage (pu)	Angle (degree)	P (pu)	Q (pu)
1	1.0240	0.0000	1.2509	0.4065
2	1.0001	-4.9488	0.0000	-0.9907
3	0.9878	-7.4958	-0.1280	-0.0620
4	0.9990	-8.9445	0.0000	0.8025
5	0.9668	-9.1202	-0.1650	-0.0800
6	0.9978	-9.0356	-0.0900	-0.0680
7	1.0185	-58.4130	-0.0013	0.2194
8	0.9864	-82.7922	0.0109	0.5290
9	0.9795	-82.9341	-0.0042	-0.0090
10	0.9981	-89.5748	0.0130	0.1832
11	0.9786	-91.5335	-0.1318	-0.0569

In Table 3.12 a wide angular lag of all nodal voltages referred to the *slack bus* is resulted. This issue proves that the network is under heavily loaded condition, mainly downstream from the bus 7. Even though, the profiles of nodal voltages are practically flat once the following bus are defined as a controlled voltage: 2, 4, 7, 8 and 10, i.e., PV-bus type, see Fig. 3.12. Moreover, in Table 3.12 the reactive power injections of all synchronous condensers are highlighted in blue and they have resulted within the operative range of ± 1 pu in all cases. The exception are the corresponding active power highlighted in red that might be equal to zero. This problem is due to the mismatches of active power at bus-7 (2.1%); -8 (2.1%) and -10 (2.6%). In the sequence, the power flows in all branches, e.g., sending and receiving end, are plotted in the one line diagram showed in Fig. 3.13. For the remaining ill-conditioned IEEE-13 and -43 bus systems the CV-LMPFA has required 4 and 5 iterations, respectively. By contrast, the RV-NRPFA and the CV-NRPFA have suffered a breakdown on all 3 IEEE-test systems.

3.7 Partial Conclusions

In this section we have presented a complex-valued Newton-Raphson and Levenberg-Marquardt algorithms to solve a power flow problem in the $\mathbb{C} - domain$. The complex-valued fourth-order Levenberg-Marquardt algorithm is addressed for ill-conditioned networks, specially those under heavily loaded condition and branches with high R/X ratio. It is shown that the implementation of the approaches is straightforward and is much easier to encode the problem formulation in the complex- than in the real-domain. All of the computations can be carried out in a very similar manner than those in the Cartesian coordinate system, making many tools and methods developed in the past readily available for the implementation in the conjugate coordinates. As a future research, we will initiate a power flow framework for hybrid AC-DC systems that include a variety of FACTS devices, including VSC-HVDC links and STATCOM devices, and will develop solution methods that are both numerically robust and compatible with real-time applications, e.g., the fourth-order Levenberg-Marquardt algorithm which performance has proved superior.

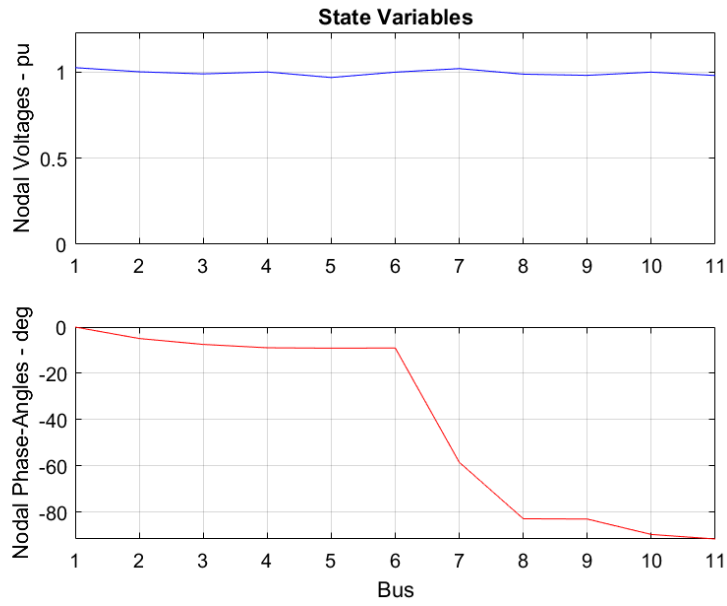


Figure 3.12: IEEE-11 Bus: Voltage profile.

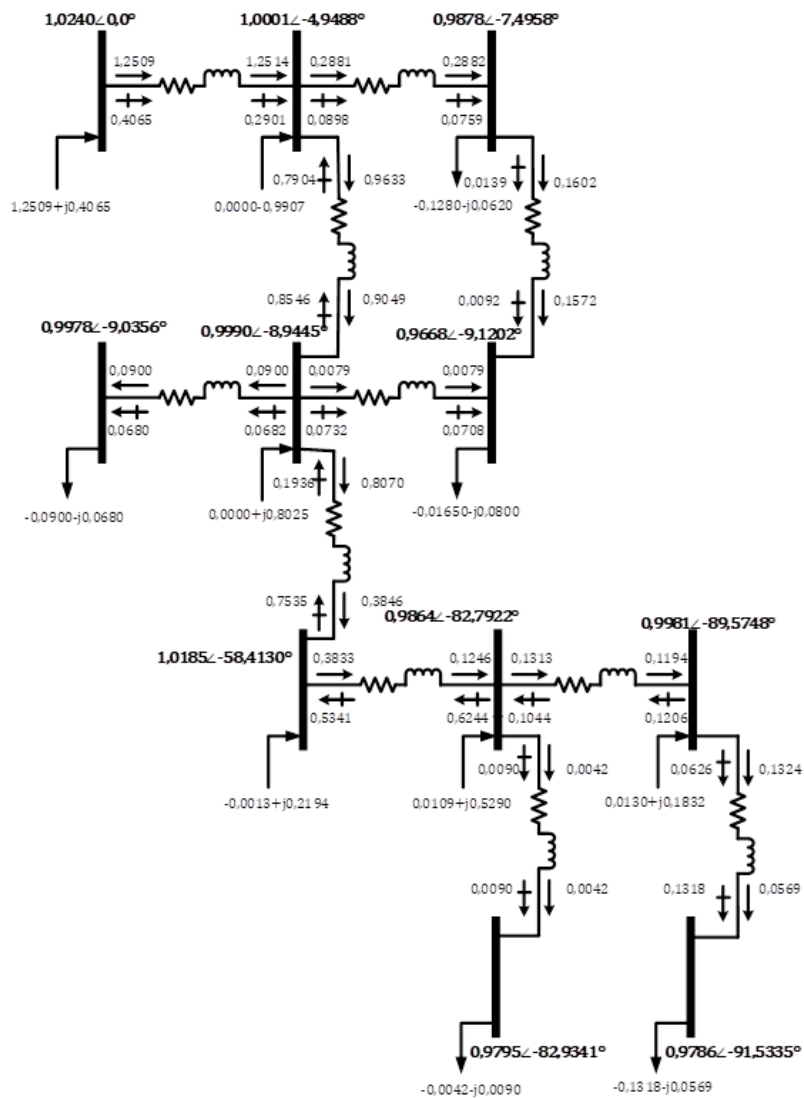


Figure 3.13: CV-Power Flows and State Variables Plotting.

4 Complex-Valued Power System State Estimation - (CV-PSSE)

4.1 Introduction

With the deployment of wide-area synchrophasor measurements that provide metered values of voltage and current phasors of a power system and the installation of power electronic devices such as FACTS devices and HVDC links, the formulation of power system state estimation in the complex domain becomes an important research topic [46], [47], [48].

Optimization problems in the complex domain are frequently encountered in applied mathematics and in signal processing [49], [11], [6], [10], [50], in control theory, in artificial neural networks [51], [52], and in biomedicine, to name a few. In power systems, a few papers have been recently published that deal with power flow calculations for power transmission and distribution systems modeled in the complex domain using both iterative and non-iterative methods [17], [16], [18], but none in power system state estimation. The solution methods of these problems often require a first- or second-order approximation of the objective function. However, such methods cannot be applied to real functions of complex variables because they are non-analytic in their arguments and therefore, for these functions Taylor series expansions do not exist. To overcome this difficulty, the objective function is usually redefined as separate functions of the real and imaginary parts of its complex arguments so that standard optimization methods can be applied. Although not widely known, it is also possible to construct an extended objective function that includes not only the original complex state variables, but also their complex conjugates and then apply the Wirtinger calculus [2], [3]. This property lies on the fact that if a function is analytic in the space spanned by $\Re\{x\}$ and $\Im\{x\}$ in \mathbb{R} , it is also analytic in the space spanned by x and x^* in \mathbb{C} .

In complex analysis of functions of complex variables, the Wirtinger operators are partial differential operators of the first order that are similar to the ordinary derivatives with respect to real variables. These operators allow the construction of a differential calculus of functions of complex variables that is entirely analogous to the ordinary differential calculus of functions of real variables [4]. In this thesis, we take advantage of the fact that the power flow equations on which the state estimation model relies lends itself well to a complex-valued formulation to derive the solution for the complex-valued power system state estimation that minimizes a WLS criterion using the Wirtinger calculus. Finally, we derive a Gauss-Newton iterative algorithm for solving the complex-valued power system state estimation problem while using the QR -factorization of the complex-valued Jacobian matrix.

The remaining part of the section is organized as follows. Subsection 2 provides a formal introduction to the complex-valued power system weighted-least-squares state estimation, including the derivation of the nonlinear measurement model; the Gauss-Newton algorithm; the high-order Levenberg-Marquardt algorithm; the QR algorithm as applied to the PSSE problems with emphasis to the direction of maximum rate of change of the cost function, all in conjugate coordinates. Finally, the Subsection 3 describes two QRD -algorithms, both addressed for the factorization of matrices in the \mathbb{C} -domain.

4.2 Complex-Valued WLS Power System State Estimation

4.2.1 Complex-Valued Nonlinear Measurement Model

In this work, the nonlinear model of the measurements includes additive errors that follow a complex multivariate Gaussian distribution as proposed by Van Den Bos [53]; the reader is referred to [49], [50] and [54] for further details on the subject matter. Let $\underline{\mathbf{z}}_c$ denote a measurement vector of complex random variables defined in the complex conjugate coordinate as

$$\underline{\mathbf{z}}_c = (z_1 \cdots z_m, z_1^* \cdots z_m^*)^T, \quad \underline{\mathbf{z}}_c \in \mathbb{C}^{2m \times 1} \quad (156)$$

with

$$z_i = a_i + j b_i \quad \text{and} \quad z_i^* = a_i - j b_i, \quad (157)$$

where $a_i, b_i \in \mathbb{R}$. Moreover, we assume that the real variables a_i and b_i , for $i = 1, \dots, m$, are normally distributed. Therefore, the power system state estimation nonlinear model in the \mathbb{C} -domain is expressed as

$$\underline{\mathbf{z}}_c = \underline{\mathbf{h}}_c(\underline{\mathbf{x}}_c) + \underline{\omega}_c, \quad (158)$$

$$E(\underline{\omega}_c) = 0, \quad E(\underline{\omega}_c \underline{\omega}_c^H) = \underline{\Omega}_c. \quad (159)$$

where $\underline{\mathbf{z}}_c = (\underline{\mathbf{z}}, \underline{\mathbf{z}}^*)$ is a vector of complex-valued measurements of dimension $(2m \times 1)$; $\underline{\mathbf{x}}_c = (\underline{\mathbf{x}}, \underline{\mathbf{x}}^*)$ is a vector of complex-valued state variables of dimension $(2n \times 1)$; $\underline{\mathbf{h}}_c(\underline{\mathbf{x}}_c)$ is a vector of nonlinear functions of dimension $(2m \times 1)$ that maps $\underline{\mathbf{z}}_c$ to $\underline{\mathbf{x}}_c$; $\underline{\omega}_c$ is a vector of a complex measurement random errors of dimension $(2m \times 1)$; $\underline{\Omega}_c$ is a Hermitian positive-definite covariance matrix of $\underline{\omega}_c$ of dimension $(2m \times 2m)$. The superscript $(\cdot)^H$ stands for Hermitian operator, that is, the transpose complex conjugate operation.

4.2.2 Complex-Valued Gauss-Newton Algorithm

As shown in [6], the complex-valued WLS state estimator minimizes an objective function defined as

$$\underset{\underline{\mathbf{x}}_c}{\operatorname{argmin}} \mathcal{J}(\underline{\mathbf{x}}_c) = \frac{1}{2} (\underline{\mathbf{z}}_c - \underline{\mathbf{h}}_c(\underline{\mathbf{x}}_c))^H \underline{\Omega}_c^{-1} (\underline{\mathbf{z}}_c - \underline{\mathbf{h}}_c(\underline{\mathbf{x}}_c)). \quad (160)$$

The necessary condition of optimality is given by

$$\frac{\partial \mathcal{J}(\underline{\mathbf{x}}_c)}{\partial \underline{\mathbf{x}}_c} = -\mathbf{H}(\underline{\mathbf{x}}_c)^H \underline{\Omega}_c^{-1} (\underline{\mathbf{z}}_c - \underline{\mathbf{h}}_c(\underline{\mathbf{x}}_c)) = 0. \quad (161)$$

By applying a first order Taylor series expansion of $\underline{\mathbf{h}}_c(\underline{\mathbf{x}}_c)$ about $\underline{\mathbf{x}}_c^{(\nu)}$, we get

$$\underline{\mathbf{h}}_c(\underline{\mathbf{x}}_c) = \underline{\mathbf{h}}_c(\underline{\mathbf{x}}_c^{(\nu)}) + \mathbf{H}(\underline{\mathbf{x}}_c^{(\nu)}) (\underline{\mathbf{x}}_c - \underline{\mathbf{x}}_c^{(\nu)}). \quad (162)$$

By replacing (162) into (161), we obtain

$$\mathbf{H}(\underline{\mathbf{x}}_c^{(\nu)})^H \underline{\Omega}_c^{-1} \left[\underline{\mathbf{z}}_c - \underline{\mathbf{h}}_c(\underline{\mathbf{x}}_c^{(\nu)}) - \mathbf{H}(\underline{\mathbf{x}}_c^{(\nu)}) (\underline{\mathbf{x}}_c - \underline{\mathbf{x}}_c^{(\nu)}) \right] = 0, \quad (163)$$

yielding the updated estimated state vector expressed as

$$\underline{\mathbf{x}}_c^{(\nu+1)} = \underline{\mathbf{x}}_c^{(\nu)} + \mathbf{G}(\underline{\mathbf{x}}_c^{(\nu)})^{-1} \mathbf{H}(\underline{\mathbf{x}}_c^{(\nu)})^H \underline{\Omega}_c^{-1} \underline{\Delta \mathbf{z}}_c^{(\nu)}, \quad (164)$$

where $\mathbf{G}(\underline{\mathbf{x}}_c^{(\nu)}) = \mathbf{H}(\underline{\mathbf{x}}_c^{(\nu)})^H \boldsymbol{\Omega}_c^{-1} \mathbf{H}(\underline{\mathbf{x}}_c^{(\nu)})$ and $\Delta \underline{\mathbf{z}}_c^{(\nu)} = \underline{\mathbf{z}}_c - \underline{\mathbf{h}}_c(\underline{\mathbf{x}}_c^{(\nu)})$. The iterations are stopped when

$$\left\| \Delta \underline{\mathbf{x}}_c^{(\nu)} \right\|_{\infty} \leq \text{tol}, \text{ e.g., } 10^{-3}, \quad (165)$$

where $\|\cdot\|_{\infty}$ is the infinity norm and ν is the iteration counter.

Note that in (161), $\mathbf{H}(\underline{\mathbf{x}}_c)$ is the Jacobian matrix of dimension $(2m \times 2n)$ defined in the complex domain as

$$\mathbf{H}(\underline{\mathbf{x}}_c) \triangleq \frac{\partial \underline{\mathbf{h}}_c(\underline{\mathbf{x}}_c)}{\partial \underline{\mathbf{x}}_c} \triangleq \begin{pmatrix} \frac{\partial \underline{\mathbf{h}}_c(\underline{\mathbf{x}}_c)}{\partial \underline{\mathbf{x}}} & \frac{\partial \underline{\mathbf{h}}_c(\underline{\mathbf{x}}_c)}{\partial \underline{\mathbf{x}}^*} \\ \frac{\partial \underline{\mathbf{h}}_c^*(\underline{\mathbf{x}}_c)}{\partial \underline{\mathbf{x}}} & \frac{\partial \underline{\mathbf{h}}_c^*(\underline{\mathbf{x}}_c)}{\partial \underline{\mathbf{x}}^*} \end{pmatrix}. \quad (166)$$

Let $\mathbf{J}_h = \frac{\partial \underline{\mathbf{h}}_c(\underline{\mathbf{x}}_c)}{\partial \underline{\mathbf{x}}}$ and $\mathbf{J}_h^d = \frac{\partial \underline{\mathbf{h}}_c(\underline{\mathbf{x}}_c)}{\partial \underline{\mathbf{x}}^*}$ be Jacobian submatrices of dimension $(m \times n)$. They are obtained through the Wirtinger partial derivatives with respect to the complex and the complex conjugate state vector using the rule stated in (17) and (18), respectively. Let us define the Jacobian matrix as

$$\mathbf{J}_c(\underline{\mathbf{x}}_c) = (\mathbf{J}_h \quad \mathbf{J}_h^d). \quad (167)$$

In the important special case given by (160) where $\mathcal{J}(\underline{\mathbf{x}}_c)$ is a real-valued function of complex variables, the following property holds:

$$\mathcal{J}(\underline{\mathbf{x}}_c) \in \mathbb{R} \Rightarrow \frac{\partial \mathcal{J}(\underline{\mathbf{x}}_c)}{\partial \underline{\mathbf{x}}} = \left(\frac{\partial \mathcal{J}(\underline{\mathbf{x}}_c)}{\partial \underline{\mathbf{x}}^*} \right)^* = (\mathbf{J}_h^d)^*. \quad (168)$$

Therefore, taking into account the rule expressed in (48) and the property stated in (168), (166) becomes

$$\mathbf{H}(\underline{\mathbf{x}}_c) = \begin{pmatrix} \mathbf{J}_h & \mathbf{J}_h^d \\ (\mathbf{J}_h^d)^* & (\mathbf{J}_h)^* \end{pmatrix} = \begin{pmatrix} \mathbf{J}_c(\underline{\mathbf{x}}_c) \\ \mathbf{J}_c^*(\underline{\mathbf{x}}_c) \mathbf{S} \end{pmatrix}, \quad (169)$$

where \mathbf{S} is a swap operator that permutes blocks of m rows or blocks of n columns depending upon whether \mathbf{S} pre-multiplies or post-multiplies a matrix, respectively. Moreover, this operator is an isomorphism from \mathbb{C} to the dual space \mathbb{C}^* , which obeys the properties $\mathbf{S}^{-1} = \mathbf{S}^T = \mathbf{S}$. It shows that \mathbf{S} is symmetric and is equal to its own inverse, that is, $\mathbf{S}^2 = I$. For instance, as shown in [5], this matrix is defined as

$$\mathbf{S} \triangleq \begin{bmatrix} 0 & I_n \\ I_n & 0 \end{bmatrix}, \quad (170)$$

where I_n is the $(n \times n)$ -identity matrix.

Now, the complex-valued gain matrix $\mathbf{G}(\widehat{\underline{\mathbf{x}}}_c)$ is expressed as

$$\mathbf{G}(\widehat{\underline{\mathbf{x}}}_c) = \begin{pmatrix} \mathbf{G}_{\underline{\mathbf{x}}\underline{\mathbf{x}}} & \mathbf{G}_{\underline{\mathbf{x}}^*\underline{\mathbf{x}}} \\ \mathbf{G}_{\underline{\mathbf{x}}\underline{\mathbf{x}}^*} & \mathbf{G}_{\underline{\mathbf{x}}^*\underline{\mathbf{x}}^*} \end{pmatrix}, \quad (171)$$

where $\mathbf{G}_{\underline{\mathbf{x}}^*\underline{\mathbf{x}}} = (\mathbf{G}_{\underline{\mathbf{x}}\underline{\mathbf{x}}})^*$ and $\mathbf{G}_{\underline{\mathbf{x}}\underline{\mathbf{x}}^*} = (\mathbf{G}_{\underline{\mathbf{x}}^*\underline{\mathbf{x}}})^*$, all of dimension $(n \times n)$. Then, it follows from (168) that

$$\begin{aligned} \mathbf{G}_{\underline{\mathbf{x}}\underline{\mathbf{x}}} &= \\ &= \frac{1}{2} \left[\left(\frac{\partial \underline{\mathbf{h}}}{\partial \underline{\mathbf{x}}} \right)^H \boldsymbol{\Omega}_c^{-1} \left(\frac{\partial \underline{\mathbf{h}}}{\partial \underline{\mathbf{x}}} \right) + \left(\left(\frac{\partial \underline{\mathbf{h}}}{\partial \underline{\mathbf{x}}} \right)^H \boldsymbol{\Omega}_c^{-1} \left(\frac{\partial \underline{\mathbf{h}}}{\partial \underline{\mathbf{x}}^*} \right) \right)^* \right], \\ &= \frac{1}{2} \left[\mathbf{J}_h^H \boldsymbol{\Omega}_c^{-1} \mathbf{J}_h + \left(\mathbf{J}_h^d{}^H \boldsymbol{\Omega}_c^{-1} \mathbf{J}_h^d \right)^* \right], \end{aligned} \quad (172)$$

Similarly, we get

$$\begin{aligned}
\mathbf{G}_{\underline{\mathbf{x}}^* \underline{\mathbf{x}}} &= \\
&= \frac{1}{2} \left[\left(\frac{\partial \mathbf{h}}{\partial \underline{\mathbf{x}}} \right)^H \boldsymbol{\Omega}_c^{-1} \left(\frac{\partial \mathbf{h}}{\partial \underline{\mathbf{x}}^*} \right) + \left(\left(\frac{\partial \mathbf{h}}{\partial \underline{\mathbf{x}}^*} \right)^H \boldsymbol{\Omega}_c^{-1} \left(\frac{\partial \mathbf{h}}{\partial \underline{\mathbf{x}}} \right) \right)^* \right], \\
&= \frac{1}{2} \left[\mathbf{J}_h^H \boldsymbol{\Omega}_c^{-1} \mathbf{J}_h^d + \left(\mathbf{J}_h^d{}^H \boldsymbol{\Omega}_c^{-1} \mathbf{J}_h \right)^* \right].
\end{aligned} \tag{173}$$

4.2.3 Complex-Valued High-Order Levenberg-Marquardt Algorithm

As stated before, the key idea is to enhance the condition number of the complex-valued Jacobian matrix when updating the estimated state variables in (176), yielding

$$\Delta \underline{\mathbf{x}}_c^{(\nu)} = \begin{pmatrix} \tilde{\mathbf{H}}(\hat{\underline{\mathbf{x}}}_c) \\ \sqrt{\eta} \mathbf{I} \end{pmatrix}^\dagger \begin{pmatrix} \Delta \tilde{\underline{\mathbf{z}}}_c \\ \mathbf{0} \end{pmatrix}, \tag{174}$$

where $\eta > 0$ is the Levenberg-Marquardt regularization parameter which influences both the length and direction of the update to be added to the estimated variables that minimize the objective function. Notice that the \dagger operator is defined as the Moore-Penrose pseudoinverse [42]. A detailed derivation regarding this enhancement that adds numerical robustness and better performance to the power system state estimation, regardless the coordinate numbers domain, can be found in our paper [55].

4.2.4 Complex-Valued PSSE Numerical Solutions

The complex-valued power system state estimation numerical solution is addressed by solving the weighted form of the right-hand side (*rhs*) of (161), yielding

$$\tilde{\mathbf{H}}(\hat{\underline{\mathbf{x}}}_c) \Delta \underline{\mathbf{x}}_c^{(\nu)} = \Delta \tilde{\underline{\mathbf{z}}}_c, \tag{175}$$

where $\tilde{\mathbf{H}}(\hat{\underline{\mathbf{x}}}_c) = \boldsymbol{\Omega}_c^{-1/2} \mathbf{H}(\hat{\underline{\mathbf{x}}}_c)$ is of dimension $(2m \times 2n)$ and $\Delta \tilde{\underline{\mathbf{z}}}_c = \boldsymbol{\Omega}_c^{-1/2} \Delta \underline{\mathbf{z}}_c$ is of dimension $(2m \times 1)$. The incremental change in the state vector is calculated via

$$\Delta \underline{\mathbf{x}}_c^{(\nu)} = \tilde{\mathbf{H}}(\hat{\underline{\mathbf{x}}}_c)^\dagger \Delta \tilde{\underline{\mathbf{z}}}_c, \tag{176}$$

where the \dagger operator is defined as the Moore-Penrose pseudoinverse [56].

Two QR -algorithms in the \mathbb{C} domain based on the Givens rotations and as described in [7], [8] have been implemented and tested. Similarly, the well-known real-valued algorithm proposed in [26] and applied to PSSE by [27], [28], and [29] can be accordingly converted to the complex domain. To avoid explicitly storing the Q -matrix, we apply the QR -transformation to the augmented matrix, $\mathbf{H}_a(\hat{\underline{\mathbf{x}}}_c)$, given by

$$\mathbf{H}_a(\hat{\underline{\mathbf{x}}}_c) = \begin{bmatrix} \tilde{\mathbf{H}}(\hat{\underline{\mathbf{x}}}_c) & \Delta \tilde{\underline{\mathbf{z}}}_c \end{bmatrix}. \tag{177}$$

By storing the rotations in compact form the complex-valued Jacobian matrix can be kept constant and only the right-hand-side vector is updated throughout the final iterations. The solution of the state vector increment given by (176) is found by executing a simple back-substitution of (177) after performing unitary transformations to the latter matrix, resulting in

$$\tilde{\mathbf{H}}_a(\hat{\underline{\mathbf{x}}}_c) = \begin{bmatrix} \mathbf{T}_c & \Delta \tilde{\underline{\mathbf{z}}}_c \end{bmatrix}. \tag{178}$$

Here, \mathbf{T}_c is an upper triangular matrix of dimension $(2n \times 2n)$ and $\Delta\tilde{\mathbf{z}}_c$ comprises the corresponding rows in the updated *RHS* vector of dimension $(2n \times 1)$. Finally, (176) is solved by performing a back-substitution via

$$\Delta\mathbf{x}_c^{(\nu)} = \mathbf{T}_c \Delta\tilde{\mathbf{z}}_c. \quad (179)$$

Note that when executing the algorithm given by (179), only the complex conjugate state vector, \mathbf{x}^* , has to be updated. Indeed, in the sequel is shown that the complex conjugate gradient gives the direction of maximum rate of change of the cost function. Therefore, the steps defined in (165) and (179) can be numerically decoupled; consequently, only the Jacobian matrix as stated in (167), i.e., associated with $\Delta\mathbf{z}_c^{(\nu)} = \mathbf{z}_c - \mathbf{h}_c(\mathbf{x}_c^{(\nu)})$, has to be stored and factorized. It becomes possible because the Jacobian matrix is redundant and has a very nice property as stated in (168) and also showed in (169). In the sequel this issue is better clarified and explored.

4.2.5 Direction of Maximum Rate of Change of the Cost Function

As shown by Bonet [11], the necessary and sufficient conditions satisfied by the minimum point of the WLS objective function, $\mathcal{J}(\hat{\mathbf{x}}_c)$, given by (160) with respect to a complex vector $\hat{\mathbf{x}}_c$ are expressed as

$$\nabla_{\mathbf{x}} \mathbf{h}_c(\hat{\mathbf{x}}_c) = \mathbf{0}, \quad (180)$$

$$\nabla_{\mathbf{x}^*} \mathbf{h}_c(\hat{\mathbf{x}}_c) = \mathbf{0}. \quad (181)$$

They state that the cogradient and the conjugate cogradient of $\mathcal{J}(\hat{\mathbf{x}}_c)$ are equal to zero at the minimum point. Consequently, any small change in the state vector, $\Delta\mathbf{x}_c$, may or may not result in a change in the cost function value depending on the search direction. In the \mathbb{C} domain, Bonet [11] proved that the direction of maximum rate of change of the cost function is that of the cogradient given by (181). Let us summarize the main steps of Bonet's proof by using the differential rule given by (48) for vectors, which leads to

$$d\mathbf{h}_c = (\nabla_{\mathbf{x}_c} \mathbf{h}_c(\mathbf{x}_c))^T d\mathbf{x}_c + (\nabla_{\mathbf{x}_c^*} \mathbf{h}_c(\mathbf{x}_c))^T d\mathbf{x}_c^* \in \mathbb{R}. \quad (182)$$

Identifying the expression $\nabla_{\mathbf{a}} = \frac{1}{2}(\nabla_{\mathbf{x}_c} + \nabla_{\mathbf{x}_c^*})$ of the real part of a complex vector results in

$$d\mathbf{h}_c = 2 \times \Re \left\{ (\nabla_{\mathbf{x}_c} \mathbf{h}_c(\mathbf{x}_c))^T d\mathbf{x}_c \right\}, \quad (183)$$

By applying the multivariate equivalent property stated in (168) to (183), we get

$$d\mathbf{h}_c = 2 \times \Re \left\{ (\nabla_{\mathbf{x}_c^*} \mathbf{h}_c(\mathbf{x}_c))^H d\mathbf{x}_c \right\}. \quad (184)$$

which is proportional to the inner product of two complex-valued vectors, $\nabla_{\mathbf{x}_c^*} \mathbf{h}_c(\mathbf{x}_c)$ and $d\mathbf{x}_c$. When the vectors $\nabla_{\mathbf{x}_c^*} \mathbf{h}_c(\mathbf{x}_c)$ and $d\mathbf{x}_c$ are orthogonal, then the inner product is null, which makes the rate of change of the cost function to vanish at a stationary point. Recall that in this special case the cogradient vector $\nabla_{\mathbf{x}_c^*} \mathbf{h}_c(\mathbf{x}_c)$ is orthogonal to the contours of the cost function as shown in Fig. 2.1.

4.2.6 Numerical Decoupled Solutions

Two algorithms are proposed aiming to mitigate the computational overhead, i.e., the iterative searching for the final state variables vector. Both are based on the very nice properties stated in

(168) and (184). These properties allow us to decouple the numerical solution of the weighted form referred to the right-hand side of (161) yielding

$$\tilde{\mathbf{J}}_c(\hat{\mathbf{x}}_c)^{(\nu)} \Delta \mathbf{x}_c^{(\nu)} = \Delta \tilde{\mathbf{z}}^{(\nu)}, \quad (185)$$

which in expanded form leads to

$$\mathbf{\Omega}^{-1/2} \begin{bmatrix} \mathbf{J}_h & \mathbf{J}_h^d \end{bmatrix}^{(\nu)} \begin{pmatrix} \Delta \mathbf{x}^{(\nu)} \\ \Delta \mathbf{x}^{*(\nu)} \end{pmatrix} = \mathbf{\Omega}^{-1/2} \Delta \mathbf{z}^{(\nu)}, \quad (186)$$

where $\mathbf{\Omega}^{-1/2}$ and $(\mathbf{J}_h \ \mathbf{J}_h^d)$ are of dimension $(m \times m)$ and $(m \times 2n)$, respectively. Moreover, $\Delta \mathbf{z}^{(\nu)} = \mathbf{z} - \mathbf{h}(\hat{\mathbf{x}}^{(\nu)})$. Thus, the solution of (186) allows to update the state variables for the first time at current iteration, as

$$\mathbf{x}_c^{(\nu)} = \mathbf{x}_c^{(\nu-1)} + \Delta \mathbf{x}_c^{(\nu)}, \quad (187)$$

Similarly, the other half linear system of equations in (161) is given by

$$\tilde{\mathbf{J}}_c^*(\hat{\mathbf{x}}_c) \mathbf{S} \Delta \mathbf{x}_c^{(\nu)} = \Delta \tilde{\mathbf{z}}^{*(\nu)} \quad (188)$$

where \mathbf{S} is a swap matrix which post-multiplies $\tilde{\mathbf{J}}_c^*(\hat{\mathbf{x}}_c)$, yielding

$$\left(\mathbf{\Omega}^{-1/2}\right)^* \left[\left(\mathbf{J}_h^d\right)^* \ \left(\mathbf{J}_h\right)^*\right]^{(\nu)} \begin{pmatrix} \Delta \mathbf{x}^{(\nu)} \\ \Delta \mathbf{x}^{*(\nu)} \end{pmatrix} = \left(\mathbf{\Omega}^{-1/2}\right)^* \Delta \mathbf{z}^{*(\nu)}, \quad (189)$$

thus, the solution of (189) updates the state variables vector for the second time at the current iteration, yielding

$$\mathbf{x}_c^{(\nu)} = \mathbf{x}_c^{(\nu-1)} + \Delta \mathbf{x}_c^{(\nu)}. \quad (190)$$

The steps (185-190) is the algorithm called complex-valued fast decoupled state estimation, CV-FDSE for short, which allows to speed up the convergence process once the state variables vector is twice updated at each iteration.

On the other hand, the second algorithm is based just on the two first steps of CV-FDSE, i.e., (186-187), because the solution obtained through this sub-system of equations depicts the direction of maximum rate of change in the cost function (see Fig. 2.1).

In this thesis, the results produced by these two algorithms are not presented but will be discussed in the forthcoming papers.

4.3 Complex-Valued Factorization Algorithms

Two *QR-Decomposition (QRD)* algorithms are investigated in this thesis. The first one is the *Three-Angle Complex Rotations (TACR)*, which is derived in polar coordinates [7] whereas the second algorithm is based on the *Fast Plane Rotations* [8] that is derived in complex plane. Both approaches are presented in the the sequel. Nonetheless, we have recommended the TACR algorithm for performing the Jacobian matrix factorization in \mathbb{C} -domain because it is very easy encoding. Notice that both algorithms are derived from their counterpart in \mathbb{R} -domain [26]. Thus, one believe that both follow the same standards of *fill-in suppression* when ordering schemes addressed for *QR-decomposition* in real domain are applied. Nonetheless, this issue should be investigated later. In this sense, the set of algorithms reported in [57] should be tried in \mathbb{C} -domain, besides news ones proposed in the updated state-of-the-art, e.g., [58], [59].

4.3.1 Three-Angle Complex Rotation Algorithm

The *TACR* algorithm is a *QR-Decomposition (QRD) unitary transformation (not orthogonal!.)* because it operates in *complex domain*. Aiming this target, consider the following complex matrix $H_{2 \times 2}$ defined by

$$H_{2 \times 2} = \begin{bmatrix} A e^{j\theta_a} & C e^{j\theta_c} \\ B e^{j\theta_b} & D e^{j\theta_d} \end{bmatrix} \quad (191)$$

where $j = \sqrt{-1}$; A, B, C, D represent the magnitude and $\theta_a, \theta_b, \theta_c, \theta_d$ stand for the angle of the matrix entries.

The *complex Givens rotations* is described by two rotation angles θ_1, θ_2 , through the following matrix transformation:

$$\begin{bmatrix} \cos \theta_1 & \sin \theta_1 e^{j\theta_2} \\ -\sin \theta_1 e^{-j\theta_2} & \cos \theta_1 \end{bmatrix} \begin{bmatrix} A e^{j\theta_a} & C e^{j\theta_c} \\ B e^{j\theta_b} & D e^{j\theta_d} \end{bmatrix} = \begin{bmatrix} X e^{j\theta_x} & Y e^{j\theta_y} \\ 0 & Z e^{j\theta_z} \end{bmatrix} \quad (192)$$

where angles θ_1, θ_2 are chosen to set to zero the matrix element below the main diagonal, and are defined by

$$\begin{aligned} \theta_1 &= \tan^{-1}(B/A) \\ \theta_2 &= \theta_a - \theta_b \end{aligned} \quad (193)$$

It is easy to verify that using (193) leads to an upper triangular matrix with complex diagonal elements (192).

On the other hand, an alternative approach for the aforementioned *QRD* may be realized through a *unitary* matrix transformation which can be reached as follows:

$$Z = \begin{bmatrix} \cos \theta_1 e^{j\theta_2} & \sin \theta_1 e^{j\theta_3} \\ -\sin \theta_1 e^{-j\theta_2} & \cos \theta_1 e^{j\theta_3} \end{bmatrix} \quad (194)$$

where

$$\begin{aligned} \theta_1 &= \tan^{-1}(B/A) \\ \theta_2 &= -\theta_a \\ \theta_3 &= -\theta_b \end{aligned} \quad (195)$$

Remark that in (195) the *three angles* that give a name to the algorithm are function of $Ae^{j\theta_a}$ and $Be^{j\theta_b}$, i.e., depend only of two planes to be rotated. Then, the suggested *TACR* technique results in a new triangular matrix as showed below:

$$\begin{bmatrix} \cos \theta_1 e^{j\theta_2} & \sin \theta_1 e^{j\theta_3} \\ -\sin \theta_1 e^{-j\theta_2} & \cos \theta_1 e^{j\theta_3} \end{bmatrix} \begin{bmatrix} A e^{j\theta_a} & C e^{j\theta_c} \\ B e^{j\theta_b} & D e^{j\theta_d} \end{bmatrix} = \begin{bmatrix} X & Y e^{j\theta_y} \\ 0 & Z e^{j\theta_z} \end{bmatrix}, \quad (196)$$

Note that the *TACR* matrix transformation in (196) introduces the real element X on the matrix diagonal. Application of the *TACR* approach for an $n \times n$ matrix will lead to the appearance of real elements on the matrix diagonal except for the lowest one.

In order to avoid complex division, for instance, when doing the backsubstitution step within the solution of linear system of equations, it is advantageous to eliminate the complex lowest diagonal element. Therefore, aiming this target, the further simple unitary transformation is required:

$$\begin{bmatrix} 1 & 0 \\ 1 & e^{-j\theta_z} \end{bmatrix} \begin{bmatrix} X & Y & e^{j\theta_y} \\ 0 & Z & e^{j\theta_z} \end{bmatrix} = \begin{bmatrix} X & Y & e^{j\theta_y} \\ 0 & Z & \end{bmatrix}. \quad (197)$$

On the other hand, the aforementioned additional unitary transformation can be needless if the *TACR* algorithm operates over an augmented coefficient matrix (178) aiming the solution of the same linear system of equations. In other words, it means that the original coefficient matrix should be added of one column comprised by the *right hand side* of the linear system of equations to be solved. Consequently, the lowest diagonal element of the coefficient matrix naturally appears as a real number.

4.3.2 Complex-Valued Fast Givens Rotations

The complex-valued fast Givens rotations (CVFGR) is a very interesting algorithm aiming a *QR-Decomposition* of matrices once the computations are performed incrementally, i.e., as the data arrives sequentially in time [8]. It allows us to reduce the overall latency and hardware resources drastically. In the forthcoming papers, the *TACR*; the CVFGR and those which are well known because they were successfully applied to power system state estimation by [27], [28], and [29], once they are accordingly converted from real- toward complex-domain, their performance will be compared.

5 Complex-Valued Bad Data Processing

Complex-valued signals have been applied to a great number of research areas, such as communications; radar; echocardiogram images; features for face recognition; geophysics, optics, and electromagnetics, to name a few [49]. Nowadays, in power area the electric companies around the world have deployed a large number of synchro-phasor measurement units (PMUs) for monitoring their power transmission systems. Hence, the PMU measurement is an enough motivation to extend the model of complex random variables towards the whole system of measurements in an Energy Management System (EMS). In this sense, a common assumption that is taken when dealing with complex random signals is that they are proper or circular, which implies that some aspect of the statistics of a complex signal is ignored [60], [61], [62], [63], [64]. A proper complex random variable is uncorrelated with its complex conjugate, and a circular complex random variable has a probability density function (*pdf*) such that for any α , the *pdf* of Z and $Z' = e^{j\alpha}Z$ are invariant [60]. Although, these assumptions are mathematically convenient targeting low computational overhead, there are also many situations where proper and circular signals are very poor models of the underlying physics. To exploit the improper or noncircular nature of signals, the complete statistical characterization of complex-valued random signal, e.g., the complementary correlations (or pseudo-) correlation is required.

This section is organized as follows. Subsection 2 defines the nature of complex random signals. Subsection 3 presents the complex-valued multivariate generalized Gaussian distribution (CV-GGD). Subsection 4 presents the complex linear and nonlinear models of measurements. Subsection 5 shows the derivation of bad-data processing, detection and identification methods in complex domain. In Subsection 6 is presented the numerical results as applied to a small example and large systems as showed before within this section. Finally, in Subsection 7 some partial conclusions are stated.

5.1 Nature of Complex Random Signals

Considering a complex random variable $z = z_R + j z_I$, besides the covariance matrix calculation given by

$$\mathbf{C}_c = E[zz^H] = E[z_R^2] + E[z_I^2] = \sigma_R^2 + \sigma_I^2, \quad (198)$$

it is also necessary to include the so-called pseudo-covariance matrix [65], yielding

$$\begin{aligned} \mathbf{P}_c &= E[zz^T], \\ &= E[z_R^2] - E[z_I^2] + 2j E[z_R z_I], \\ &= \sigma_R^2 - \sigma_I^2 + 2j\rho, \end{aligned} \quad (199)$$

where σ^2 is the variance and ρ is the correlation $E[z_R z_I]$. Then, under such condition a complex Gaussian random signal is called second-order circular *iff* it is zero-mean and proper and its variance is twice the variance of real and imaginary parts: $\sigma^2 = 2 \sigma_R^2 = 2 \sigma_I^2$. However, among other many practical reasons, being the most common that due to short observation windows, the pseudo-covariance matrix should be taking into account, i.e., $\mathbf{P}_c \neq 0$. Thus, to cater for noncircularity, the literature in signal processing [61], [62], [63] have recommended the signal model based on the complex variable in the complex conjugate coordinate, i.e.

$$Z = \mathbf{M} \begin{bmatrix} z_R \\ z_I \end{bmatrix} = \begin{bmatrix} z \\ z^* \end{bmatrix}, \quad (200)$$

where the matrix $\mathbf{M} \in \mathbb{C}^{2 \times 2}$ is defined as

$$\mathbf{M} = \begin{pmatrix} 1 & j \\ 1 & -j \end{pmatrix}, \quad (201)$$

being $j = \sqrt{-1}$, and for what follows it is important to note that

$$\mathbf{M}^{-1} = \frac{1}{2} \mathbf{M}^H. \quad (202)$$

Thus, the following covariance matrix [65] can be defined

$$\boldsymbol{\Omega}_c = E[Z Z^H] = \begin{bmatrix} \mathbf{C}_c & \mathbf{P}_c \\ \mathbf{P}_c^* & \mathbf{C}_c^* \end{bmatrix}, \quad (203)$$

where $(\cdot)^*$, $(\cdot)^T$ and $(\cdot)^H$ denotes the complex conjugate, complex transpose and complex conjugate transpose (Hermitian matrix), respectively. Therefore, both second-order circular and noncircular nature of signals can be modeled for general complex processes. Remark that the $\boldsymbol{\Omega}_c$ matrix in (203) will have real-valued diagonal elements while complex-valued off-diagonal elements. For Z as defined in (200) to be second-order circular the variance of Z_R and Z_I are the same and Z_R and Z_I are uncorrelated. In this sense, a measure of second-order noncircularity is known as [66]

$$\text{The degree of impropriety} = \frac{|E[Z^2]|}{E[ZZ^*]}, \quad (204)$$

with bounds $0 \leq |E[Z^2]|/E[ZZ^*] \leq 1$, while $|E[Z^2]| = 0$ indicates circular data. Furthermore, in the complex signals processing literature the circularity measure ξ is proposed as the ratio between the standard deviation of the real and imaginary components of the signal [67]

$$\xi = \sqrt{\frac{\sigma_{Z_R}}{\sigma_{Z_I}}}. \quad (205)$$

where the value of $\xi = 1$ indicates equal powers in the real and imaginary components and thus a proper signal, whereas $\xi > 1$ indicates improperness.

Summing up, observe that circularity implies zero mean and propriety, but not vice versa. Either, impropriety implies noncircularity, but not vice versa.

5.2 CV-Multivariate Generalized Gaussian Distribution

As aforementioned, the complex statistics are not a straightforward extension of real-valued statistics. Then, let us consider the distribution of samples from a complex process in which the real and imaginary parts are Gaussian distributed. The key concept herein is to derive a compact form of the density function which can be written directly as a function of a complex argument rather than its real and imaginary parts. In this sense, a collection of m complex numbers is simply a collection of $2 \times m$ real numbers. Thus, a collection of m complex random variables is really just a collection of

$2 \times m$ real random variables with some joint distribution (density) of its real and imaginary parts in \mathbb{R}^{2m} .

Firstly, let us taking into account a vector $\underline{\eta} \in \mathbb{R}^{2m \times 1}$ as the corresponding random error of measurements as defined in *real domain*, i.e.,

$$\underline{\eta} = \left(\eta_{R_1}, \eta_{I_1}, \dots, \eta_{R_m}, \eta_{I_m} \right)^T, \quad (206)$$

and $E \left[\eta_{R_i} \right] = E \left[\eta_{I_i} \right] = 0$ for all i . In other words, the random errors have a Gaussian distribution and are samples of a circular and proper complex stochastic process. Then, the covariance matrix of $\underline{\eta}$ can be defined as

$$\mathbf{R} = E \left[\underline{\eta} \underline{\eta}^T \right]. \quad (207)$$

The distribution function of η_{R_i} and η_{I_i} is described by

$$f(\underline{\eta}) = \frac{1}{(2\pi)^m (\det \mathbf{R})^{1/2}} e^{(-\frac{1}{2} \underline{\eta}^T \mathbf{R}^{-1} \underline{\eta})}. \quad (208)$$

On the other hand, based on what was stated in (200) and equation (208), follows that

$$\begin{pmatrix} \omega_i \\ \omega_i^* \end{pmatrix} = \mathbf{M} \begin{pmatrix} \eta_{R_i} \\ \eta_{I_i} \end{pmatrix}, \quad (209)$$

where $\omega_i = (\eta_{R_i} + j \eta_{I_i})$ and \mathbf{M} is defined as in (201). Now, defining $\underline{\omega}_c \in \mathbb{C}^{2m \times 1}$ as the random error of measurements in the complex conjugate coordinate becomes

$$\underline{\omega}_c = (\omega_1, \omega_1^*, \dots, \omega_m, \omega_m^*)^T. \quad (210)$$

Then, by (209) yields

$$\underline{\omega}_c = \mathbf{A} \underline{\eta}, \quad (211)$$

where the block-diagonal matrix $\mathbf{A} \in \mathbb{C}^{2m \times 2m}$ is defined as

$$\mathbf{A} = \text{diag}(\mathbf{M}, \mathbf{M}, \dots, \mathbf{M}). \quad (212)$$

Hence, by (211) and (202) results

$$\underline{\eta} = \mathbf{A}^{-1} \underline{\omega}_c = \frac{1}{2} \mathbf{A}^H \underline{\omega}_c, \quad (213)$$

and since $\underline{\eta}$ is a real vector, thus

$$\underline{\eta} = \frac{1}{2} \mathbf{A}^T \underline{\omega}_c^*. \quad (214)$$

The covariance matrix $\mathbf{\Omega}_c \in \mathbb{C}^{2m \times 2m}$ of $\underline{\omega}_c$, by (211) becomes

$$\mathbf{\Omega}_c = \mathbf{A} \mathbf{R} \mathbf{A}^H. \quad (215)$$

Now, let us consider the quadratic form in (208) as in [53], yielding

$$\underline{\eta}^T \mathbf{R}^{-1} \underline{\eta}. \quad (216)$$

By (213), (214) and (215) this form may be written as

$$\begin{aligned} \underline{\omega}_c^H \left(\frac{1}{2}\mathbf{A}\right) \mathbf{R}^{-1} \left(\frac{1}{2}\mathbf{A}^H\right) \underline{\omega}_c &= \underline{\omega}_c^H \left(\mathbf{A} \mathbf{R} \mathbf{A}^H\right)^{-1} \underline{\omega}_c, \\ &= \underline{\omega}_c^H \mathbf{\Omega}_c^{-1} \underline{\omega}_c. \end{aligned} \quad (217)$$

Moreover, the determinant in (208) may be written as

$$\begin{aligned} \det \mathbf{R} &= \det\left(\frac{1}{2}\mathbf{A}^H \mathbf{\Omega}_c \frac{1}{2}\mathbf{A}\right), \\ &= \left(\frac{1}{2}\right)^{2m} (\det \mathbf{M}^H)^m \det \mathbf{\Omega}_c \left(\frac{1}{2}\right)^{2m} (\det \mathbf{M})^m, \\ &= \left(\frac{1}{2}\right)^{4m} (2j)^m (-2j)^m \det \mathbf{\Omega}_c, \\ &= \left(\frac{1}{2}\right)^{2m} \det \mathbf{\Omega}_c. \end{aligned} \quad (218)$$

Substitution of (217) and (218) in (208), allow to obtain the *complex-valued multivariate generalized Gaussian distribution*, yielding

$$f(\underline{\omega}_c) = \frac{1}{\pi^m (\det \mathbf{\Omega}_c)} e^{(-\underline{\omega}_c^H \mathbf{\Omega}_c^{-1} \underline{\omega}_c)}. \quad (219)$$

with $\underline{\omega}_c$ defined by (210). Moreover, note that the *pdf* depends algebraically on $\underline{\omega}_c$, i.e., ω_i and ω_i^* , but is interpreted as the joint *pdf* of η_{R_i} and η_{I_i} , and can be used for proper and improper ω_i . Now, it is straightforward to introduce a non-zero mean μ , which is the complex vector isomorphic to the mean of its real counterpart. The resulting *pdf* is

$$f(\underline{\omega}_c) = \frac{1}{\pi^m (\det \mathbf{\Omega}_c)} e^{-(\underline{\omega}_c - \mu)^H \mathbf{\Omega}_c^{-1} (\underline{\omega}_c - \mu)}. \quad (220)$$

Finally, aiming to meet the definition and format assumed before within this section, recall that $\underline{\omega}_c$ can be rearranged as follows

$$\underline{u}_c = \mathbf{S} \underline{\omega}_c = (\omega_1 \cdots \omega_m, \omega_1^* \cdots \omega_m^*)^T, \quad (221)$$

where $\mathbf{S} \in \mathbb{R}^{2m \times 2m}$ is a permutation matrix, which entries are either equal to one or to zero, and the following property holds: $\mathbf{S}^T = \mathbf{S}^{-1}$ and $|\det \mathbf{S}| = 1$, i.e., \mathbf{S} is an orthogonal matrix [68].

In Fig. 5.1 are shown different complex-valued signals nature [69]. This picture shows the scatter plots for three nature of signals: (a) ice multiparameter imaging -band radar (IPIX) data from the website <http://soma.crl.mcmaster.ca/ipix/>; (b) a 16-quadrature amplitude modulated (QAM) signal; and (c) wind data obtained from <http://mesonet.agron.iastate.edu>. While Fig. 5.2 depicts their corresponding covariance functions and complementary covariance functions.

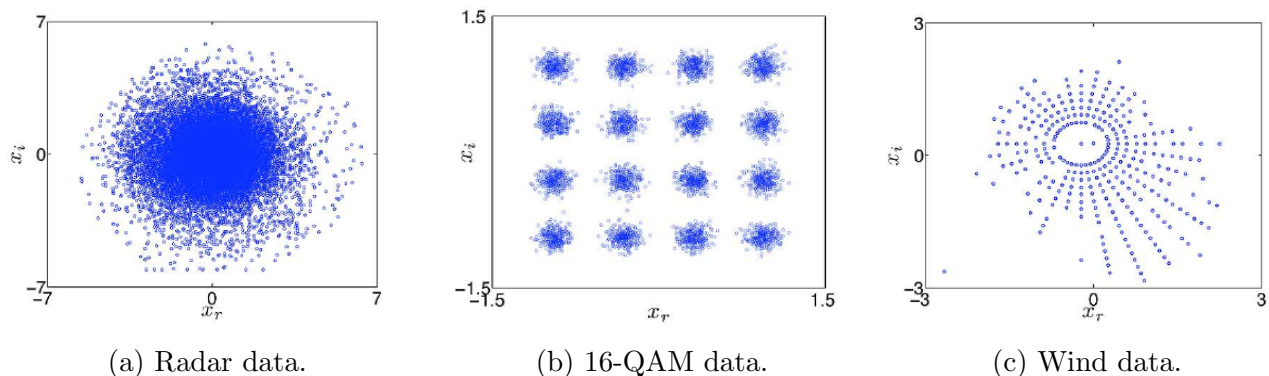


Figure 5.1: Scatter plots for (a) circular, (b) proper but noncircular, and (c) improper (and thus noncircular) data.

The radar signal in Fig. 5.2 (a) is narrow-band. Evidently, the gain and phase of the in-phase and quadrature channels are matched, as the data appear circular (and therefore proper). The uniform phase is due to carrier phase fluctuation from pulse-to-pulse and the amplitude fluctuations are due to variations in the scattering cross-section. The 16-QAM signal in Fig. 5.2 (b) has zero complementary covariance function and is therefore proper (second-order circular). However, its distribution is not rotationally invariant and therefore it is noncircular. The wind data in Fig. 5.2 (c) is noncircular and improper.

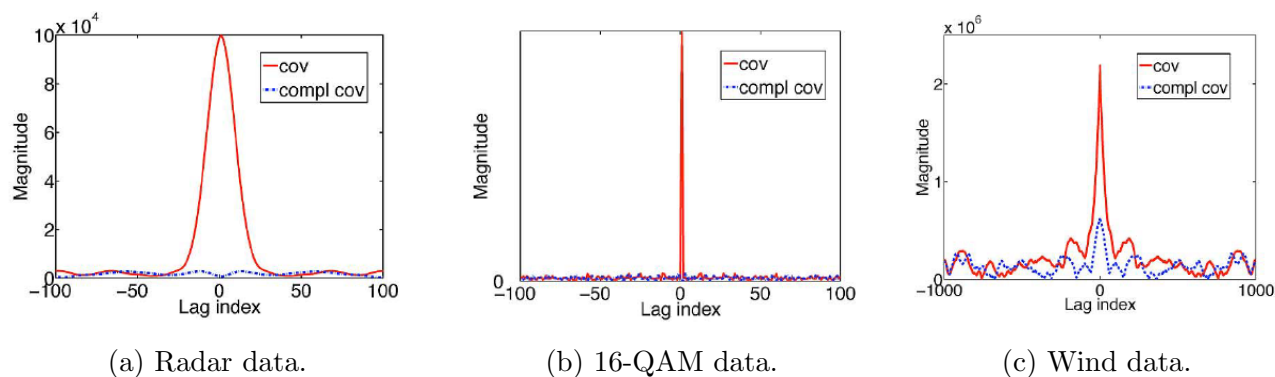


Figure 5.2: Covariance and complementary covariance function plots for the corresponding processes in Fig. 5.1: (a) circular (b) proper but noncircular; and (c) improper.

Further insights regarding the nature of complex random signals can be found in [], [70], [66] [54], [64], [9], [67], [60], [61], [62], [71], [72]. Near future, our intend is to investigate the nature of the data set that comes from a low-voltage widearea measurement system consisting of 24 PMUs installed nationwide in Brazilian university campuses: <http://www.medfasee.ufsc.br/temporeal/>. Additionally, key issues should be taken into account when a complex-valued signal is modeled within the state estimation applications, as presented in [73], [74] and [75], to cite a few.

5.3 Complex-Valued Measurements Models

5.3.1 Complex Linear Model

If the data model is linear, the minimum variance unbiased (MVU) estimator can be easily found [72]. The complex linear model has the form

$$\underline{\mathbf{z}}_c = \mathbf{H} \underline{\mathbf{x}}_c + \underline{\omega}_c, \quad (222)$$

$$E(\underline{\omega}_c) = 0, \quad E(\underline{\omega}_c \underline{\omega}_c^H) = \mathbf{\Omega}_c. \quad (223)$$

where $\underline{\mathbf{z}}_c$ is a vector of complex-valued measurements, $m \times 1$; \mathbf{H} is a known $m \times n$ complex observation matrix and full rank; $\underline{\mathbf{x}}_c$ is a complex $n \times 1$ *true* state variables vector, e.g., $(\underline{\mathbf{x}}, \underline{\mathbf{x}}^*)$, while, $\underline{\omega}_c$ is a $m \times 1$ complex random noise vector with *pdf* $\underline{\omega}_c \sim \mathcal{CN}(0, \mathbf{C}_c, \mathbf{P}_c = 0)$. Nonetheless, it is well known that strictly linear transformations of proper complex Gaussian random vectors yield again proper complex Gaussian distributed random vectors. Thus, $\underline{\mathbf{z}}_c \sim \mathcal{CN}(E[\underline{\mathbf{z}}_c], \mathbf{C}_c, \mathbf{P}_c = 0)$, where it can be shown that $E[\underline{\mathbf{z}}_c] = \mathbf{H} \underline{\mathbf{x}}_c$ and $\mathbf{\Omega}_c = \mathbf{C}_c$. Therefore, the MVU estimator of $\underline{\mathbf{x}}_c$ is given by

$$\hat{\underline{\mathbf{x}}}_c = (\mathbf{H}^H \mathbf{\Omega}_c^{-1} \mathbf{H})^{-1} \mathbf{H}^H \mathbf{\Omega}_c^{-1} \underline{\mathbf{z}}_c. \quad (224)$$

5.3.2 Complex Nonlinear Model

As already stated above, let us assume $\underline{\mathbf{z}}_c$ as a measurement vector of a complex random variables defined as

$$\underline{\mathbf{z}}_c = (z_1 \cdots z_m, z_1^* \cdots z_m^*)^T, \quad \underline{\mathbf{z}}_c \in \mathbb{C}^{2m \times 1} \quad (225)$$

with

$$z_i = z_{R_i} + j z_{I_i} \quad \text{and} \quad z_i^* = z_{R_i} - j z_{I_i}, \quad (226)$$

where $z_{R_i}, z_{I_i} \in \mathbb{R}$. Moreover, the real quantities z_{R_i} and z_{I_i} , for $i = 1, \dots, m$ are normal distributed. Therefore, under these assumptions the nonlinear complex-valued model of measurements referred to PSSE problem in \mathbb{C} -domain can be stated as follows

$$\underline{\mathbf{z}}_c = \underline{\mathbf{h}}_c(\underline{\mathbf{x}}_c) + \underline{\omega}_c, \quad (227)$$

$$E(\underline{\omega}_c) = 0, \quad E(\underline{\omega}_c \underline{\omega}_c^H) = \mathbf{\Omega}_c. \quad (228)$$

where $\underline{\mathbf{h}}_c$ is a vector of nonlinear functions that maps a complex-valued measurements, e.g., $(\underline{\mathbf{z}}, \underline{\mathbf{z}}^*)$ towards a complex-valued *true* state variables, e.g., $(\underline{\mathbf{x}}, \underline{\mathbf{x}}^*)$. The remaining variables stated in (227) and (228) are defined as aforementioned and the estimates of $\underline{\mathbf{x}}_c$, i.e., $\hat{\underline{\mathbf{x}}}_c$, are known as showed before within this section.

5.4 Complex-Valued Bad Data Detection and Identification Methods

In this work a classical bad data detection and identification methods in power system state estimation are revisited [76], [77], except that both are herein derived in complex domain.

5.4.1 Detection: Complex-Valued Chi-squared Test

It is well known that a common test performed aiming bad data detection is to compute the sum of squared magnitudes of the residual vector and compare this to a threshold. The resulting test statistic has a behavior modeled by the χ^2 -squared distribution [78].

Thus, let us assume the set of measurements as a m complex Gaussian random variables, independent and identically distributed with mean 0 and variance 1 (meaning that the covariance matrix for the residual vector, \mathbf{r}_c , is \mathbf{I}). Recall that central distributions are usually associated with the null hypothesis in a detection problem and are used to compute the probability of false alarm. In this sense, defining the real non-negative random variable $\mathcal{J}(\mathbf{r}_c)$ according to

$$\mathcal{J}(\mathbf{r}_c) = \sum_i^m |r_{c_i}|^2. \quad (229)$$

The density χ^2 -squared distribution function for $\mathcal{J}(\mathbf{r}_c)$, for simplicity this latter with its argument omitted, is given by

$$f_{\mathcal{J}}(\mathcal{J}) = \frac{1}{(m-1)!} \mathcal{J}^{m-1} e^{-\mathcal{J}} U(\mathcal{J}), \quad (230)$$

which is derived assuming the *pdf* for $|r_{c_i}|^2$ is a simple exponential. Then, Eq. (230) is the m -fold convolution of this exponential density function with itself [78]. Also, recall that $f_{\mathcal{J}}(\mathcal{J})$ is a gamma density function with an integer parameter m , and like the *pdf* defined in (219), it is cleaner and simpler than its real counterpart. Likewise, in (230) we often say that \mathcal{J} is χ^2 with m complex degrees of freedom. However, note that although a “complex degree of freedom” is like $2 \times m$ real degrees of freedom, Eq. (230) is not the usual χ^2 -squared density function with $2 \times m$ real degrees of freedom. Indeed, recall that in (219) each real random variable going into the computation of \mathcal{J} has variance $1/2$, not 1 [78], i.e.,

$$\int_{\mathbb{C}^m} f_z(z) dz = 1. \quad (231)$$

The probability that $z \in \kappa$, where κ is some subset of \mathbb{C}^m , is given by

$$p(\kappa) = \int_{\kappa} f_z(z) dz, \quad (232)$$

and the differential element dz is understood to be

$$dz = dz_{R_1} dz_{I_1} dz_{R_2} dz_{I_2} \dots dz_{R_m} dz_{I_m}. \quad (233)$$

5.4.2 Identification: Largest Normalized Residual Method

The main concern in this method is to becoming known the covariance matrix of residual prior to normalize the residual vector. Recall that the normalized residual values are obtained through the weighting of residual values by the corresponding variance values of the residual [77]. Indeed, as the same assumptions can be assumed aiming the derivation of its counterpart in complex domain through an equivalent expression, yields

$$\Sigma = [\mathbf{I} - \mathbf{H} (\mathbf{H}^H \mathbf{\Omega}_c^{-1} \mathbf{H})^{-1} \mathbf{H}^H \mathbf{\Omega}_c^{-1}] \mathbf{\Omega}_c. \quad (234)$$

where Σ is the *covariance matrix of residual* and \mathbf{H} is the power system state estimation's Jacobian matrix, as defined in (169). Hence, the complex normalized residual values are computed as follows

$$r_{n_i} = \frac{r_i}{\sqrt{\Sigma_{ii}}}. \quad (235)$$

In this sense, only an individual checking of a *real* and *imaginary* parts of r_{n_i} allows to identify which measurement violates the complex-valued measurement model. Recall that the searching for the largest normalized residual value can be processed as follows

$$\max |\underline{\mathbf{r}}_N| > \lambda (\approx 2.5). \quad (236)$$

5.4.3 Bad Data Redemption as Pseudo Measurement

Once a bad data has been identified among the measured quantities, it is advised to rescue the gross error as a pseudo measurement rather than reject it, and the reasons are twofold:

1. To mitigate the risk of loss of observability;
2. To avoid further computational overhead caused by the refactorization of Jacobian matrix.

In this section the approach aiming to become a gross error toward pseudo measurement after its redemption is employed as proposed in [79]. In this sense, the following estimates of the magnitude of the error can be posed

$$\hat{\beta}_i = \frac{\sigma_i}{\Sigma_{ii}} r_{n_i}, \quad (237)$$

Thus, the pseudo-measurement is determined as follows

$$z_i^{new} = z_i^{old} - \frac{\sigma_i}{\Sigma_{ii}} r_{n_i}. \quad (238)$$

5.5 Numerical Results Without Bad Data Processing

We first solve the complex-valued WLS estimator in a small 2-bus power system and then apply the solution method to the IEEE 14- and 30-bus systems and to the Brazilian equivalents 340- and 730-bus systems. The small power system example was simulated considering perfect measurements and a unitary co-variance matrix for the measurement errors. As for the IEEE-test systems and the two Brazilian equivalent systems, the accuracy assigned to the PMU and the SCADA measurements are 10^{-4} and 10^{-2} , respectively.

5.5.1 Small Power System Example

The one-line diagram of a 2-bus system is depicted in Fig. 5.8. The system is provided with two PMU measurements that meter the nodal voltage magnitudes and phase angles and two real and reactive power flow measurements, which are identified by means of black bullets and red triangles, respectively. In Table 5.1, the network parameters are given in *pu*.

From Fig. 5.8, the complex power injections at both buses are derived as

$$S_1 = V_1 [(y_{12}^* - j b_{12}^{sh}) V_1^* - y_{12}^* V_2^*], \quad (239)$$

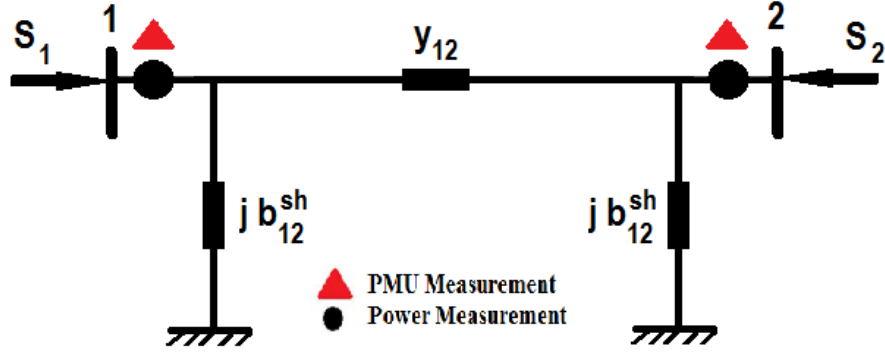


Figure 5.3: 2-Bus power system.

Table 5.1: Branches Data

Branch	Serie		Shunt	
	R	X	Charging	Y/2
$i \rightarrow j$	pu	pu	MVAr	pu
1-2	0.0203	0.1318	62.62	0.3131

$$S_2 = V_2 [(y_{12}^* - j b_{12}^{sh}) V_2^* - y_{12}^* V_1^*]. \quad (240)$$

Applying the Wirtinger calculus to (239-240) yields

$$\left. \frac{\partial S_1}{\partial V_1} \right|_{V_1^* = const.} = (y_{12}^* - j b_{12}^{sh}) V_1^* - y_{12}^* V_2^*,$$

$$\left. \frac{\partial S_1}{\partial V_1^*} \right|_{V_1 = const.} = (y_{12}^* - j b_{12}^{sh}) V_1, \quad (241)$$

$$\left. \frac{\partial S_1}{\partial V_2^*} \right|_{V_2 = const.} = -y_{12}^* V_1,$$

and

$$\left. \frac{\partial S_2}{\partial V_2} \right|_{V_2^* = const.} = (y_{12}^* - j b_{12}^{sh}) V_2^* - y_{12}^* V_1^*.$$

$$\left. \frac{\partial S_2}{\partial V_1^*} \right|_{V_1 = const.} = -y_{12}^* V_2. \quad (242)$$

$$\left. \frac{\partial S_2}{\partial V_2^*} \right|_{V_2 = const.} = (y_{12}^* - j b_{12}^{sh}) V_2.$$

Let us provide the Jacobian matrix given by (167). Here, the complex power injection measurements, S_1 and S_2 , are equal to the power flow measurements, S_{12} and S_{21} , respectively.

Table 5.3: CV-Estimated Quantities

\hat{z}_i	$\hat{z}^{(\nu=0)}$	$\hat{z}^{(\nu=1)}$	$\hat{z}^{(\nu=2)}$	$\hat{z}^{(\nu=3)}$
S_{12}	0.0000 -j 0.3131	1.4747 j 0.1745	1.8873 j 0.4815	1.8827 j 0.4248
S_{21}	0.0000 -j 0.3131	-1.4014 -j 0.0707	-1.8036 -j 0.5094	-1.7997 -j 0.4500
S_1	0.0000 -j 0.3131	1.4747 j 0.1745	1.8873 j 0.4815	1.8827 j 0.4248
S_2	0.0000 -j 0.3131	-1.4014 -j 0.0707	-1.8036 -j 0.5094	-1.7997 -j 0.4500

Table 5.4: CV-Residual Vector

<i>CV-Residual Vector</i>				
$\underline{r}^{(\nu=i)}$	$\underline{r}^{(\nu=0)}$	$\underline{r}^{(\nu=1)}$	$\underline{r}^{(\nu=2)}$	$\underline{r}^{(\nu=3)}$
r_{V_1}	0.0000 j 0.0000	0.1991 j 0.0000	-0.0097 j 0.0018	0.0000 -j 0.0000
r_{V_2}	-0.1349 -j 0.2333	0.1634 -j 0.0000	-0.0017 -j 0.0015	0.0006 -j 0.0001
$r_{S_{12}}$	1.8827 j 0.7375	0.4080 j 0.2499	-0.0046 -j 0.0571	-0.0000 -j 0.0004
$r_{S_{21}}$	-1.7998 -j 0.1366	-0.3984 -j 0.3790	0.0038 j 0.0597	-0.0001 j 0.0003
r_{S_1}	1.8827 j 0.7375	0.4080 j 0.2499	-0.0046 -j 0.0571	-0.0000 -j 0.0004
r_{S_2}	-1.7998 -j 0.1366	-0.3984 -j 0.3790	0.0038 j 0.0597	-0.0001 j 0.0003
$\mathcal{J}(\hat{\underline{x}})^{\nu=i}$	14.7654	1.1288	0.013825	8.8×10^{-7}

5.5.2 IEEE-Test Systems and the Brazilian Equivalent Systems

Table 5.5 provides for the two IEEE-test systems and the two Brazilian equivalent power systems, the total numbers of the state variables, the PMUs, and the SCADA-based measurements along with the total numbers of branches. Table 5.6 provides for the four power systems the numbers of non-zero entries of the Jacobian and the gain matrices along with the number of iterations and the total computing times of the Gauss-Newton algorithm without the implementation of any sparsity technique.

We investigate the sparsity structure of the augmented Jacobian matrix given by (169). Comparison of Figs. 5.4-5.7 reveal that the Jacobian matrices in the \mathbb{C} -domain are sparser than those in the \mathbb{R} -domain [57]. For instance, for the Brazilian equivalent 730-bus system, the Jacobian matrix in the \mathbb{C} -domain has 10,396 non-zero-elements while in the \mathbb{R} -domain, it has 18,403 non-zero-elements; it is about 45% sparser.

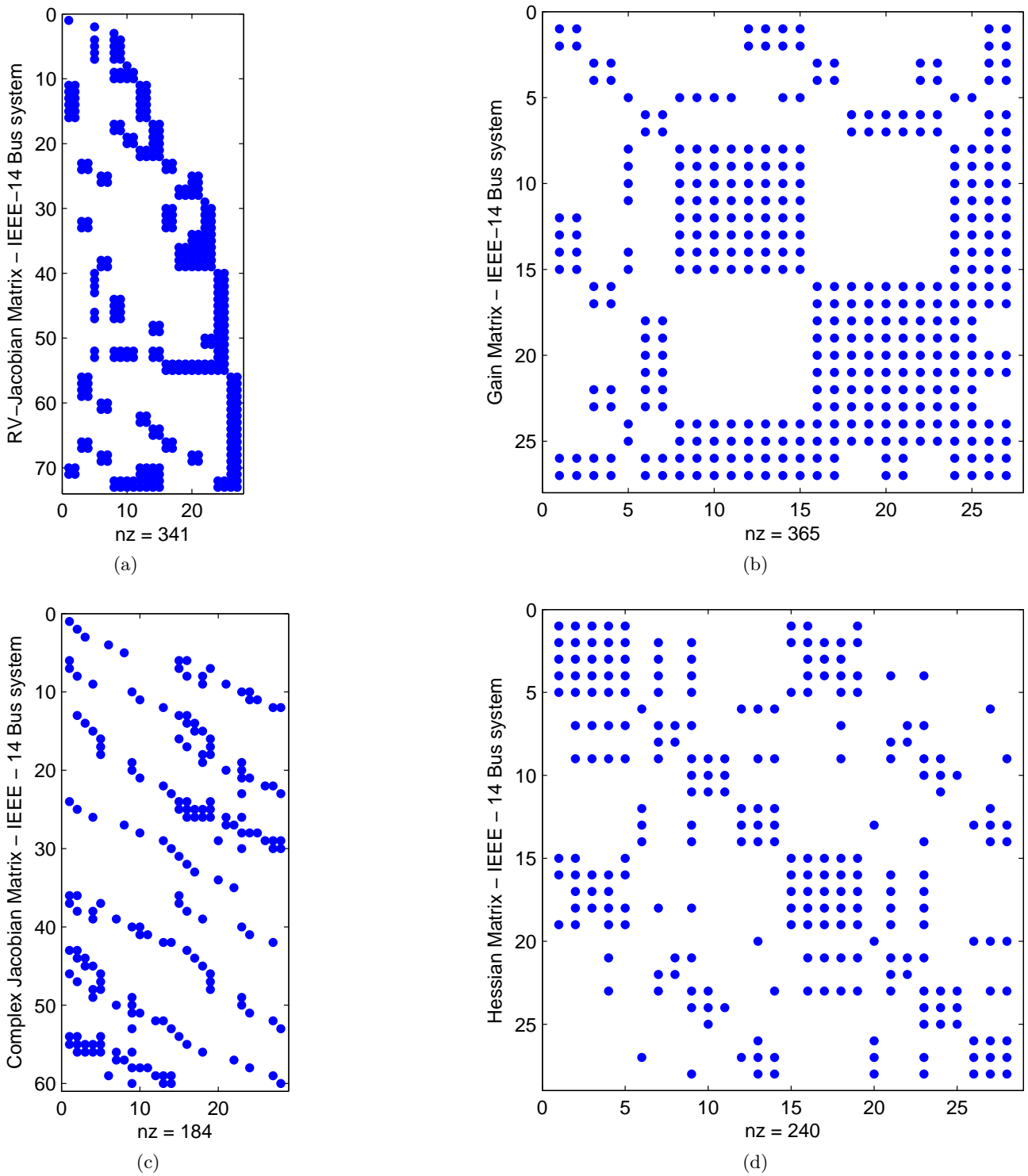


Figure 5.4: Sparsity structure of (a) real-valued Jacobian matrix; (b) real-valued gain matrix; (c) complex-valued Jacobian matrix; (d) complex-valued Hessian matrix of the IEEE 14-bus system.

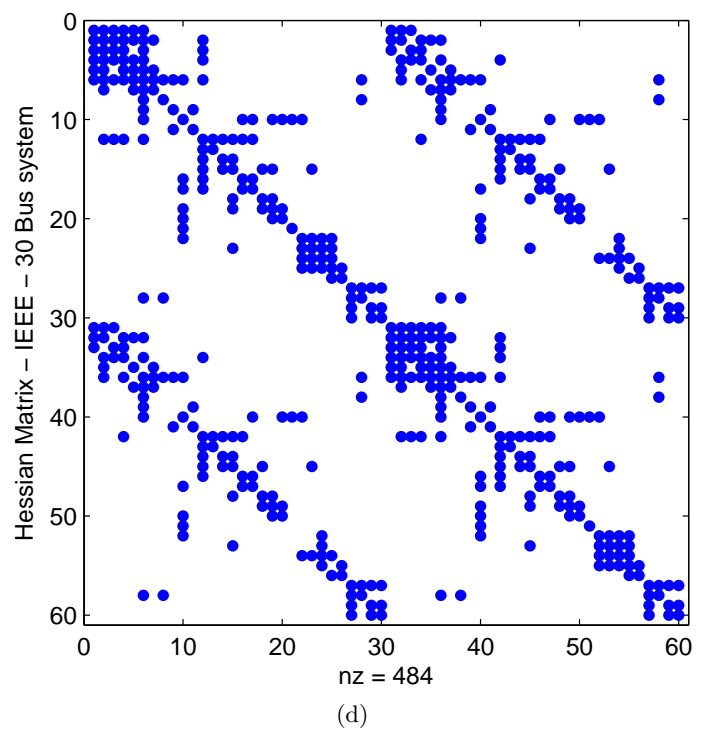
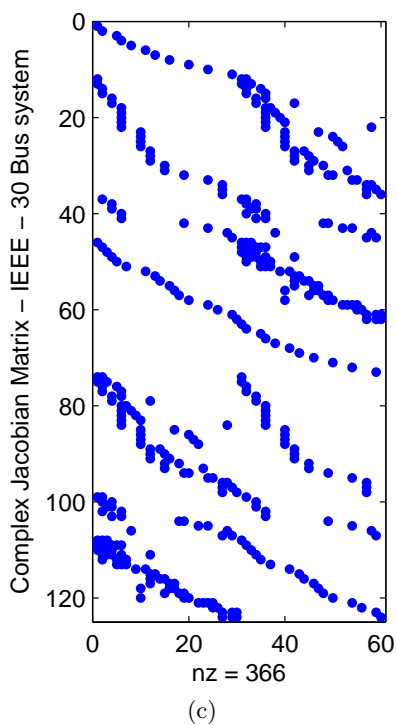
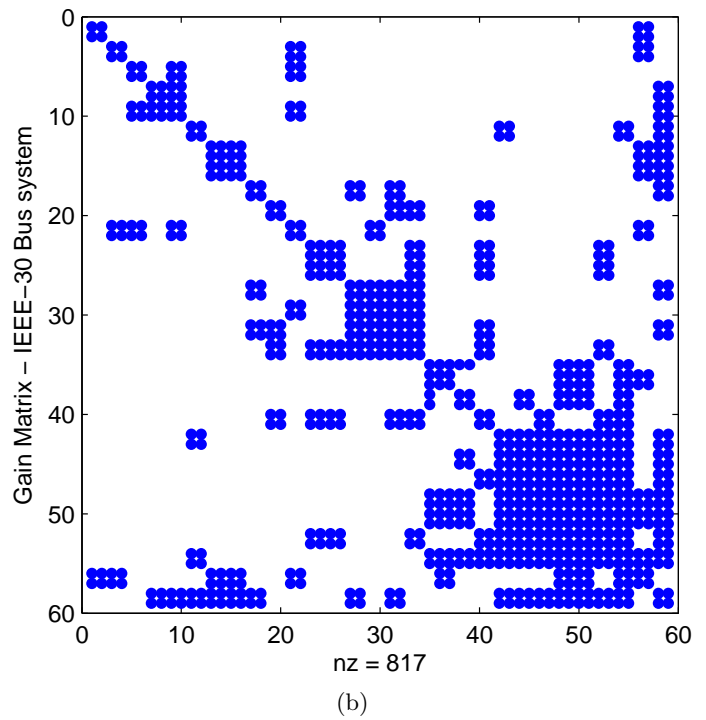
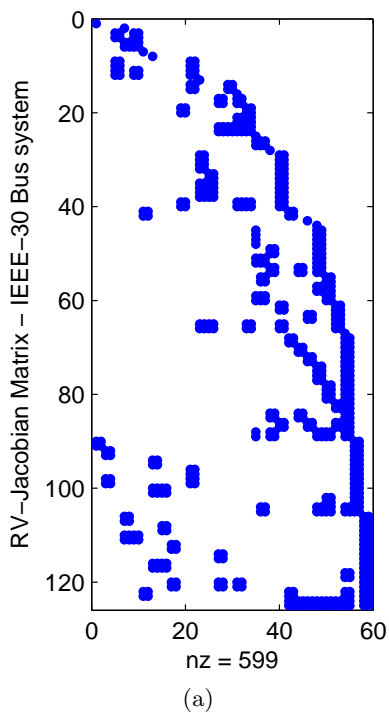


Figure 5.5: Sparsity structure of (a) real-valued Jacobian matrix; (b) real-valued gain matrix; (c) complex-valued Jacobian matrix; (d) complex-valued Hessian matrix of the IEEE 30-bus system.

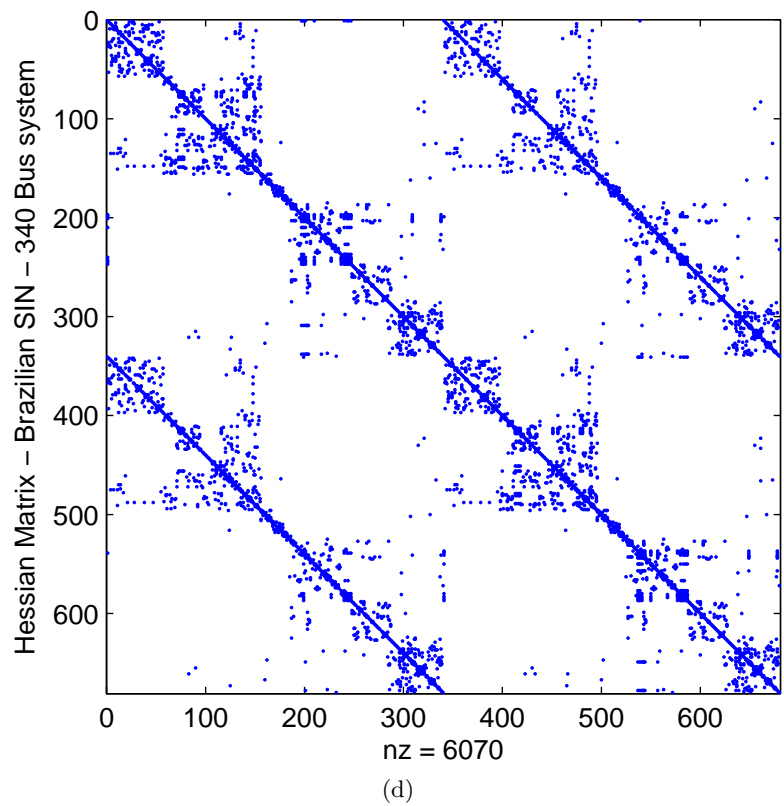
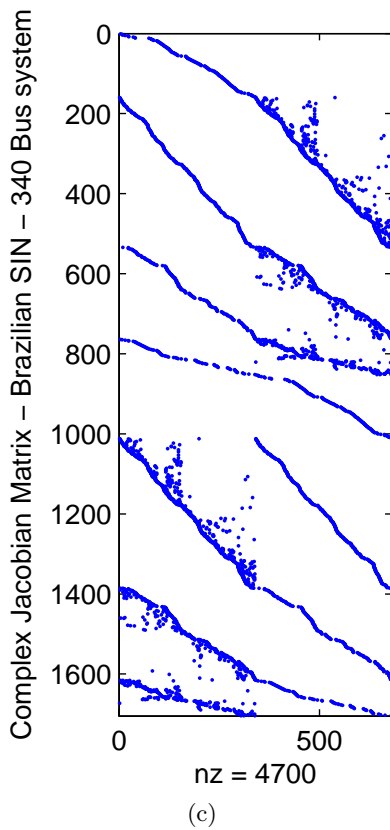
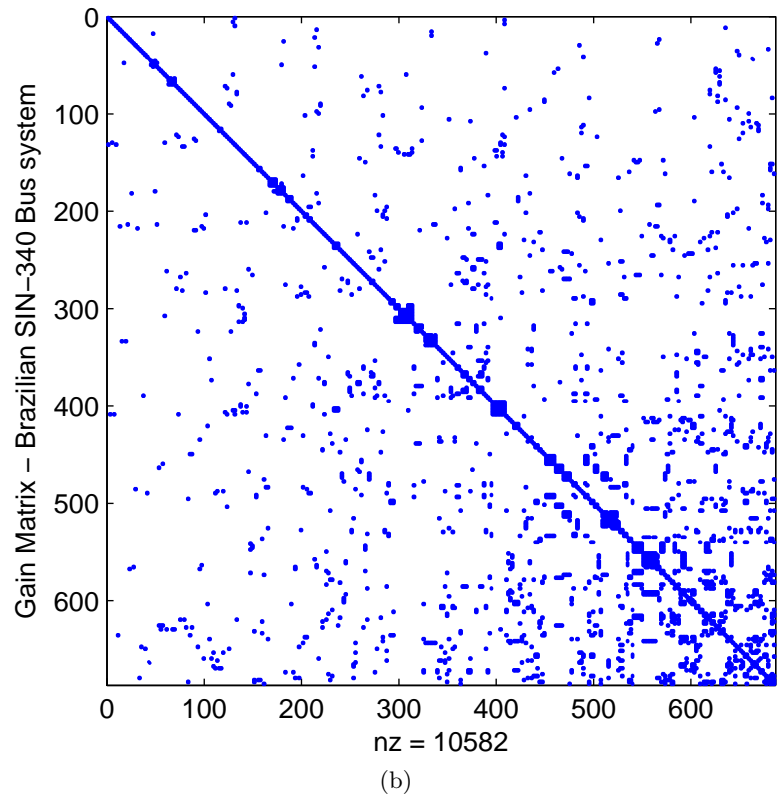
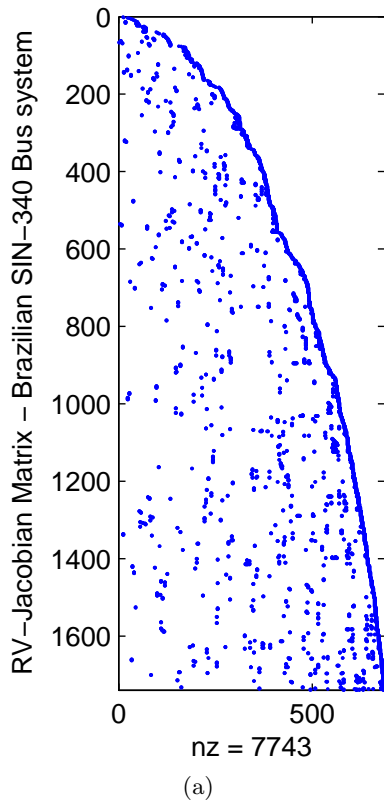
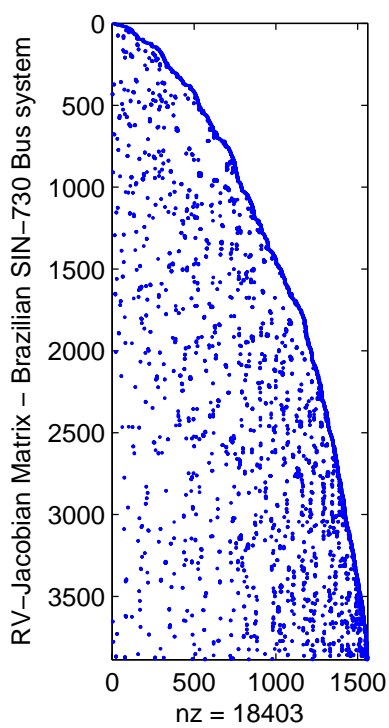
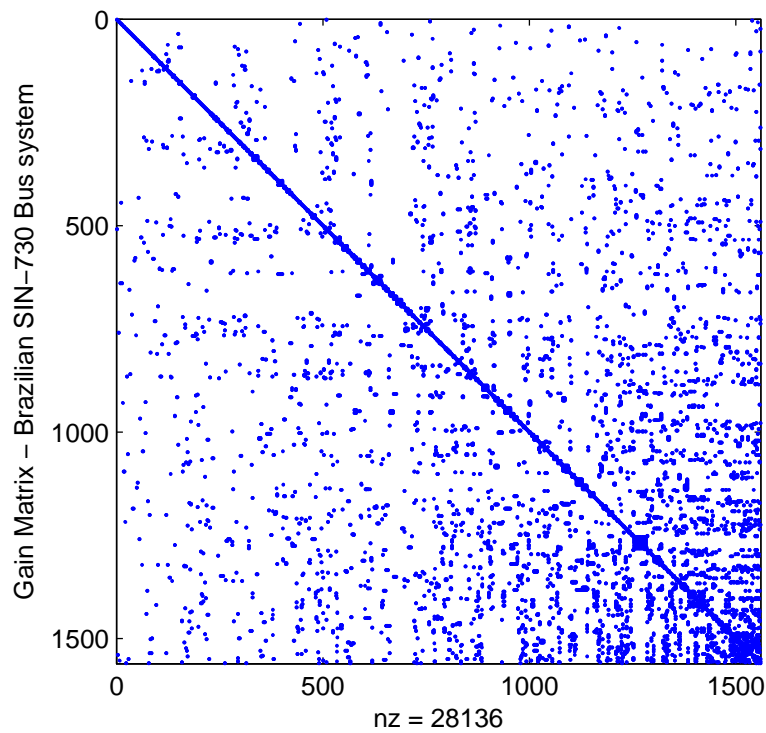


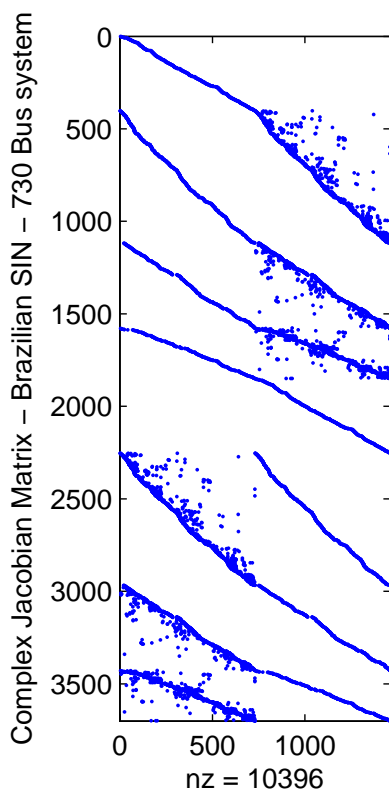
Figure 5.6: Sparsity structure of (a) real-valued Jacobian matrix; (b) real-valued gain matrix; (c) complex-valued Jacobian matrix; (d) complex-valued Hessian matrix of the Brazilian equivalent 340-bus system.



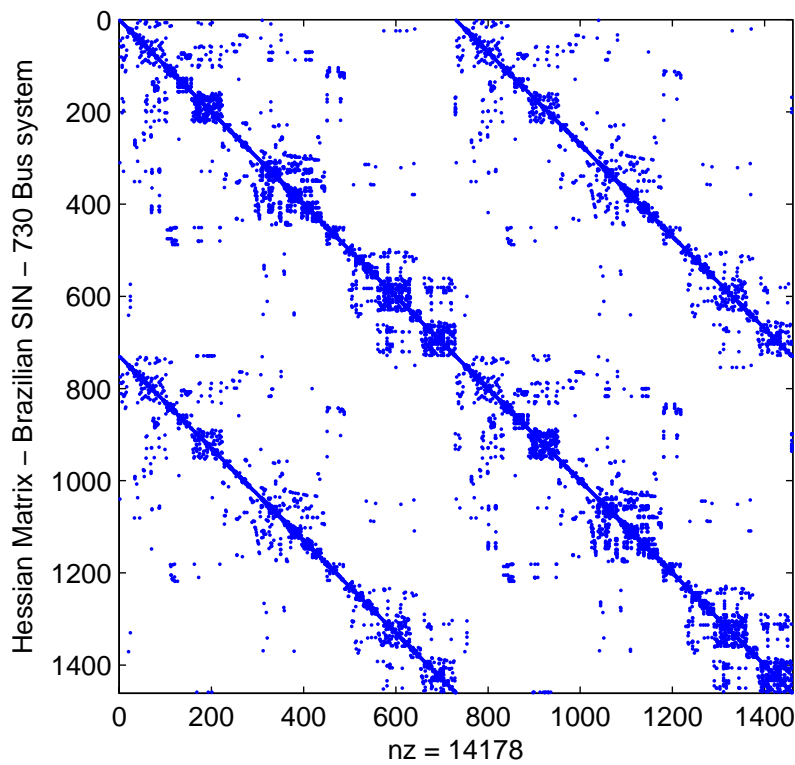
(a)



(b)



(c)



(d)

Figure 5.7: Sparsity structure of (a) real-valued Jacobian matrix; (b) real-valued gain matrix; (c) complex-valued Jacobian matrix; (d) complex-valued Hessian matrix of the Brazilian equivalent 730-bus system.

5.6 Numerical Results Including Bad Data

In the sequel is presented the application of a classical bad data processing in a small example system aiming to track its performance in complex-domain. Firstly, the linear complex model of measurements is considered and compared to those cases discussed in [80]. Likewise, the nonlinear complex model will be applied to the same 2-bus example system as presented before.

5.6.1 Circular and Proper Complex Linear Model

The one-line diagram of an example system, including the measurement configuration identified by means of black bullets placed at each measurement point, is shown in Fig. 5.8. All lines are assumed to have zero resistance and 1.0 pu, reactance, x_{ij} .

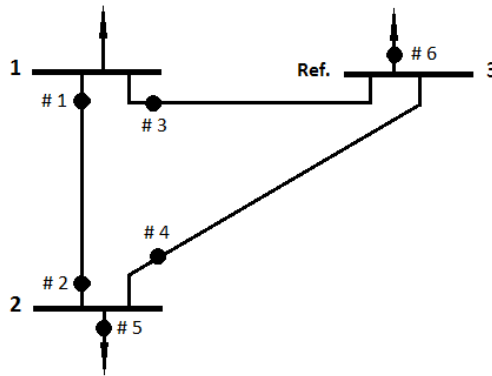


Figure 5.8: Small 3-Bus Example System.

Taking bus 3 as reference bus ($\delta_3 = 0.0$), the problem is to estimate the two bus voltage angles δ_1 and δ_2 based on a set of 6 real power measurements. Also, namely that the true measurement values are zero and that the standard deviation of the errors are of 0.01 pu, i.e., $\mathbf{\Omega}_c = 10^{-4} \mathbf{I}_{12 \times 12}$, which means a proper and circular data. Then, applying the complex DC model, the contents of equation (224) to be solved are

Table 5.5: Features of the IEEE-Standards and Brazilian Grids

Number of bus	14	30	340	730
branches	20	41	494	973
states (n)	27	59	686	1560
voltage meas. (V_i)	5	11	159	402
active p. flow meas. (t_{ij})	23	34	604	1176
reactive p. flow meas. (u_{ij})	23	34	604	1176
active p. inj. meas. (p_i)	11	23	89	241
reactive p. inj. meas. (q_i)	11	23	85	260
measurements (m)	73	125	1732	3784

Table 5.6: Parameters and Performance Indices

Number of bus	14	30	340	730
Jacobian Matrix, as in (169):				
- Number of rows -> m	30	62	852	1850
- Number of columns -> n	14	30	340	730
Number of nonzero entries in:				
- H matrix, as in Eq. (169) ->	184	366	4700	10396
- G matrix, as in Eq. (171) ->	240	484	6070	14178
Number of iterations	3	3	5	6
Total time (s) without sparsity	7.69	10.63	16.93	89.67

$$\mathbf{H}_c = j \begin{bmatrix} 1 & -1 & 0 & 0 \\ -1 & 1 & 0 & 0 \\ 1 & 0 & 0 & 0 \\ 0 & 1 & 0 & 0 \\ -1 & 2 & 0 & 0 \\ -1 & -1 & 0 & 0 \\ 0 & 0 & -1 & 1 \\ 0 & 0 & 1 & -1 \\ 0 & 0 & -1 & 0 \\ 0 & 0 & 0 & -1 \\ 0 & 0 & 1 & -2 \\ 0 & 0 & 1 & 1 \end{bmatrix}; \quad \mathbf{z}_c = \begin{bmatrix} 0 \\ 0 \\ 0 \\ 0 \\ 0 \\ 0 \\ 0 \\ 0 \\ 0 \\ 0 \\ 0 \\ 0 \end{bmatrix}; \quad \hat{\delta}_c = j \begin{bmatrix} \delta_1 \\ \delta_2 \\ -\delta_1 \\ -\delta_2 \end{bmatrix}.$$

Strictly speaking, when the data are proper and circular the complex linear model can be solved likewise its counterpart in real domain. The covariance matrix becomes a diagonal and real-valued matrix as stated in (198), i.e., $\mathbf{\Omega}_c = \mathbf{C}_c$, although the complex arithmetics have to be used. Otherwise, i.e., when the pseudo-covariance cannot be neglected ($\mathbf{P}_c \neq 0$), the above formulation must be employed.

Case A.1:

$\mathbf{z}_c = [0 \ 0 \ 0 \ 0 \ 1 \ 0 \ : \ 0 \ 0 \ 0 \ 0 \ 1 \ 0]^T \text{ pu}$ \rightarrow Measurement 5 is a bad data. The corresponding normalized residual vector is

$$\mathbf{z}_{n_i} = [33.0 \ -33.0 \ 7.5 \ -24.7 \ \underline{69.5} \ 25.9 \ : \ 33.0 \ -33.0 \ 7.5 \ -24.7 \ \underline{69.5} \ 25.9]^T \therefore \text{It works.}$$

Case A.2:

$\mathbf{z}_c = [0 \ -1 \ 0 \ 0 \ 1 \ 0 \ : \ 0 \ -1 \ 0 \ 0 \ 1 \ 0]^T \text{ pu}$ \rightarrow Measurements 2 and 5 are bad data. Both bad data are not conforming, i.e., not interacted. Thus, the corresponding normalized residual vector is

$$\mathbf{z}_{n_i} = [7.3 \ -\underline{121.0} \ -11.2 \ -17.6 \ 111.3 \ 41.5 \ : \ 7.3 \ -\underline{121.0} \ -11.2 \ -17.6 \ 111.3 \ 41.5]^T \therefore \text{It also works.}$$

Case A.3:

$\mathbf{z}_c = [0 \ 1 \ 0 \ 0 \ 1 \ 0 \ : \ 0 \ 1 \ 0 \ 0 \ 1 \ 0]^T \text{ pu}$ \rightarrow Measurements 2 and 5 are bad data.

But, in this case they are interacting or conforming, and the corresponding normalized residual vector is

$\underline{z}_{n_i} = [\underline{58.6} \ 55.0 \ 26.2 \ -31.7 \ 27.8 \ 10.4 \vdots \ \underline{58.6} \ 55.0 \ 26.2 \ -31.7 \ 27.8 \ 10.4]^T$ ∴ It fails!... Remark that the largest residual occurs at measurement 1, which is a good data.

It is now time to give some insights regarding the existence of leverage points in complex domain, even if this issue is beyond of this work now. Aiming this purpose, let us take the same simulation of bad leverage points discussed in [81] and carried out in the example system presented in Fig. 5.8 as showed in the sequel,

Case A.4:

$\underline{z}_c = [0 \ 0 \ -0.55 \ 0 \ 0 \ 1 \ \vdots \ 0 \ 0 \ -0.55 \ 0 \ 0 \ 1]^T \ pu$ → Measurements 3 and 6 are bad leverage points.

$\underline{z}_{n_i} = [21.1 \ -21.1 \ -6.2 \ \underline{34.0} \ 18.1 \ 30.8 \ \vdots \ 21.1 \ -21.1 \ -6.2 \ \underline{34.0} \ 18.1 \ 30.8]^T$ ∴ It fails!... Remark that the largest residual occurs at measurement 4, which is a good data. And, the identification by elimination based on largest $|r_{n_i}|$ leads towards next case.

Case A.5:

$\underline{z}_c = [0 \ 0 \ -0.55 \ 0 \ 1 \ \vdots \ 0 \ 0 \ -0.55 \ 0 \ 1]^T \ pu$ → Measurements 3 and 6 are bad leverage points and measurement 4 is suppressed as suggested in **Case A.4**.

$\underline{z}_{n_i} = [18.4 \ -18.4 \ -2.0 \ \underline{32.2} \ 17.3 \ \vdots \ 18.4 \ -18.4 \ -2.0 \ \underline{32.2} \ 17.3]^T$ ∴ It fails again!... Now the largest residual occurs at measurement 5, which is a good data.

5.6.2 Circular and Proper Complex NonLinear Model

The one-line diagram, including the measurement placement, is shown in Fig. 5.9. Recall it is that presented before and within this section. Therefore, the whole set of results are already known, including the intermediary ones.

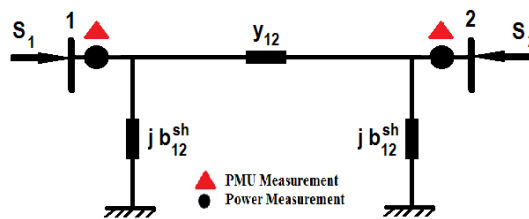


Figure 5.9: Small 2-Bus Example System.

The main concern here is to extend the application of the classical bad data processing algorithms towards nonlinear model of measurements in complex domain. In this sense, we are going to consider bad data regardless it is in real or imaginary parts, being both uncorrelated and have equal variances of a complex data. Thus, it is intended to simulate bad data in two classes of measurements. Firstly, we are going to consider as a bad data a complex power simulated as follows:

Case B.1:

$$\underline{\mathbf{z}}_c = \begin{bmatrix} V_k \\ V_m \\ S_{km} \\ S_{mk} \end{bmatrix} = \begin{bmatrix} 1.0000 + j0.0000 \\ 0.8651 - j0.2333 \\ -1.8827 + j0.4244 \\ -1.7998 - j0.4497 \end{bmatrix},$$

where the active power (real part) of the complex power at the sending end terminal, i.e., $P_{km} = \Re(S_{km})$ is a bad data.

$$\underline{\mathbf{r}}_{n_i} = \begin{bmatrix} 12.9295 + j11.1486 \\ 6.1186 - j14.5367 \\ -185.5201 + j20.0240 \\ -183.3210 + j18.3333 \end{bmatrix}.$$

The complex normalized residual vector showed above points out the bad data properly.

Case B.2:

The real part of the voltage at the receiving end of the Pi-circuit, i.e., $\Re(V_m)$ is a bad data.

$$\underline{\mathbf{z}}_c = \begin{bmatrix} V_k \\ V_m \\ S_{km} \\ S_{mk} \end{bmatrix} = \begin{bmatrix} 1.0000 + j0.0000 \\ -0.8651 - j0.2333 \\ 1.8827 + j0.4244 \\ -1.7998 - j0.4497 \end{bmatrix},$$

and the corresponding complex normalized residual vector allows to identify the bad data correctly.

$$\underline{\mathbf{r}}_{n_i} = \begin{bmatrix} 49.6222 + j53.3528 \\ -100.4777 + j34.5800 \\ 9.0977 - j33.8791 \\ -16.1844 - j40.5206 \end{bmatrix}.$$

Case B.3:

The imaginary part of the voltage at the receiving end of the Pi-circuit, i.e., $\Im(V_m)$ is a bad data.

$$\underline{\mathbf{z}}_c = \begin{bmatrix} V_k \\ V_m \\ S_{km} \\ S_{mk} \end{bmatrix} = \begin{bmatrix} 1.0000 + j0.0000 \\ 0.8651 + j0.2333 \\ 1.8827 + j0.4244 \\ -1.7998 - j0.4497 \end{bmatrix}.$$

and the corresponding complex normalized residual vector is,

$$\underline{\mathbf{r}}_{n_i} = \begin{bmatrix} 1.5464 - j23.0929 \\ -4.2318 + j25.5528 \\ 1.3930 + j 1.2796 \\ -1.0985 + j 2.0941 \end{bmatrix},$$

and it clearly works.

5.6.3 Noncircular/Proper Complex NonLinear Model

The deployment of a large number of synchro-phasor measurement units (PMUs) for monitoring power transmission systems around the world is a newly trend [82]. Definitely, a hybrid monitoring system is already a reality at EMS of many utilities in most of the countries. This is an enough motivation for investigating statistical models able to better deal with this new endeavour. The PMU statistical model cannot overlook the fact that a malfunction in whichever voltage or current channels implies in errors which may violate the measurement model and give rise to a bad data. As we are dealing with complex signals, then the error in the real and imaginary parts are correlated, thus the complex signals are non-circular.

5.6.4 Noncircular/Improper Complex NonLinear Model

Not available yet.

5.7 Partial Conclusions

The power system weighted-least-squares estimator in the \mathbb{C} -domain has been formulated using the Wirtinger calculus. The estimator has been solved through the complex-valued Gauss-Newton iterative algorithm. The sparsity structure of the Jacobian and the Hermitian matrices has been investigated on two IEEE test-systems and the Brazilian equivalent 340- and 730-bus system. As a future work, partial factorization of the Jacobian matrix will be investigated and residual statistical analysis for bad data detection and identification will be developed.

In this thesis is derived a covariance matrix which contains information from both the covariance and pseudo-covariance matrices. This approach allows to deal with any nature of a complex random variables, e.g., regardless they are proper or improper, circular or non-circular. The classical bad data processing when applied in complex coordinates behaves likewise in real domain. Nonetheless, highlights that we are just starting the investigation of keys issues in complex-valued power system state estimation.

Definitely, complex random signals play an increasingly important role in array, communications, and biomedical signal processing and related fields. The wider deployment of complexvalued signal processing is often hindered by the fact that the concepts, tools and algorithms for handling complex-valued signals are lacking, or, are simply too scattered in the literature. Due to extensive research in this area during the past few years, as reviewed here, these obstacles no-longer exist, or, are at least less pronounced. We also wish to point out that due to lack of space, several important topics in complex-valued signal processing were not discussed here.

6 General Conclusions

In this thesis a new framework in \mathbb{C} – *domain* specially addressed for nonlinear Power Flow Analysis (CV-PFA) and Power System State Estimation (CV-PSSE) problems is derived. The main features of these classical tools usually employed for planning electrical network expansion and its operative security supervision, respectively, are highlighted from Section 3 to 5. But the whole mathematical fundamentation that is based on Wirtinger’s Work [3], is outlined in Section 2. In Sections 3 and 4 the main qualitative and numerical analysis obtained till now are presented and discussed. Therefore, it shall deem advisable that some insights should pointed out towards next steps of this research, as follows:

1. The Matlab code regarding the CV-PFA should be generalized in order to exploit the sparsity features and potentially speed up the solution of the problem as it is already done for the CV-PSSE after the proposed enhancements have been embedded.
2. Besides the adoption of recommended actions stated before, the bad data processing, i.e., the — classical approach for detection and identification of gross errors in \mathbb{C} – *domain* should be extended to robust methods. For instance, SHGM estimator [57].
3. Moreover, the behavior of CV-Power Flow and CV-Power System State Estimation algorithms should be investigated when applied to unbalanced polyphase distribution systems.
4. This *Thesis* may become a *draft* of a near future Chapter or even a Book on *Complex-Valued Steady-State Models as Applied to Power Systems Problems - Power Flow Analysis and Power System State Estimation* - intended to be published in English aiming the whole Power and Energy Society, i.e., Academy and Power Industry community.

6.1 Future Investigations

It seems opportune to outline the near future trends and works to be done based on the framework proposed in this thesis. The complex-valued power flow and complex-valued power system state estimation open up the path for embed toward new smart grid technologies.

Definitively, power electronic devices are already a reality in modern power system control. For instance, VSC-STATCOM and VSC-HVDC [46], [83], [47], [84] and [85] to cite a few. In this sense, as a future research, we will initiate a power flow framework for hybrid AC-DC systems that include a variety of FACTS devices, including VSC-HVDC links and STATCOM devices, and will develop solution methods that are both numerically robust and compatible with real-time applications.

Consequently, the monitoring hybrid network requires advances on PMU and SCADA technologies [75], [48] and [74]. The power system weighted-least-squares estimator in the \mathbb{C} -domain has been formulated using the Wirtinger calculus. The estimator has been solved through the complex-valued Gauss-Newton iterative algorithm. The sparsity structure of the Jacobian and the Hermitian matrices has been investigated on two IEEE test-systems and the Brazilian equivalent 340- and 730-bus system. As a future work, partial factorization of the Jacobian matrix will be investigated and residual statistical analysis for bad data detection and identification will be developed.

Currently, it is initiated the derivation of a covariance matrix which contains information from the covariance and pseudo-covariance matrices. This approach allows to deal with any nature of a complex random variables, e.g., regardless they are proper or improper, circular or non-circular. The

classical bad data processing when applied in conjugate coordinates behaves likewise in real domain. Nonetheless, highlights that we are just starting the investigation of keys issues in complex-valued power system state estimation.

6.2 Papers Under Review

1. Pires, R. and Mili, L. - "Complex-Valued Power Flow Analysis Using the Wirtinger Calculus", IEEE Transaction on Power Systems, TPWRS-01513-2017, pp. 1-8.
2. Pires, R. and Mili, L. - "Complex-Valued WLS State Estimation of Power Systems Using the Wirtinger Calculus", IEEE Transaction on Power Systems, TPWRS-01530.R1-2017, pp. 1-8.
3. Zhao, J and Mili, L. and Pires, R. - "Statistical and Numerical Robust State Estimator for Heavily Loaded Power Systems", IEEE Transaction on Power Systems, TPWRS-01728-2017, pp. 1-8.

6.3 Advised Students

1. Chagas, G.S. - "Fluxo de Potência Numericamente Robusto via Método de Levenberg-Marquardt de Ordem Superior", Dissertação de Mestrado; *Conclusion: June / 2018*.
2. Custódio, J. F. - "O Método de Newton-Raphason Aplicado ao Problema de Fluxo de Potência - Uma Alternativa Vantajosa para Análise de Redes Inteligentes", Trabalho Final de Graduação (TFG), Engenharia Elétrica-NIFEI, October / 2016.
3. Pereira, M. A. e Silva, M. C. M. - "Modelo de links-HVDC incorporado ao problema de fluxo de potência derivado no domínio de números complexos", Trabalho Final de Graduação (TFG), Engenharia Elétrica-NIFEI, October / 2017.
4. Neto, R. A. e Oliveira, F. F. J. - "Propriedades de convergência do algoritmo de Newton-Rapshon formulado no domínio de números complexos", Trabalho Final de Graduação (TFG), Engenharia Elétrica-NIFEI, October / 2017.
5. Alvarenga, I. V. - "Análise de Perturbações no Sistema Interligado Nacional via Projeto MED-FASEE", Trabalho Final de Graduação (TFG), Engenharia Elétrica-NIFEI; *Conclusion: October / 2018*.
6. Barbosa, M. T. - "Incorporação do Modelo de Transformadores com Tape em Quadratura em Estudos de Fluxo de Potência Construído no Domínio de Números Complexos", Trabalho Final de Graduação (TFG), Engenharia Elétrica-NIFEI; *Conclusion: October / 2018*.

Bibliography

- [1] C. P. Steinmetz, “Complex quantities and their use in electrical engineering,” *Proceedings of the International Electrical Congress*, pp. 33–74, 1893.
- [2] Wikipedia, “Wilhelm Wirtinger — wikipedia, the free encyclopedia,” 2015, [Online: accessed 5-February-2016]. [Online]. Available: https://en.wikipedia.org/w/index.php?title=Wilhelm_Wirtinger&oldid=680448303
- [3] W. Wirtinger, “Zur Formalen Theorie der Functionen Von Mehr Complexen Veranderlichen,” *Math. Ann.*, vol. 97, pp. 357–375, 1927.
- [4] R. Remmert, *Theory of Complex Functions*, Springer-Verlag, Ed. Springer-Verlag, New York, 1991.
- [5] K. Kreutz-Delgado, “The complex gradient operator and the CR-calculus,” *ArXIV e-print, arXIV:0906.4835v1 [math.OA]*, pp. 1–74, June 25, 2009.
- [6] L. Sorber, M. V. Barel, and L. de Lathauwer, “Unconstrained optimization of real functions in complex variables,” *Society for Industrial and Applied Mathematics - SIAM*, vol. 22, No. 3, pp. 879–898, 2012.
- [7] A. Maltsev, V. Pestretsov, R. Maslennikov, and A. Khoryaev, “Triangular systolic array with reduced latency for QR-decomposition of complex matrices,” *IEEE International Symposium on Circuits and Systems - ISCAS*, pp. 385–388, 2006.
- [8] A. Awasthi, R. Guttal, N. Al-Dhahir, and P. T. Balsara, “Complex QR decomposition using fast plane rotations for MIMO applications,” *IEEE Communications Letters*, vol. 18, No. 10, pp. 1743–1746, 2014.
- [9] D. P. Mandic and V. S. L. Goh, *Complex Valued Nonlinear Adaptive Filters: Noncircularity, Widely Linear and Neural Models*. John Wiley and Sons, Ltd, 2009.
- [10] A. Hjørungnes, *Complex-Valued Matrix Derivatives - With Applications in Signal Processing and Communications*. Cambridge University Press, New York, 2011.
- [11] P. A. Bonet, “Theory and applications of bounded component analysis in complex valued signal processing,” Ph.D. dissertation, Department of Signal Theory and Communications, University of Seville, Spain, February 2013.
- [12] J. Glover, M. Sarma, and T. Overbye, *Power System Analysis and Design*. Cengage Learning, 2011. [Online]. Available: <https://books.google.com.br/books?id=uQcJAAAAQBAJ>

- [13] H. L. Nguyen, “Newton-raphson method in complex form [power flow analysis],” in *Transmission and Distribution Conference, 1996. Proceedings., 1996 IEEE*, Sep 1996, pp. 591–595.
- [14] —, “Newton-raphson method in complex form [power system load flow analysis],” *Power Systems, IEEE Transactions on*, vol. 12, no. 3, pp. 1355–1359, Aug 1997.
- [15] T. Nguyen and C. Vu, “Complex-variable newton-raphson load-flow analysis with facts devices,” in *Transmission and Distribution Conference and Exhibition, 2005/2006 IEEE PES*, May 2006, pp. 183–190.
- [16] Z. Wang, B. Cui, and J. Wang, “A necessary condition for power flow insolvability in power distribution systems with distributed generators,” *IEEE Transactions on Power Systems*, vol. PP, no. 99, pp. 1–1, 2016.
- [17] S. S. Baghsorkhi and S. P. Suetin, “Embedding AC power flow with voltage control in the complex plane : The case of analytic continuation via padé approximants,” *CoRR*, vol. abs/1504.03249, 2015. [Online]. Available: <http://arxiv.org/abs/1504.03249>
- [18] A. Trias, “The holomorphic embedding load flow method,” in *2012 IEEE Power and Energy Society General Meeting*, July 2012, pp. 1–8.
- [19] D. H. Brandwood, “A complex gradient operator and its application in adaptive array theory,” *Communications, Radar and Signal Processing, IEE Proceedings F*, vol. 130, no. 1, pp. 11–16, February 1983.
- [20] T. T. Nguyen and C. Vu, “Complex-variable newton-raphson load-flow analysis with FACTS devices,” in *Transmission and Distribution Conference and Exhibition, 2005/2006 IEEE PES*, IEEE, Ed. <http://dx.doi.org/10.1109/TDC.2006.1668480>: IEEE, 2006, pp. 183 – 190.
- [21] L. Barboza, H. Zürn, and R. Salgado, “Load tap change transformer: A modeling reminder,” *IEEE Power Engineering Review*, pp. 51–52, 2001.
- [22] R. Pires, “Unbalanced phase-to-phase voltage compensators applied to radial distribution feeders,” *Power Delivery, IEEE Transactions on*, vol. 19, no. 2, pp. 806–812, April 2004.
- [23] J. Verboomen, D. V. Hertem, P. H. Schavemaker, W. L. Kling, and R. Belmans, “Phase shifting transformers: principles and applications,” in *2005 International Conference on Future Power Systems*, Nov 2005, pp. 6 pp.–6.
- [24] S. Bhowmick, *Flexible Transmission Systems (FACTS) - Newton Power Flow Modeling of Voltage-Sourced Converter Based Controllers*, ser. International Standard Book Number-13: 978-1-4987-5620-4 (eBook - PDF), C. P. T. . F. Group, Ed., 2016.
- [25] X.-P. Zhang, “Multiterminal voltage-sourced converter-based **HVDC** models for power flow analysis,” *IEEE Transactions on Power Systems*, vol. 19, no. 4, pp. 1877–1884, Nov 2004.
- [26] W. Gentleman, “Least Squares Computations by Givens Transformations Without Square Roots,” *Journal of Mathematics Applications*, vol. 12, pp. 329–336, 1974.
- [27] A. Simões-Costa and V. Quintana, “An Orthogonal Row Processing Algorithm for Power Sequential State Estimation,” *IEEE-Transaction on Power Apparatus and Systems*, vol. 100, no. 8, pp. 3791–3800, August 1981.

- [28] J. W. Wang and V. H. Quintana, “A decoupled orthogonal row processing algorithm for power system state estimation,” *IEEE Transactions on Power Apparatus and Systems*, vol. PAS-103, no. 8, pp. 2337–2344, Aug 1984.
- [29] N. Vempati, I. W. Slutsker, and W. F. Tinney, “Enhancement to givens rotations for power system state estimation,” *IEEE Transactions on Power Systems*, vol. 6, no. 2, pp. 842–849, May 1991.
- [30] K. M. Brown, “A quadratically convergent newton-like method based upon gaussian elimination,” *SIAM Journal on Numerical Analysis*, vol. 6, no. 4, pp. 560–569, 1969. [Online]. Available: <https://doi.org/10.1137/0706051>
- [31] R. P. Brent, “Some efficient algorithms for solving systems of nonlinear equations,” *SIAM Journal on Numerical Analysis*, vol. 10, no. 2, pp. 327–344, 1973. [Online]. Available: <https://doi.org/10.1137/0710031>
- [32] J. M. Martinez, “Generalization of the Methods of Brent and Brown for Solving Nonlinear Simultaneous equations,” *SIAM Journal on Numerical Analysis*, vol. 16, no. 3, pp. 434–448, 1979. [Online]. Available: <https://doi.org/10.1137/0716036>
- [33] J. J. Moré and M. Y. Cosnard, “Numerical solution of nonlinear equations,” *ACM Trans. Math. Softw.*, vol. 5, no. 1, pp. 64–85, Mar. 1979. [Online]. Available: <http://doi.acm.org/10.1145/355815.355820>
- [34] J. M. Martínez, “Solving nonlinear simultaneous equations with a generalization of brent’s method,” *BIT Numerical Mathematics*, vol. 20, no. 4, pp. 501–510, Dec 1980. [Online]. Available: <https://doi.org/10.1007/BF01933643>
- [35] A. Klos and A. Kerner, “The non-uniqueness of load flow solutions,” *Proceedings of 5th power system computation conference (PSCC) - Cambridge - UK*, pp. 268–276, July 1975.
- [36] S. Iwamoto and Y. Tamura, “A load flow calculation method for ill-conditioned power systems,” *IEEE Transactions on Power Apparatus and Systems*, vol. PAS-100, no. 4, pp. 1736–1743, April 1981.
- [37] S. C. Tripathy and G. S. S. S. K. P. Prasad, “Load flow solution for ill-conditioned power systems by quadratically convergent newton-like method,” *IEE Proceedings C - Generation, Transmission and Distribution*, vol. 127, no. 5, pp. 273–280, September 1980.
- [38] S. C. Tripathy, G. D. Prasad, O. P. Malik, and G. S. Hope, “Load-flow solutions for ill-conditioned power systems by a newton-like method,” *IEEE Power Engineering Review*, vol. PER-2, no. 10, pp. 25–26, Oct 1982.
- [39] —, “Late discussion and closure to ”load-flow solutions for ill-conditioned power systems by a newton-like method”,,” *IEEE Transactions on Power Apparatus and Systems*, vol. PAS-103, no. 8, pp. 2368–2368, Aug 1984.
- [40] Y. Tamura, K. Sakamoto, and Y. Tayama, “Voltage instability proximity index (vipi) based on multiple load flow solutions in ill-conditioned power systems,” in *Proceedings of the 27th IEEE Conference on Decision and Control*, Dec 1988, pp. 2114–2119 vol.3.

- [41] R. Pourbagher and S. Y. Derakhshandeh, “Application of high-order Levenberg -Marquardt method for solving the power flow problem in the ill-conditioned systems,” *IET Generation, Transmission Distribution*, vol. 10, no. 12, pp. 3017–3022, 2016.
- [42] X. Yang, “A higher-order Levenberg–Marquardt method for nonlinear equations,” *Applied Mathematics and Computation*, vol. 219, no. 22, pp. 10 682 – 10 694, 2013. [Online]. Available: <http://www.sciencedirect.com/science/article/pii/S0096300313004487>
- [43] J. Fan, “Accelerating the modified Levenberg-Marquardt method for nonlinear equations,” *Mathematics of Computation*, vol. 287, no. 83, pp. 1173 – 1187, 2014.
- [44] K. Amini and F. Rostami, “A modified two steps Levenberg-Marquardt method for nonlinear equations,” *Journal of Computational and Applied Mathematics*, vol. 288, no. Supplement C, pp. 341 – 350, 2015. [Online]. Available: <http://www.sciencedirect.com/science/article/pii/S0377042715002666>
- [45] —, “Three-steps modified Levenberg-Marquardt method with a new line search for systems of nonlinear equations,” *Journal of Computational and Applied Mathematics*, vol. 300, no. Supplement C, pp. 30 – 42, 2016. [Online]. Available: <http://www.sciencedirect.com/science/article/pii/S0377042715006251>
- [46] E. Acha and L. M. Castro, “A generalized frame of reference for the incorporation of multi-terminal vsc-hvdc systems in power flow solutions,” *Electric Power Systems Research*, vol. 136, no. Supplement C, pp. 415 – 424, 2016. [Online]. Available: <http://www.sciencedirect.com/science/article/pii/S0378779616300566>
- [47] S. Bhowmick, *Flexibal AC Transmission Systems (FACTS): Newton Power-Flow Modeling of Voltage-Sourced-Converter Base Controllers*, C. P. T. . F. Group, Ed., 2016.
- [48] A. de la Villa Jaen, E. Acha, and A. G. Exposito, “Voltage source converter modeling for power system state estimation: Statcom and vsc-hvdc,” *IEEE Transactions on Power Systems*, vol. 23, no. 4, pp. 1552–1559, Nov 2008.
- [49] T. Adalý and P. J. Schreier, “Optimization and estimation of complex-valued signals,” *IEEE Signal Processing Magazine*, pp. 112–128, September 2014.
- [50] T. Adalý and S. Haykin, *Adaptive Signal Processing: Next-Generation Solutions*, S. H. Tülay Adalý, Ed. John Wiley and Sons, Inc., Hoboken, New Jersey, 2010.
- [51] M. F. Amin and K. Murase, *Complex-Valued Neural Networks - Advances and Applications*, ser. IEEE Press Series on Computational Intelligence, A. Hirose, Ed., 2013.
- [52] H. G. Zimmermann, A. Minin, and V. Kusherbaeva, “Comparison of the Complex Valued and Real Valued Neural Networks Trained with Gradient Descent and Random Search Algorithms,” in *European Symposium on Artificial Neural Networks (ESANN), Computational Intelligence and Machine Learning, Bruges (Belgium) 27-29 April 2011*, Proceedings, Ed., 2011, pp. 213–218, [Online: accessed 22-July-2016]. [Online]. Available: <https://www.i6doc.com/en/livre/?GCOI=28001100817300>.
- [53] B. A. Van Den, “The multivariate complex normal distribution - A Generalization,” *Information Theory, IEEE Transactions on*, vol. 41, no. 2, pp. 537–539, Mar 1995.

- [54] P. J. Schreier and L. L. Scharf, *Statistical Signal Processing of Complex-Valued Data - The Theory of Improper and Noncircular Signals*. Cambridge University Press, 2010.
- [55] Z. Junbo, L. Mili, and R. Pires, “Statistical and Numerical Robust State Estimator for Heavily Loaded Power Systems,” *IEEE - Transactions on Power Systems - TPWRS-01728-2017*, pp. 1–8, 2017.
- [56] C. D. Meyer, *Matrix Analysis and Linear Algebra*. Society for Industrial and Applied Mathematics - SIAM, 2000.
- [57] R. Pires, L. Mili, and F. Lemos, “Constrained robust estimation of power system state variables and transformer tap positions under erroneous zero-injections,” *Power Systems, IEEE Transactions on*, vol. 29, no. 3, pp. 1144–1152, May 2014.
- [58] U. V. Catalyurek, C. T. Aykanat, and E. Kayaaslan, “Hypergraph Partitioning-Based Fill-Reducing Ordering for Symmetric Matrices,” *Siam J. Sci. Comput.*, vol. 4, pp. 1996–2023, 2011.
- [59] O. Kaya, E. Kayaaslan, B. Uçar, and I. S. Duff, “Fill-in reduction in sparse matrix factorizations using hypergraphs,” Research Report RR-8448, Jan 2014. [Online]. Available: <https://hal.inria.fr/hal-00932882>
- [60] B. Picinbono, “On circularity,” *IEEE Transactions on Signal Processing*, vol. 42, no. 12, pp. 3473–3482, Dec 1994.
- [61] B. Picinbono and P. Chevalier, “Widely linear estimation with complex data,” *IEEE Transactions on Signal Processing*, vol. 43, no. 8, pp. 2030–2033, Aug 1995.
- [62] B. Picinbono, “Second-order complex random vectors and normal distributions,” *IEEE Transactions on Signal Processing*, vol. 44, no. 10, pp. 2637–2640, Oct 1996.
- [63] P. J. Schreier and L. L. Scharf, “Second-order analysis of improper complex random vectors and processes,” *IEEE Transactions on Signal Processing*, vol. 51, no. 3, pp. 714–725, March 2003.
- [64] D. Mandic and S. Goh, *Complex Valued Nonlinear Adaptive Filters: Noncircularity, Widely Linear and Neural Models*, Wiley, Ed., 2009.
- [65] D. Looney and D. P. Mandic, “Augmented complex matrix factorisation,” in *2011 IEEE International Conference on Acoustics, Speech and Signal Processing (ICASSP)*, May 2011, pp. 4072–4075.
- [66] P. J. Schreier, “The degree of impropriety (noncircularity) of complex random vectors,” in *2008 IEEE International Conference on Acoustics, Speech and Signal Processing*, March 2008, pp. 3909–3912.
- [67] S. Javidi, D. P. Mandic, and A. Cichocki, “Complex blind source extraction from noisy mixtures using second-order statistics,” *IEEE Transactions on Circuits and Systems I: Regular Papers*, vol. 57, no. 7, pp. 1404–1416, July 2010.
- [68] H. Li and T. Adalý, “Optimization in the complex domain for nonlinear adaptive filtering,” in *Signals, Systems and Computers, 2006. ACSSC '06. Fortieth Asilomar Conference on*, Oct 2006, pp. 263–267.

- [69] T. Adali, P. J. Schreier, and L. L. Scharf, "Complex-valued signal processing: The proper way to deal with impropriety," *IEEE Transactions on Signal Processing*, vol. 59, no. 11, pp. 5101–5125, Nov 2011.
- [70] P. J. Schreier and L. L. Scharf, "Second-order analysis of improper complex random vectors and processes," *IEEE Transactions on Signal Processing*, vol. 51, no. 3, pp. 714–725, March 2003.
- [71] E. Ollila, V. Koivunen, and H. V. Poor, "Complex-valued signal processing - essential models, tools and statistics," in *2011 Information Theory and Applications Workshop*, Feb 2011, pp. 1–10.
- [72] S. Trampitsch, "Complex-valued data estimation: Second-order statistics and widely linear estimators," Master's thesis, Institut für Vernetzte und Eingebettete Systeme, Klagenfurt, Austria, April 2013.
- [73] S. Wang, J. Zhao, Z. Huang, and R. Diao, "Assessing gaussian assumption of PMU measurement error using field data," *IEEE Transactions on Power Delivery*, vol. PP, no. 99, pp. 1–1, 2017.
- [74] Y. Chakhchoukh, V. Vittal, and G. T. Heydt, "PMU based state estimation by integrating correlation," *IEEE Transactions on Power Systems*, vol. 29, no. 2, pp. 617–626, March 2014.
- [75] Q. Zhang, Y. Chakhchoukh, V. Vittal, G. T. Heydt, N. Logic, and S. Sturgill, "Impact of PMU measurement buffer length on state estimation and its optimization," *IEEE Transactions on Power Systems*, vol. 28, no. 2, pp. 1657–1665, May 2013.
- [76] H. Merrill and F. Schweppe, "Bad data suppression in power system static state estimation," *Power Apparatus and Systems, IEEE Transactions on*, vol. PAS-90, no. 6, pp. 2718–2725, Nov 1971.
- [77] E. Handschin, F. C. Schweppe, J. Kohlas, and A. Fiechter, "Bad data analysis for power system state estimation," *IEEE Transactions on Power Apparatus and Systems*, vol. 94, no. 2, pp. 329–337, Mar 1975.
- [78] D. Fuhrmann, *Chapter 60 - Complex Random Variables and Stochastic Processes - Digital Signal Processing Handbook*, vijay k. madisetti and douglas b. williams, editor ed., 1999.
- [79] A. Monticelli and A. Garcia, "Reliable bad data processing for real-time state estimation," *IEEE Transactions on Power Apparatus and Systems*, vol. PAS-102, no. 5, pp. 1126–1139, May 1983.
- [80] A. Monticelli, F. F. Wu, and M. Yen, "Multiple bad data identification for state estimation by combinatorial optimization," *IEEE Power Engineering Review*, vol. PER-6, no. 7, pp. 73–74, July 1986.
- [81] L. Mili, V. Phaniraj, and P. J. Rousseeuw, "Least median of squares estimation in power systems," *IEEE Transactions on Power Systems*, vol. 6, no. 2, pp. 511–523, May 1991.
- [82] R. M. Moraes, Y. Hu, G. Stenbakken, K. Martin, J. E. R. Alves, A. G. Phadke, H. A. R. Volskis, and V. Centeno, "PMU interoperability, steady-state and dynamic performance tests," *IEEE Transactions on Smart Grid*, vol. 3, no. 4, pp. 1660–1669, Dec 2012.
- [83] E. Acha and B. Kazemtabrizi, "A new statcom model for power flows using the newton-raphson method," *IEEE Transactions on Power Systems*, vol. 28, no. 3, pp. 2455–2465, Aug 2013.

- [84] S. Khan and S. Bhowmick, "A novel power-flow model of multi-terminal VSC-HVDC systems," *Electric Power Systems Research*, vol. 133, no. Supplement C, pp. 219 – 227, 2016. [Online]. Available: <http://www.sciencedirect.com/science/article/pii/S0378779615004083>
- [85] —, "A novel sequential power-flow model for hybrid AC-DC systems," in *2015 Annual IEEE India Conference (INDICON)*, Dec 2015, pp. 1–6.